Granzyme B cell death pathway: a complex I side of the story

Margiotta, Daniela

UNIVERSITÉ DE GENÈVE

FACULTÉ DES SCIENCES

Doctorat ès sciences
Mention biologie

Thèse de *Madame Daniela MARGIOTTA*

intitulée :

"Granzyme B Cell Death Pathway: a Complex I Side of the Story"

La Faculté des sciences, sur le préavis de Monsieur D. MARTINVALET, professeur assistant et directeur de thèse (Faculté de médecine, Département de physiologie cellulaire et métabolisme), Monsieur J.-C. MARTINOU, professeur ordinaire et codirecteur de thèse (Département de biologie cellulaire), Monsieur M. WALCH, docteur (Département de médecine, Université de Fribourg, Suisse) et Monsieur J. THIERY, docteur (Institut National de la Santé et de la Recherche Médicale, Unité d'Immunologie des Tumeurs Humaines: Interaction Effecteurs Cytotoxiques - Système Tumoral, Institut Gustave Roussy, Université Paris Sud Orsay, Villejuif, France), autorise l'impression de la présente thèse, sans exprimer d'opinion sur les propositions qui y sont énoncées.

Genève, le 25 juin 2014

Thèse - 4687 -

Le Décanat

N.B. - La thèse doit porter la déclaration précédente et remplir les conditions énumérées dans les "Informations relatives aux thèses de doctorat à l'Université de Genève".

UNIVERSITÉ DE GENÈVE

Département de biologie cellulaire

FACULTÉ DES SCIENCES
Professeur Jean-Claude Martinou

Département de physiologie cellulaire et métabolisme

FACULTÉ DE MÉDECINE
Professeur Denis Martinvalet

Granzyme B cell death pathway: a complex I side of the story

THÈSE

présentée à la Faculté des sciences de l'Université de Genève

pour obtenir le grade de Docteur ès sciences, mention biologie

par

Daniela MARGIOTTA

de Bari (Italie)

Thèse n° 4687

Genéve

Atelier de reproduction de Uni-Mail

2014

TABLE OF CONTENTS

LIST OF FIGURES:

LIST OF ABBREVIATION:

2D BN-gel: Two dimension blue native gel electrophoresis

3D: Three dimension

$\Delta\Psi_m$: Mitochondrial transmembrane potential

Acinus/Acn 1: Apoptotic chromatin condensation inducer

ADV100k: Adenovirus protein 100k

AIF: Apoptosis-inducing factor

Apaf-1: Apoptotic protease activating factor 1

Ape1 : Apurinic endonuclease1

APO2L/TRAIL: Apo2 ligand/tumour necrosis factor-related apoptosis-inducing ligand

ATP: Adenosine triphosphate

Bad: Bcl-2-associated agonist of cell death

Bak: Bcl-2–associated K protein

Bax: Bcl-2–associated X protein

Bcl-2: B-cell lymphoma 2

Bcl-w: Bcl-2 like 2

Bcl-xL: Bcl-2-like 1

BCR : B cell receptor

BH1, BH2, BH3 and BH4: Bcl-2 homology domain

Bid: BH3 interacting domain death agonist

Bim: Bcl2-like 11 (apoptosis facilitator)

BIR: Domains of IAPs

Blk: B lymphoid tyrosine kinase

Bmf: Bcl2 modifying factor

BNIP3: BCL2/adenovirus E1B 19kDa interacting protein 3

Bok: BCL2-related ovarian killer

C8**:** Complement component C8 alpha chain

C9: complement component 9 alpha chain

CI, II, III, IV, V: mitochondrial complex I, II, III, IV, V

C. elegans: Caenorhabditis elegans

CAD: Caspase-activated Dnase

CARD: Caspase recruitment domain

CDCs: Cholesterol dependent cytolysins

Cdk1: Cyclin-dependent kinase 1

CED-3: Protein CED-3

CED-9: Protein CED-9

cIAP1: Cellular inhibitor of apoptosis protein-1

CTLs: Cytotoxic T lymphocytes

CoQ: Coenzyme Q

COX1**:** Cytochrome c oxidase subunit I

DBP: Adenovirus DNA-binding protein

DD: Death domain

DIABLO: Direct inhibitor of apoptosis protein (IAP)-binding protein with low PI

DISC: Death inducing signaling complex DISC

DNA: Deoxyribonucleic acid

DNA-PK: DNA-dependent protein kinase

Dnm1: GTPase dynamin related protein

DR4/DR5: Tumor necrosis factor receptor superfamily,

DRP1: GTPase dynamin related protein

DKO: Double knock out

EEA1: Early endosomal antigen 1

EGF: Epidermal growth factor domain

EGL-1: Protein EGL-1

EM: Electron microscopy

Endo G: Endonuclease G

FO: ATP synthase, H+ transporting, mitochondrial Fo complex

F1**:** ATP synthase, H+ transporting, mitochondrialF1 complex, beta polypeptide

FACS: Fluorescence-activated cell sorting

FAD: Flavin adenine dinucleotide

FADD: Fas-Associated via Death Domain

FADH2: Flavin adenine dinucleotide

FAS: Fas cell surface death receptor

FASL: Fas cell surface death ligand

Fe-S: Iron Sulphur

FIS 1: Mitochondral fission 1 protein

FMN: Flavin mononucleotide

FRAP: Fluorescence recovery after photobleaching

GZMs : Granzymes

GZMA, B, C, D, E, F, G, H, K, M: Granzyme A, B, C, D, E, F, G, H, K, M

HO: Hydroxyl radical

H_2O_2: Hydrogen peroxide

Helicard: DNA helicase

HMGB2: High mobility group box 2

Hrk: BH3-only proteins

IAP: Inhibitor of apoptosis

ICAD: Inhibitor of CAD

IMM: Inner-mitochondrial membrane

IS: Immunological synapse

IKK: IκB kinase

Ku70: ATP-dependent DNA helicase 2 subunit KU70

Kir: Killer immunoglobulin-like receptor

KO: Knock out

MACPF: Membrane attack complex perforin-like

mDNA: Mitochondrial deoxyribonucleic acid

MEF: Mouse embryonic fibroblasts

MFN1: Mitofusin 1

MFN2: Mitofusin 2

MIA 40: Coiled-coil-helix-coiled-coil-helix domain containing 40

MLK: Mitogen-activated protein kinase kinase kinase 13

mn SOD: Manganese-containing SOD

MOM: Mitochondrial outer membrane

MOMP: Mitochondrial outer membrane

NAC: *N*-acetyl-L-cysteine

NADH: Nicotinamide adenine dinucleotide

NADPH: Nicotinamide adenine dinucleotide phosphate

nDNA: Nuclear deoxyribonucleic acid

Ndufa13: NADH dehydrogenase (ubiquinone) 1 alpha subcomplex, 13

Ndufv1: NADH dehydrogenase (ubiquinone) flavoprotein 1

Ndufs1: NADH dehydrogenase (ubiquinone) Fe-S protein 1

Ndufs2: NADH dehydrogenase (ubiquinone) Fe-S protein 2

Ndufs3: NADH dehydrogenase (ubiquinone) Fe-S protein 3

Ndufs7: NADH dehydrogenase (ubiquinone) Fe-S protein 7

Nec1: Necrostatin 1

NF-κB: Nuclear factor kappa-light-chain-enhancer of activated B cells

NK: Natural killers

NM-23-H: NME/NM23 nucleoside diphosphate kinase 1

NOX: Nicotinamide adenine dinucleotide phosphate oxidase

NOX1: NADPH oxidase

NOX4: NADPH oxidase 4

NOXA: BH3-only proteins

NuMa: Nuclear mitotic apparatus protein

$O_2^{\cdot -}$: Superoxide radical

Omi/HtrA2: HtrA serine peptidase 2

OMM: Mitochondrial outer membrane

OPA 1: Optic atrophy 1

OXPHOS: Oxydative phosphorylation

ρ^0: Pseudo rho

PARP-1: Poly (ADP-ribose)-Polymerase 1

PFN: Perforin

Puma: Bcl-2 binding component 3

RHIM: RIP homothypic interaction motif

RIP1/2: Receptor-interacting protein ½

RIP3: Receptor-interacting serine-threonine kinase 3

RIP: Receptor interacting protein

ROCK-1: Rho-associated, coiled-coil containing protein kinase 1

ROS: Reactive oxygen species

S100: Cyotosolic factors

SC: Supercomplex

SDHAF1: Succinate dehydrogenase complex assembly factor 1

SDS-PAGE: Sodium dodecyl sulfate polyacrylamide gel electrophoresis

SET: Histone chaperone of the nucleosome assembly protein family

SOD: Superoxide dismutases

Spike: BH3-only proteins

T Bid: Truncated BH3 interacting domain death agonist

TCA: Tricarboxylic acid cycle

TCR: T cell receptor

Tim: Translocator inner membrane

Tom: Translocator outer membrane

Type 2 FHL: Familial haemophagocytic lymphohistiocytosis disorder

TNF: Tumor necrosis factor

TNFR: Tumor necrosis factor receptor

TRADD: Tumor Necrosis Factor Receptor-1-Associated Death Domain

XO: Xanthine oxidase

XIAP: X-linked inhibitor of apoptosis

WT: Wild type

Chapter 1
RÉSUMÉ AND SUMMARY

1.1 Résumé

Le but de mon travail de thèse est d'étudier et de caractériser l'implication du stress oxydatif dans la mort cellulaire induite par Granzyme B. Les lymphocytes T cytotoxiques (CTL) et les cellules tueuses naturelles (cellules NK) sont les principaux acteurs de la défense de l'hôte contre les cellules non désirées et stressées. Ils sont nommés d'après leur capacité à tuer les cellules cibles. Cette mise à mort est initiée par la libération du contenu des granules cytotoxiques, comprenant des sérine-protéases appelées granzymes (Gzms) conjointement avec la protéine cytolytique appelée perforin (PFN) , pour déclencher de manière efficace la mort des cellules cibles. Il existe cinq types de Gzms chez l'Homme et dix chez la souris; parmi eux, les mieux caractérisés sont le Granzyme A (GzmA) et le Granzyme B (GzmB). GzmA induit une voie de mort cellulaire caspase-indépendante où les mitochondries occupent un rôle central. GzmA n'altère pas l'intégrité de la membrane mitochondriale externe (MOMP) et n'entraîne donc pas de libération des facteurs proapoptotiques

mitochondriaux; en revanche le potentiel transmembranaire mitochondrial (ΔΨm) se dissipe et une production soutenue de ROS a lieu. GzmA clive NDUFS3, une sous-unité du complexe I de la chaîne respiratoire mitochondriale afin d'induire cette production mitocentrique de ROS (Martinvalet , et al 2008). La production de ROS induite par GzmA déclenche la translocation du complexe SET du reticulum endoplasmique vers le noyau, entraînant des dommages à l'ADN et la mort cellulaire. L'équipe de recherche du Dr Green (J. Ricci, et al 2004) a également montré que la caspase- 3 cible NDUFS1, un autre sous-unité du complexe I , afin d'induire la mort cellulaire d'une manière dépendante des ROS. En raison de l'importance de la chaine respiratoire dans de nombreuses voies de mort cellulaires ROS-dépendantes, nous avons voulu vérifier l'implication de ces ROS dans la mort induite par GzmB. GzmB induit à la fois des voies de signalisation caspases-dépendante et caspases-indépendantes. GzmB clive directement et active les caspase-3 et -7 effectrices. GzmB active également par clivage la protéine Bid qui va à son tour activer les protéines pro-apoptotiques Bax et Bak. En conséquence la perméabilisation de la membrane externe mitochondriale (MOMP) a lieu et le cytochrome c est libéré et active les caspases *via* la formation de l'apoptosome. D'autre part, GzmB directement clive ICAD, DNA-PK, la tubuline, la lamine B, NuMa et PARP- 1 dans la voie de la mort cellulaire caspase-indépendante. Jusqu'à présent, la MOMP a été considérée comme le principal événement de la voie apopototique de GzmB. Cependant, une investigation plus approfondie est nécessaire pour comprendre la signification de ROS dans l'apoptose par GzmB ainsi que le mécanisme moléculaire par lequel cette production de ROS a lieu. Par conséquent, le but de ma thèse a été de caractériser le mécanisme moléculaire par lequel GzmB, un « tueur de cellules tumorales ou infectées » , induit une production de ROS et la mort cellulaire. Les premiers résultats

de notre projet sont basés sur l'utilisation de mitochondries isolées. En effet, de manière similaire à GzmA, GzmB induit une production massive de ROS directement à partir de mitochondries isolées, indépendemment de la présence de facteurs cyotosolic tel que Bid, Bax/Bak ou des caspases. De même, le traitement de cellules avec GzmB et PFN conduisent à une augmentation dose-dépendante de la production de ROS et de la mort cellulaire. D'autre part, l'utilisation d'antioxydants pour inhiber les ROS réduisent significativement la mort cellulaire. La perméabilisation de la mitochondrie (MOMP) a longtemps été considérée comme étant l'évènement central de la mort par GzmB. Toutefois, en utilisant des cellules déficientes pour Bax et Bak, qui ne subissent pas de MOMP et par conséquent ne libèrent pas le cyotochrome c, nous observons toujours une production massive de ROS et la mort cellulaire, ce qui signifie que la production de ROS ne dépends pas de la MOMP. Nous avons ensuite utilisé une approche combinée protéomique et bioinformatique qui nous a permis d'identifier NDUFV1, NDUFS2 et NDUFS1, trois sous-unités du complexe I de la chaine respiratoire mitochondriale, comme étant 3 nouveaux substrats ciblés par GzmB. Ceci suggère que le complexe I joue un rôle essentiel dans la voie de la mort cellulaire induite par GzmB. En outre, nous avons montré que GzmB clive ces trois sous-unités dans des mitochondries purifiées, ce qui indique que GzmB agit au niveau du complexe I indépendamment de la présence de facteurs cytosoliques tels que Bid ou des caspases. La présence de facteurs cytosoliques permet cependant de potentialiser et d'amplifier la signalisation apoptotique de GzmB. L'ensemble de ces résultats soutiennent le fait que la mort cellulaire induite par GzmB est dépendante à la fois de la MOMP et des ROS, ces deux événements distincts agissant en synergie pour mieux détruire la cellule cible. En outre, les mitochondries purifiées traités avec GzmB présentent une activité réduite des complexes I et III, une perturbation de la

respiration mitochondriale, une modification de l'organisation supermoléculaire de la chaîne de transport d'électrons et une altération des jonctions des cristae. Par conséquent, nous proposons que GzmB induit la mort cellulaire d'une manière dépendante de ROS. La clarification de l'importance des ROS dans le contexte de la mort cellulaire induite par les cellules cytotoxique immunitaires sera cruciale pour mieux comprendre le mécanisme de l'apoptose. En outre, le rôle important du complexe I mitochondrial dans diverses voies de mort cellulaire soulignent le rôle critique des mitochondries dans la mort cellulaire. Le complexe I pourrait-être un élément important au croisement de ces voies apoptotiques et pourrait donc représenter une nouvelle cible thérapeutique intéressante visant à augmenter ou réduire l’efficacité cytoliques de lymphocytes T cytotoxiques.

1.2 Summary

Cytotoxic T lymphocytes (CTLs) and natural killer (NK) cells are the main actors in the host defense against unwanted and stressed cells. They are named after their ability to kill their target cells. This killing is achieved by releasing the serine proteases, called granzymes (Gzms) together with the pore forming protein perforin (PFN) from their cytotoxic granules, to efficiently trigger target cells death. There are five different human Gzms and ten mouse homologous; among them the best characterized are Granzyme A (GzmA) and Granzyme B (GzmB). GzmA induces a caspase-independent cell death pathway where the mitochondria hold a central role. GzmA does not alter the integrity of the mitochondrial outer membrane (MOMP), consequently no apoptogenic factors are released; the mitochondrial transmembrane potential ($\Delta\Psi_m$) is loss and a sustained ROS production takes place. GzmA cleaves NDUFS3 - a 30 kDa subunit of the mitochondrial electron transport chain complex I - in order to induce this mitocentric ROS production (Martinvalet, et al. 2008). GzmA-induced ROS production triggers the SET complex (containing the GzmA-activated Dnases together with NM-23-H1 and TREX1) translocation to the nucleus leading to DNA damage and cell death. Importantly, the Dr. Green research team (J. Ricci, et al. 2004) have also shown that the executioner caspase-3 targets NDUFS1, another 75 kDa mitochondrial complex I subunit, in order to induce cell death in a ROS dependent manner.

GzmB kills in caspase-dependent and caspase-independent pathway. GzmB directly cleaves and activates caspase 3 and 7. GzmB also directly cleaves Bid which will activate two pro-apoptotic proteins Bax and Bak. As a consequence: MOMP takes place, cytochrome c is released and activates caspases via the apoptosome formation

highlightening the importance of mitochondrial outer membrane permeabilization (MOMP). On the other hand, GzmB directly cleaves ICAD, DNA-PK, tubulin, lamin B, NuMa and PARP-1 in the caspase-independent cell death pathway. Until now, MOMP has been considered the main event in GzmB mitochondrial-dependent apoptosis (Thomas, et al. 2001) (Han, et al. 2010). However, further investigation is required to understand the significance of ROS in GzmB-mediated apoptosis and the molecular mechanism by which this ROS production occures during apoptosis.

Therefore, the aim of my Thesis was to characterize the molecular mechanism by which GzmB, one the best characterized “malignant and pathogen-infected cell killer”, induces ROS and cell death. The first evidence supporting our project came from isolated mitochondria. Indeed, similarly to GzmA, GzmB induces a massive ROS production directly from isolated mitochondria which was unaffected by the addition of cyotosolic factors (S100). Cell loading experiments where tumor cells were treated with GzmB and PFN, showed a dose dependent increase in ROS production and cell death. Furthermore the use of ROS scavanger inhibated GzmB-induced cell death, whereas caspase inhibitors did not interfere with GzmB-induced cell death. Another crucial aspect in GzmB cell death pathway has been for long time attributed to the mitochondrial outer membrane permeabilization (MOMP). However, in order to dissect and consolidate our model, we took advantage from Bax and Bak double knockout MEF cells which do not undergo MOMP and consequently do not release cyotochrome c. Bax Bak deficient MEF treated with GzmB and PFN still experienced a potent ROS production and cell death althought to a lesser extent compared to WT MEF. To further investigate the molcular mechanism by which GzmB induces ROS and cell death we used a combination of proteomic and bioinformatic approach and identified NDUFV1, NDUFS2 and NDUFS1, three

NADH:ubiquinone oxidoreductase complex I subunits of 51, 49 and 75 kDa respectively, as three novel GzmB substrates. This indicates that complex I also plays a critical role in GzmB-induced cell death pathway. Furthermore, we showed that purified mitochondria treated with GzmB alone are unable to release apoptogenic factors from the mitochondria but still, GzmB can do its job and cleaves the mitochondrial complex I subunits. The apoptogenic factors release takes place only after adding cytosolyc factors (S100) which will potentiate GzmB killing by the caspase pathway. Furthermore, purified mitochondria treated with GzmB showed reducted complex I and III activity, loss of mitochondrial respiration, alteration of electron transport chain organization and loss of cristae junction. Therefore, we proposed that GzmB induces cell death in a ROS dependent manner. The clarification of ROS activity in the context of cytotoxic granule-mediated cell death will be crucial to further understand the mechanism of apoptosis. Moreover, the important role of mitochondrial complex I in many cell death pathways, further stress the mitochondria as a critical step for cell death. Complex I could be an important point of cross talk of these apoptotic pathways and therefore a potential key therapeutic target for intervention aimed either at increasing or reducing the susceptibility of CTL killing.

Chapter 2
INTRODUCTION

2.1 Cytotoxic Lymphocytes and Natural Killer Cells

Cytotoxic T Lymphocytes (CTLs) and natural killer (NK) cells are essential players in the cellular immune response against cancer and pathogen-infected cells (Figure 1). After recognition of their target cells, CTLs and NK cells induce cell death mainly through a molecular process where Granzymes (Gzms) and Perforin (PFN) are released from cytotoxic granules into the cytosol of target cells. Upon target cell recognition, the cytotoxic granules move into the immunological synapse (IS) where the killer and the target cell membrane fuse together, releasing cytotoxic contents by granule exocytosis (Law, et al. 2010) (Thiery, Keefe and Saffarian, et al. 2010) (Thiery, Keefe and Boulant, et al. 2011).

In mammals, cytotoxic T lymphocytes of the adaptive immunity, clonally express a T cell receptors (TCR) specific for antigens presented by the major histocompatibility complex molecules of class I (MHC). T cells express a large set of antigen receptors

resulting from genes rearrangement by somatic recombination. This large and diverse set of T cells, expressing one type of TCR, defines the T cell repertoire. The more diverse the repertoire, the more likely there will be a T lymphocyte able to recognize a specific antigen (Abbas and Lichtman 2003).

NK cells are considered killer lymphocytes of the innate immunity. They share with T lymphocytes different features such as granular morphology, some lymphoid markers and the progenitor cells-derived bone marrow origin. However, the loss of antigen specific surface receptors, allows the classification of NK cells as components of the innate immunity. Indeed, NK cells were named "natural cytolytic effector lymphocytes" because of their capacity to induce tumor and viruses-infected cells death without any immunization (Vivier, et al. 2011). In 1975, Kiessling et al., (Kiessling, Klein and Wigzell 1975) have discovered the NK capacity to produce inflammatory cytokines and to kill MHC class I negative target cells (Piontek, et al. 1985) (Lozzio and Lozzio 1975) (Kerr, Wyllie and Currie 1972). NK cells kill viruses infected or cancer cells lacking MHC class I mainly by two different classes of inhibitor receptors: killer immunoglobulin-like receptors (KIRs) and NKG2/CD94 receptors. Upon recognition of the infected cell, NK cell receptors deliver a negative signal in MHC^{+} cell preventing its destruction. On the other hand, cells with MHC low expression level will receive only a positive signal which will induce their death (Lanier 2008).

Taken together, "the stressed cells" such as chemical or physical-damaged cells, transformed and microbe or virus- infected cells can be all targets for Cytotoxic T Lymphocytes and Natural Killer cells. Lastly, CTLs and NK cells can also kill their target cells by the death receptor pathway (TNFR/TNF, Fas/FasL, TRAILR/TRAIL),

which rely on receptor-ligand interactions triggering a signal cascade that ultimately activates apoptosis inducing effector molecules, called caspases (cysteinyl, aspartate-specific proteases).

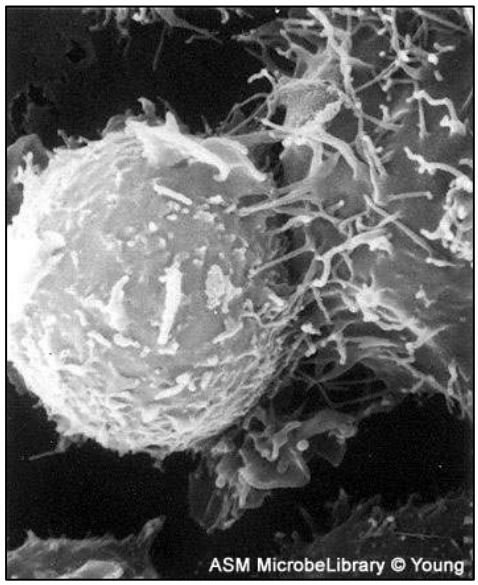

Figure 1: CTLs and NK cells kill cancer cells. Immunological synapse formation between CTLs or NK cells and target cells. Here, they probably fuse with the membrane and release the cytotoxic contents that trigger target cell death.

2.2 Apoptosis

In 1972 a common type of programmed cell death or “apoptosis” was described by Currie and colleagues (Kerr, Wyllie and Currie 1972). This molecular mechanism is a highly regulated process that plays critical roles in the development and tissue homeostasis of all the multicellular organisms (Prindull 1995). It is initiated by the interaction between tumor necrosis factor receptor family members (TNFR) and pro-apoptotic ligands (Itoh, et al. 1991). Many cells, produced in excess during the development, undergo programmed cell death in order to control tissues and organ homeostasis (Meier, Finch and Evan 2000). Apoptosis is called “fine tailoring of the organism” being implicated for instance in the elimination of the tadpoil tail in the

frog or during fetus development to remove finger interspace tissues. Apoptosis is also crucial to maintain T cells homeostasis: in fact, elimination of potentially harmful activated T cells, takes place by apoptosis through the death receptor pathway. (Kabelitz, Pohl and Pechhold 1993) (Brunner, Mogil and LaFace 1995) (Zhang, Su and Liu 1999). However, programmed cell death is also involved in the elimination of cells that represent a threat to the integrity of the organism. Indeed, dysregulation of apoptosis is implicated in cancer, autoimmune or neurodegenerative diseases and many other pathological conditions (Tompson 1995).

During apoptosis the cell starts to shrink (pyknosis), the plasma membrane blebs, the chromatin condenses and finally the DNA fragments (karryorhexis). Programmed cell death ends in distinctive features called “apoptotic bodies” that is pieces of membrane containing cytosol, fragmented DNA and organelles. Apoptotic bodies will be recognized by the macrophages and other surrounding cells (Figure 2). This recognition will facilitate the dying cells removal and consequently no inflammatory response of the surrounding area will be caused (Savill and Fadok 2000). The early genetic studies conducted on the nematode *Caenorhabditis elegans* identified apoptosis as the first mechanism through which many somatic cells are eliminated in worm organism maturation. Indeed, *C. elegans* studies have led to identify many genes such CED-3 (interleukin-1β-converting enzyme, caspases homolog), CED-4 (Apaf-1 homolog), CED-9 (Bcl-2 homolog), EGL-1 (BH3 family member homolog) encoding for protein that are the core molecular machinery of apoptosis. Furthermore, studies conducted in the fly *Drospohila melanogaster* have displayed analogy between the nematode CED-4 gene and its counterpart ARK gene in *Drosophila.* Beside some similarities, apoptosis cell death machinery in higher organism is much more complex but still, it relies on analogous genes found in *C. elegans*, suggesting

that apoptotic pathways in all three different animal phyla are quite conserved (Liu and Hengartner 1999).

Contrary to apoptosis, necrotic cell death is characterized by the traumatic loss of membrane integrity leading to swelling and finally cellular burst (Figure 3). As a consequence, by discharging their intracellular content into extracellular environment, necrotic cells induce a potent inflammatory immune response, which may result in the damaging of surrounding cells (Leist and Jaattela 2001). Therefore, necrosis has been defined as unprogrammed and uncontrolled cell death caused by different agents such as pathogens, toxins or trauma and based on morphological hallmark it has been easily distinguished from apoptosis.

In the last years a new version of programmed necrosis has been suggested. The term necroptosis has been coined to describe this special necrotic pathway involved in the early stage of development as well as in neurodegenerative disease and viral infection (Dunai, Bauer and Mihalik 2011). The same TNFR family, which activates apoptosis, is involved also in necroptosis. One of the key players of necroptosis is the receptor interacting protein 1 (RIP1); it is a serine/threonine kinase essential not only for necroptosis but also for NF-κB activation (nuclear factor kappa-light-chain-enhancer of activated B cells) and apoptosis (Holler, et al. 2000). Indeed, upon death stimuli TNFR1 activation gives rise to three different complexes: I, IIa and IIb. Complex I contains RIP1, TRADD (Tumor Necrosis Factor Receptor-1-Associated Death Domain), cIAP1 (cellular inhibitor of apoptosis protein-1) and TRAF2 (TNF receptor-associated factor 2). RIP1 ubiquitination by cIAP 1 leads to IKK (IκB kinase) complex formation and NF-κB pathway activation (Micheau and Tschopp 2003). RIP1 in association with caspases-8 and FADD (Fas-Associated via Death Domain) forms complex IIa which in turn activates caspases and induces apoptosis (Declercq,

Vanden Berghe and Vandenabeele 2009). Lastly, the association between RIP1 and RIP3 (Receptor-interacting serine-threonine kinase 3) induces complex IIb formation and necroptosis. Necrostatin 1 (Nec1), the specific RIP1 kinase activity inhibitor, prevents RIP1 and RIP3 recruitment to the complex, underlying the central role of RIP1 in necroptosis (Cho, et al. 2009). The downstream events are initiated by RIP homothypic interaction motif (RHIM) between RIP1 and RIP3 (Sun, et al. 2002). Necroptosis is highly regulated via genetic, epigenetic, and pharmacological elements and its mechanism needs more elucidations (Galluzzi and Kroemer 2008). It is mainly involved in pathological conditions such as viral infections, ischemia and neurodegenerative diseases (Dunai, Bauer and Mihalik 2011).

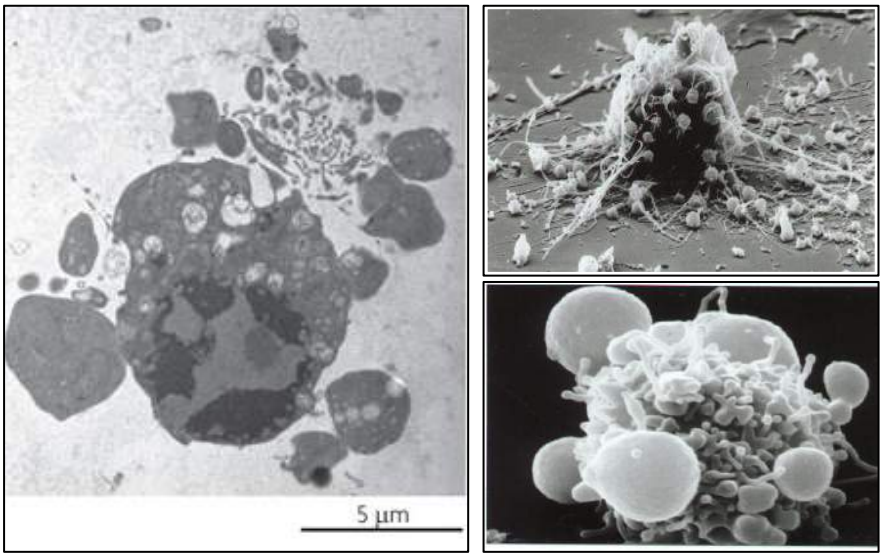

Figure 2: Morphological aspects of apoptosis. (Left) Electron microscopy shows apoptotic bodies, cell surface blebbing and rounding in apoptotic cell (Kroemer, *Nature Reviews* 2010). (Right) Scan electron microscopy showing cell surface blebbing and retraction in apoptotic cell (Malorni, Laboratory of Ultrastructures and Virology, Rome, Italy).

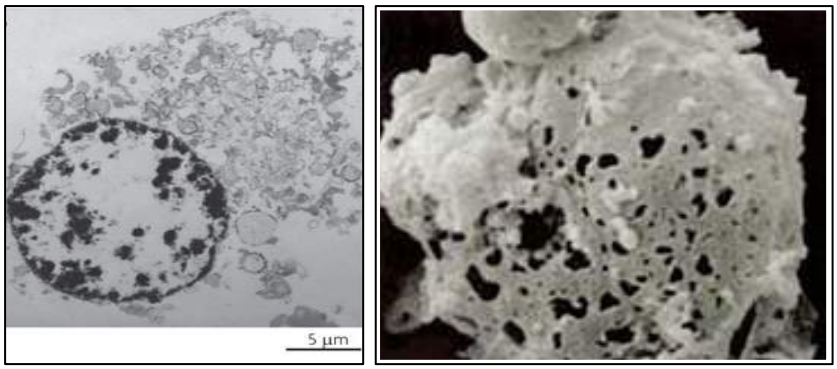

Figure 3: Morphological aspects of necrosis. (Left) Electron microscopy of necrotic cell shows clamps of chromatin and loss of membrane integrity (Kroemer, *Nature Reviews* 2010) (Right) Scan electron microscopy shows cell swelling and loss of membrane integrity in necrotic cell. 5000x magnification Reprinted from the Purdue CDROM Vol 4, Purdue University with permission.

2.2.1 Apoptotic extrinsic pathway

Elimination of malignant and pathogen-infected cells as well as physiological cell homeostasis is mediated by apoptosis. There are two major apoptotic pathways: the extrinsic or “death receptor pathway” and the intrinsic or “mitochondrial pathway”. The extrinsic pathway begins outside the cell by external signals, which activates cell surface receptors. The so called “death receptors” are all members of the tumor necrosis factor receptors family (TNFR), which are activated by pro-apoptotic ligands. Upon apoptotic stimuli, cytotoxic immune cells initiate cell death through FASL, APO2L/TRAIL or TNF are ligands of death receptors (Ashkenazi and Dixit 1998), (Nagata 1997).

The ligands specific recognition to the FAS/CD95/ApoI DR4/DR5 or TNFR1 receptors counterpart is due to a cysteine enriched extracellular domain, which allows the activation and trimerization of the death receptors on the target cell side (Naismith and Sprang 1998). The apoptotic signaling is then transduced through the death

domain (DD), a highly conserved region found into the cytoplasmic region of death receptors. The activated receptors will then recruit the DD domain containing-adaptor molecules such as FADD or TRADD. Together, with diverse initiator caspases-8 and -10, these molecules will constitute a bridge to form the death inducing signaling complex (DISC) in the target cell cytosol (Kischkel, et al. 1995).

Subsequently, procaspase-8 will be autocatalytically turned on and released as active caspase-8, ready to activate many effector caspases such as caspase-3, -6 and -7. The caspases are cysteine proteases homologous to *C. elegans* CED-3 gene (Bratton, et al. 2000) that notably cleave their substrates after aspartic acid residue. They are the degrading effector proteases activated in many cell death pathways. The effector caspases will cleave many other downstream proteins to dismantle the cell.

So far, more than 280 caspases substrates have been identified (Cryns, et al. 1997) (Kamada, et al. 1998). The caspase substrates are involved in many different cellular processes such as DNA repair, cell cycle, cytoplasm and nucleus scaffold, signal transduction and apoptosis. For example, caspase-3 cleaves ICAD, to induce DNA fragmentation. Additionally, acinus and helicard (DNA helicase) induce chromatin condensation. Another key apoptotic feature is membrane blebbing. Caspases-3 cleaves gelsolin and ROCK-1 kinase (Rho-associated coiled-coil containing protein kinase1) facilitating F-actin depolimerization and myosin light chain phosphorylation, respectively. As a result, the actin will contract in a myosin-depndent manner, the cytosol will be forced to move and the blebs will start to form where the cytoskeleton has been impaired (Fischer, Janicke and Schulze-Osthoff 2003).

Cells, such as thymocytes, capable to support directly initiatior caspases-mediated apoptotic pathway are called type I cells (Scaffidi, et al. 1998). On the contrary, type

II cells such as hepatocytes and pancreatic β-cells are unable to sustain a caspases signal strong enough to induce cell death. Indeed, after receptor activation, the efficiency of target cell killing is achieved by a second signal, which relies on the mitochondria (Figure 4). The discovery of these two cell types came from experiments where Bcl-2, an anti-apoptotic molecule that preserves the integrity of the mitochondrial membrane, was over expressed. While in some cells (type I) Bcl-2 over expression did not interfere with the extrinsic cell death pathway, in other cells (type II) the extrinsic pathway was affected. Indeed, stimulation with anti-FAS antibody leads to DISC enrichment in type I but not in type II cells. This suggests that type II cells rely mainly on the mitochondrial pathway to undergo apoptosis (Scaffaldi, et al. 1999).

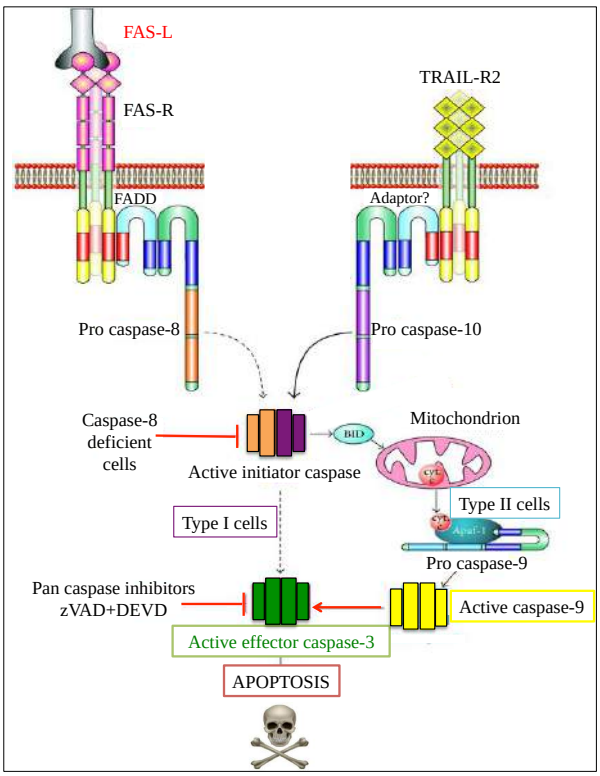

Figure 4: Apoptotic extrinsic pathway. Extrinsic cell death pathway relies on external signals which activate cell surface receptors. In cell type I the receptor, the adaptor molecule and the procaspase together form the DISC complex. Active caspases-8 lead to executioner caspase-3 activation and cell death. Type II cells, deficient in active caspase 8 in the DISC complex, relies on mitochondrial cell death pathway (Krug HF - J Toxicol, 2012).

2.2.2 Apoptotic intrinsic pathway

Intrinsic or mitochondrial apoptotic pathway is initiated from inside the cell following DNA damage, oxidative stress, nutrients deprivation as well as after chemotherapeutic drugs treatment (Wang 2001) (Kaufmann and Earnshaw 2000). These stimuli are able to induce changes in the mitochondrial outer membrane, in a very early step, leading to the mitochondrial outer membrane permeabilization (MOMP) and loss of transmembrane potential ($\Delta\psi$) to finally release pro-apoptotic proteins into the target cell cytosol (Ashkenazi, Holland and Eckhardt 2008) (Roy and Nicholson 2000) (Elmore 2007). The release of cytochrome c from mitochondria is one of the critical events in the intrinsic apoptotic pathway. After cytosolic release, cytochrome c binds to the Apaf-1 containing multiple WD-40 motifs in its C-terminus (Benedict, et al. 2000). This event will lead to the Apaf-1 oligomerization. In the presence of dATP and cytochrome c, Apaf-1 exposes its caspase recruitment domain (CARD) to engage and activate procaspase-9 in order to assemble the multimeric complex “apoptosome” (LI, et al. 1997), (Cain, et al. 1999), (Zou, et al. 1999), (Saleh, et al. 1999), (Rodriguez and Lazebnik 1999). Caspase-9 cleaves and activates the effector caspases-3 and -7, which will cleave many downstream proteins enhancing the cell suicide. Importantly, many other apoptogenic factors such as Smac (second mitochondria-derived activator of caspase)/DIABLO (direct inhibitor of apoptosis protein (IAP)-binding protein with low PI), Omi/HtrA2, will be released from the mitochondria (Cande, Cecconi and Kroemer 2002) (Saelens, Festjens, et al. 2004). It has been suggested that only after a massive mitochondrial devastation, that includes inner membrane rupture, other apoptogenic factors such as apoptosis-inducing factor (AIF) or endonuclease G (Endo G) will be released to further induce cell damage

(Arnoult, et al. 2003). Endo G and AIF translocate to the nucleus to induce DNA fragmentation and cell death (Figure 5) (Susin, et al. 1999b), (Li, Luo and Wang 2001). Furthermore, Smac/DIABLO and Omi/HtrA2s, both nuclear-encoded mitochondrial proteins, have been identified in mammals as two antagonist of the inhibitor of apoptosis (IAP) (Du, et al. 2000), (Verhagen, et al. 2000), (Hegde , et al. 2002), (Martins, et al. 2002), (van Loo, et al. 2002). Upon apoptotic stimuli, they translocate from the mitochondria to be released into the cytosol. Through their IAP-binding motif, Smac and HtrA2 bind to the BIR domains of IAPs, leading to the release and subsequent activation of the IAP-bound effector caspases to trigger caspase dependent cell death (Liu, et al. 2000) (Wu, et al. 2000) (Srinivasula, et al. 2001). Importantly, mitochondrial apoptosis can occur in a caspase independent manner. Indeed, HtrA2 can also activate cell death by using its serine protease activity (Suzuki, et al. 2001).

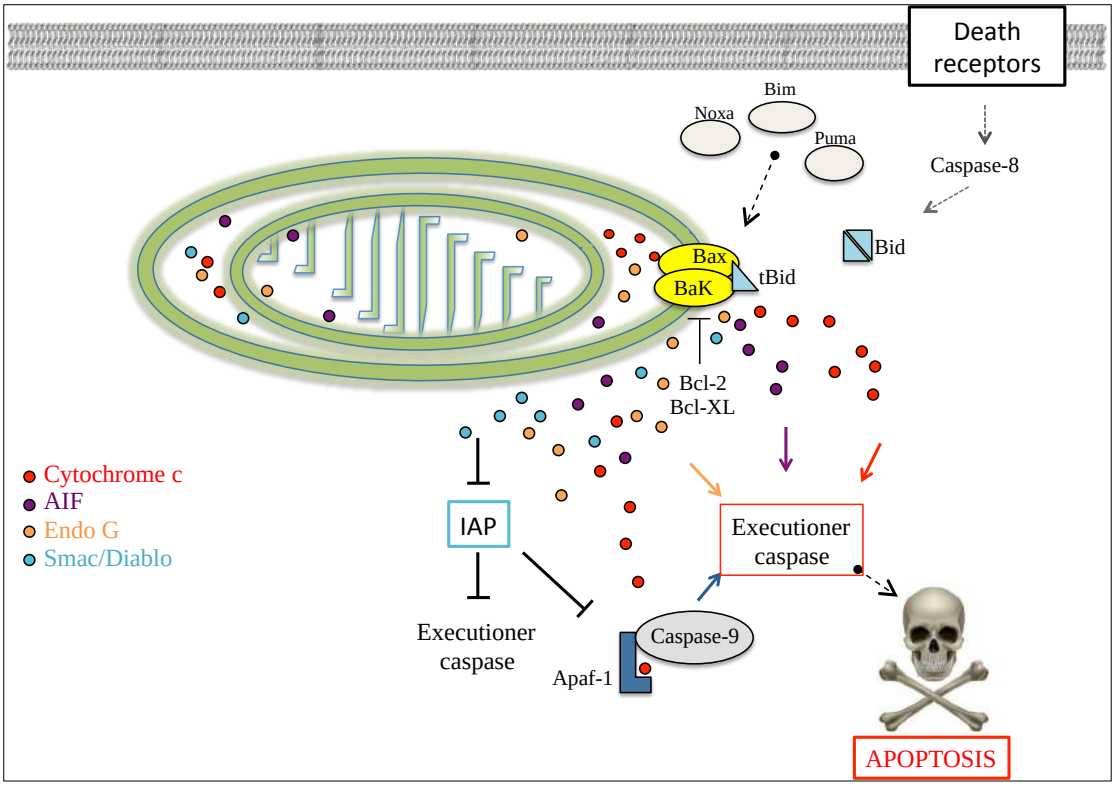

Figure 5: Apoptotic extrinsic pathway. Different stimuli will induce mitochondrial outer membrane permeabilization and loss of mitochondrial potential with consequent apoptogenic factor release into the cytosol. Cyotchrome c with Apaf-1 and caspase-9 form to the apoptosome. Active caspase 9 and the apoptogenic factor AIF, Endo G and Smac/Diablo contribute to the activation of the executioner caspase and apoptosis.

The key molecule used to connect the mitochondria and the cell death pathway is Bid, one member of the "BH3 domain only" belonging to the Bcl-2 family. Hepatocytes and pancreatic β-cells, which cannot commit suicide only by mean of the extrinsic pathway, will integrate the receptor pathway with the mitochondrial signals in order to induce cell death. In this case the death receptor-engagement induces caspase-8 dependent cleavage of Bid giving rise to truncated Bid (tBid). tBid will interact with the pro-apoptotic proteins Bax and Bak in order to initiate the mitochondrial pathway. The Bcl-2 family includes pro- and anti-apoptotic molecules (Figure 6). The induction of cell suicide mainly relies on the interaction between these two groups of molecules (Oltvai, Milliman and Korsmeyer 1993). It has been shown that the Bcl-2 proteins

contains up to four Bcl-2 homology domain named BH1, BH2, BH3 and BH4, all of them structured in α helix (Adams and Cory 1998), (Kelekar and Thompson 1998), (Reed 1998). In general, the anti-apoptotic proteins such as Bcl-2, Bcl-xL, Bcl-w, A1, and Mcl-1 share conserved BH domains. Bax, Bak, and Bok possess the domains BH1, BH2, and BH3 whereas Bid, Bim, Bik, Bad, Bmf, Hrk, Noxa, Puma, Blk, BNIP3, and Spike belong to the BH3-only proteins meaning that they only have a small BH3 domain (Cory and Adams 2002), (Mund, et al. 2003). The importance of Bcl-2 family in apoptosis is seen by their link between extrinsic and intrinsic pathway. BH3-only proteins following postranslational modifications (proteolysis, dephosphorylation) activate proapoptotic members Bax and Bak. This activation induces MOMP and the releasing of the apoptogenic factors, which in turn trigger or amplify the caspase cascade.

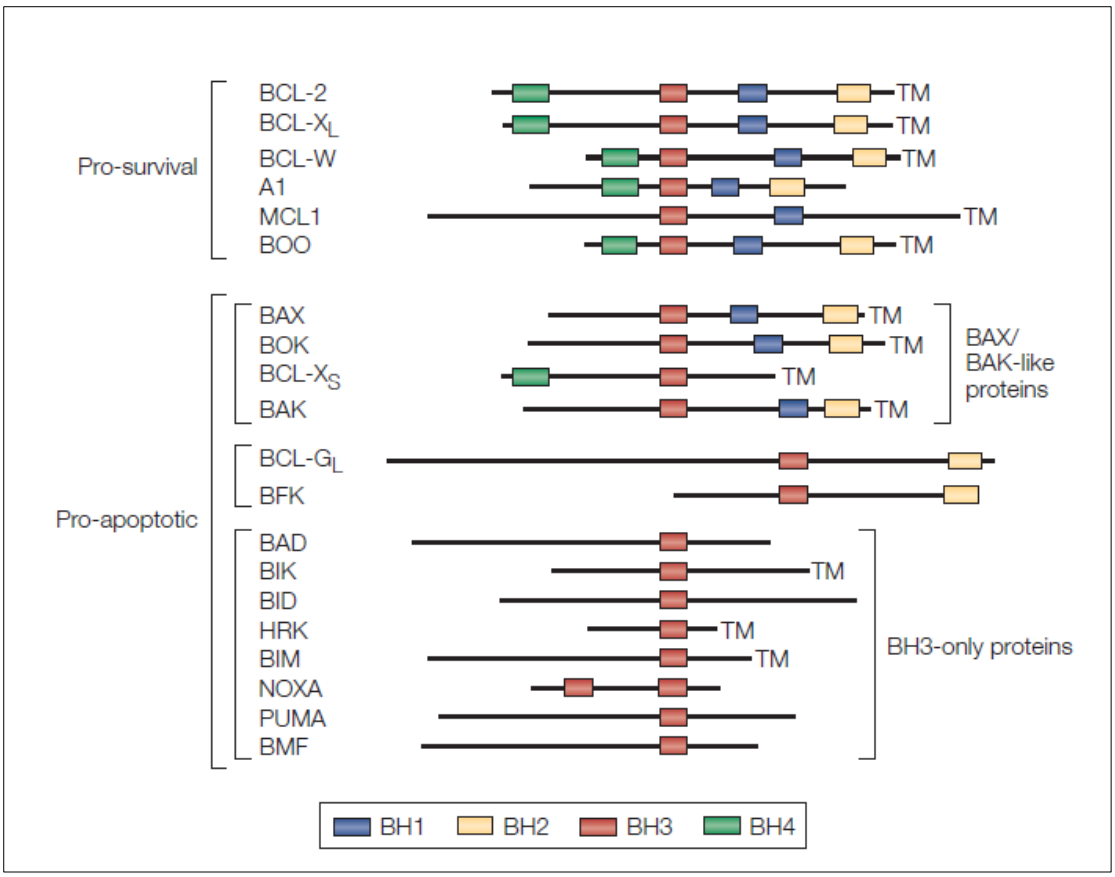

Figure 6: Bcl2 family members. Scheme of the mammalian Bcl2 family members shows anti and pro-apoptotic proteins with distinct BCL-2-homology (BH) domains. The pro-apoptotic proteins can be divided in BAX/BAK-like proteins and BH3-only proteins with short BH3 domain (Andreas Strasser 2005 Nature Review).

2.3 Cytotoxic Granules

Upon recognition and binding of malignant and virus- or bacterial-infected cells, CTLs and NK cells form an immunological synapse (IS) through which cytotoxic granule contents are released (Russell and Ley 2002). On the target cell side of the IS, PFN starts to multimerize forming small pores through which Ca^{++} can enter. This triggers a plasma membrane response, which results in the fusion of the endosome and the damaged plasma membrane. PFN and Gzms are internalized by dynamin/clathrin dependent endocytosis. Endosomes fuse together by rapid Rab5

dependent homotypic fusion to form a new structure called “gigantosome”. Meanwhile PFN continues to multimerize to form new and biggest pores that endosomalize the gigantosome to finally induce PFN and Gzms release into the cytosol of the target cells (Figure 7) (Thiery, Keefe and Boulant, et al. 2011).

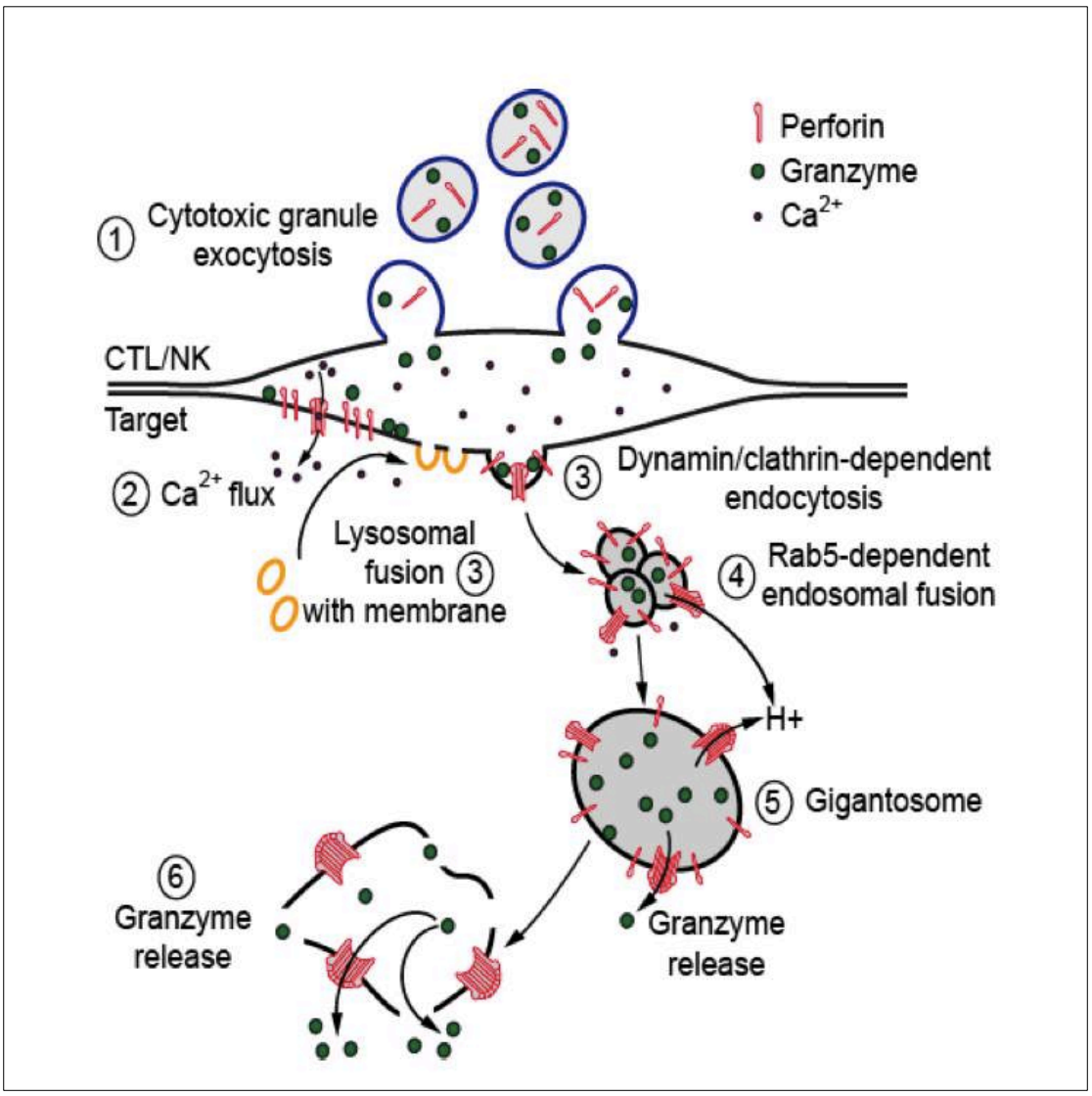

Figure 7: Release of cytotoxic granule contents into the target cell. (1) PFN and Gzms are released into the immunological synapse. (2) PFN multimerization leads to small pores formation and Ca^{++} entry into the target cell. (3) Lysosomes and the target cell damaged membrane fuse together leading to Gzms and PFN endocytosis in a dynamin and clathrin dependent manner. (4) Endosomes fuse together in Rab5 dependent manner forming gigantosome. (5) PFN multimerization leads to endosomal rupture of gigantosome and Gzms release into the target cell cytoplasm (Thiery, Keefe and Boulant, et al. 2011).

Electron microscopy images have shown two different cytotoxic granules area: the electron dense area containing all the machinery to kill the target cells and a peripheral cortical space enriched in lysosomal proteins (Figure 8). The electron dense area consists of granulysin (GNLY), PFN and its inhibitor calreticulin, serine proteases enzymes termed granzymes (Gzms) and serglycin (secretory granule proteoglycan core protein), whereas the peripheral cortical area mostly cathepsins. Granulysin is a protein that binds to lipids and belongs to the family of saposin-like proteins (SAPLIP) similarly to the bacterial defensines. GNLY, found exclusively in cytotoxic granules of humans and some other mammals but not mice, kills a wide range of bacteria including Gram-positive and Gram-negative, fungi parasites and tumor cells (Stenger, Hanson and Teitelbaum 1998). Calreticulin, a chaperone and Ca^{2+} binding protein, is able to bind to PFN, inhibiting its polymerization and activation inside the killer cells cytosol. Serglycin helps PFN and the Gzms in their packaging. Cytotoxic granules and lysosomes have many features in common. Indeed, the granules pH is acid like the lysosomal compartment and similarly to the early endosome, cytotoxic granules are enriched in the 270 kDa-receptor mannose-6-phosphate. Among all these molecules, Gzms and PFN are the crucial executioner of cell death (Smyth, et al. 2001), (Lieberman 2003).

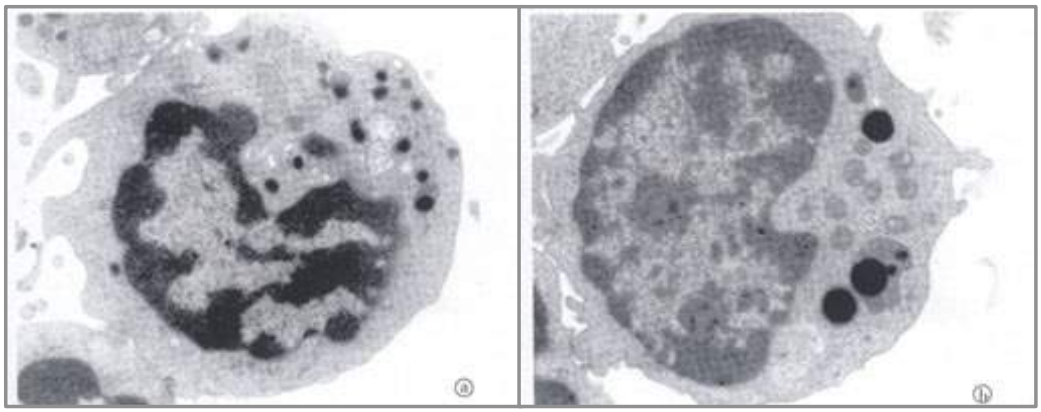

Figure 8: Cytotoxic granule area. NK cell Transmission Electron microscopy shows cytotoxic granules with the electron dense area and a peripheral cortical space enriched in lysosomal proteins (Luo DZ et al., 2000).

2.3.1 Perforin structure and mechanism

The pore forming protein perforin (PFN) is a 67 kDa protein involved in Gzms endocytosis into the cytosol of target cells in order to kill them. More than 50 PFN mutations are implicated in familial haemophagocytic lymphohistiocytosis disorder (type 2 FHL). Indeed, these mutations lead to an unbalanced immune response resulting in a hyper activation of T and B cells, NK cells and macrophages (Voskoboinik, Smyth and Trapani 2006). PFN is a complex and potentially harmful protein therefore it needs many checkpoints to be correctly stored in the cytotoxic granules before being released together with the Gzms to kill the target cell. PFN biosynthesis occurs in the endoplasmic reticulum where PFN binds to its inhibitor calreticulin. Through the trans-Golgi compartment, PFN is released into the cytotoxic granules where it is associated with Gzms and serglycin in an inactive form. The acidic granule compartment inhibits PFN bindind to the Ca^{2+} and also contributes to PFN stabilization. Upon release into the synaptic cleft, the neutral pH will favor PFN detachment from serglycin and its insertion into the target cell membrane, in a Ca^{2+}-

dependent manner. Killer cells must protect themselves from PFN lysis. The granule membrane, that leans the effector cell side of the synaptic cleft, has cathepsin B that may inactivates PFN back-clash avoiding its lethal hit on the killer cell (Balaji, et al. 2002). Another mechanism, which protects CTLs from their cytotoxic component, is due to the Gzms specific inhibitor serpin. Serpin acts by covalently and irreversibly binding to the Gzms active site. This binding will inactivate the Gzms when released accidentally inside the killer cells cytosol (Sun, et al. 1996). Recently, an elegant study on the PFN structure reveals the mechanistic mode of action of this protein (Law, et al. 2010). In fact, by using a model of murine monomeric PFN, Ruby et al., have characterized the PFN X-ray crystal structure and reconstituted the complete PFN pore by using cryo-electron microscopy (Figure 9 i). The molecular structure of PFN showed that, the amino-terminal region contains the MACPF/CDC domain (membrane attack complex perforin-like/cholesterol dependent cytolysins), a carboxyl-terminal sequence linked to an epidermal growth factor domain (EGF) and a C-terminal C2 domain implicated in PFN Ca^{2+}binding. These regions are most likely involved in the early step of PFN pore formation. Moreover, PFN and the components of the complement C8, C9 pore forming proteins, have a high sequence similarity suggesting a crucial role for MACPF pore forming protein fold in the mammalian immune system to finally destroy the target cell. According to these authors, PFN-MACPF domain is in an opposite orientation compared to the similar CDCs bacterial protein (Law, et al. 2010). This suggests a possible different mechanism of PFN membrane binding and pores forming, which need further elucidations (Figure 9 ii).

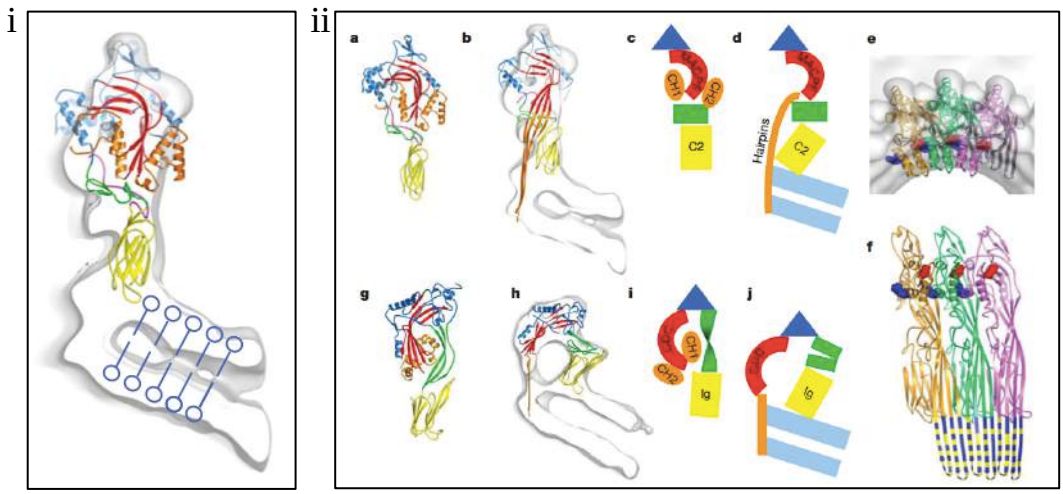

Figure 9: PFN pore structure. (i) PFN monomer obtained by its overlapped crystal structure. (ii) Pore structure in CDCs and PFN. The PFN-MACPF domain orientation (a-f) is in an opposite orientation compared to the similar CDCs bacterial protein (g-j). Blue: MACPF domain. Red: Central b-sheet. Orange: CH1, CH2. Green: EGF domain. Yellow: C2 domain (Ruby H. P. Law et al., Nature 2010).

To date, two different mechanisms have been conceptualized to explain how PFN and Gzms are released into the cytosol of the target cells. In the first model, PFN simply makes holes in the target cell plasma membrane inducing a passive Gzms diffusion into the target cells (Millard, et al. 1984). This model has been subjected to many critics. The initial PFN pores size (5-20 nm) might be unable to allow passage of big molecules as 30-50 kDa Gzms. However, at a later stage, bigger holes in the target cell plasma membrane were visible, maybe capable to release Gzms. This late larger pores could induce necrosis rather than apoptosis cell death challenging this model. Recently, more effort has been made to study this mechanism. The first evidence supporting a different model of Gzms uptake was the observation of GzmB entry into target cells even in PFN absence. However, only after PFN addition, GzmB could induce apoptosis, suggesting that PFN releases Gzms from another compartment inside the cell, most likely the endosome (Froelich, et al. 1996). Another piece of evidence came from streptolysin O, a bacterial pore forming protein, that enables to

break the endosomal membrane and therefore inducing Gzms release independently of PFN (Pinkoski, et al. 1998). Moreover, at physiological and sublytic dose of PFN (10% necrotic cells induced), small pores and transient Ca^{2+} influx into the target cell membrane occurs. The damaged plasma membrane on the target cell side is repaired through the coupled endocytosis and exocytosis of vesicles and lysosomes, in a Ca^{2+} dependent manner (Reddy, Caler and Andrews 2001), (McNeil and Steinhardt 2003), (Keefe, et al. 2005). Supporting this latter model, target cells treated with PFN and Gzms undergo endocytosis in a clathrin and dynamin dependent manner leading to the formation of gigantosomes containing PFN and Gzms and positive for the early endosomal antigen (EEA1) (Keefe, et al. 2005) (Thiery, Keefe and Saffarian, et al. 2010). In a recent paper, Dr. Thiery J. and collaborators, have shown that firstly PFN creates membrane pores to facilitate Gzms endocytosis, and then the endosomolytic action of PFN solubilize the gigantosome containing Gzms, leading to their release into the target cell cytosol (Figure 10). In particular, they have observed that after PFN addition, Gzms were detectable in the early endosome up to 15 minutes later before it was released into the cytosol of the target cell, confirming that PFN pores formation cannot be the only mechanism involved in Gzms release. Furthermore, by different PFN staining they suggested that PFN multimerization occurs in the gigantosome concurrently with Gzms release, supporting their two-step model. Again, further elucidations are necessary to clarify how PFN works in vivo (Thiery, Keefe and Boulant, et al. 2011).

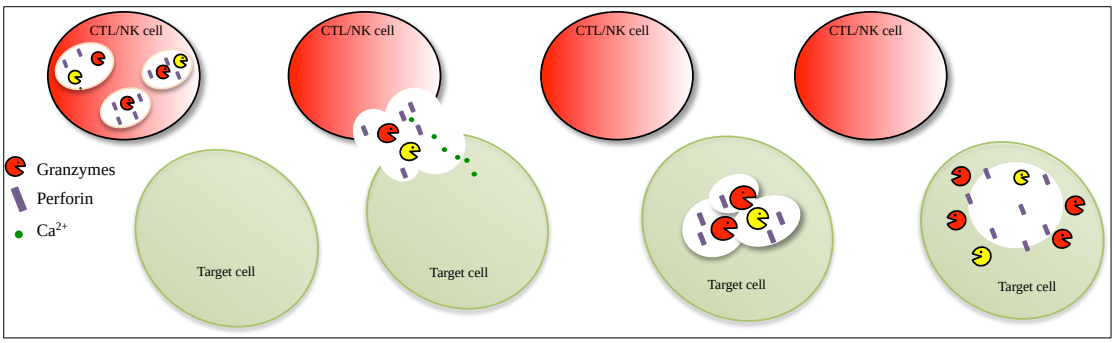

Figure 10: Scheme of Granzymes release into the target cell. Upon recognition CTLs or NK cells release the cyototoxic granules stored molecules Gzms and PFN into the immunological synapse. PFN makes hole to facilitate Gzms entry into the target cell. Granzymes and PFN are endocytosed into the target cell forming a gigantosome. The endosomalytic action of PFN solubilize the gigantosome releasing Gzms into the target cell cytosol.

2.3.2 Human Granzymes vs Mice Gramzymes

Among all the Granzymes, GzmA and GzmB are the best characterized. 5 human and 10 mice Gzms have been identified. The expression of these different Gzms originates from three different clusters (Figure 11).

Human chromosome 5 and mouse chromosome 13 carry the genes encoding for GzmA and GzmK. Chromosome 14 carries human GzmB, GzmH and the mouse homologous GzmB and GzmC, whereas human chromosome 19 and mouse chromosome 10 carry GzmM gene. In mice, GzmB encoding region was duplicated, yielding GzmD, GzmE, GzmF, GzmG, GzmL and GzmN genes. Even though their role is not fully understood, it is possible that they are important to destroy natural mice microorganisms.

Human GzmA is a homodimer protease with a MW of 50 kDa. It belongs to the family of the tryptase since it preferentially cleaves after Arginine or Lysine residues. Human GzmA substrates were identified such as lamins, histones, Ku70 as well as

proteins of the SET complex, Ape1 and HMGB2 (Chowdhury and Lieberman 2008). After GzmA and PFN treatment, target cells display mitochondrial damage. GzmA cleaves the mitochondrial complex I subunit NDUFS3 triggering ROS production and loss of $\Delta\Psi_m$, in a caspase-independent manner. Furthermore, ROS production cause the SET complex translocation into the nucelus in order to induce DNA single strand damage and finally cell death (Martinvalet, et al. 2008).

Human GzmH and its mouse homologous GzmC share a chymase activity. They cleave after phenylalanine and aromatic aminoacids. They induce apoptotic cell death pathway in a caspase-independent manner (Fellows, et al. 2007), (Johnoson, et al. 2003). ROS are generated, mitochondrial transmembrane potential is dissipated and single strand DNA break is occurring. It has been shown that GzmH cleaves the adenovirus DNA-binding protein DBP (also a GzmB substrates) and ADV 100k proteins (inhibitor of GzmB) suggesting an involvement in anti-adenoviral immune defense. GzmK similarly to GzmA cleaves arginine and lysine residues but it is a monomer unlike human GzmA. GzmK seems to activate the same caspase independent GzmA-cell death pathway associated with increase in ROS generation, loss of $\Delta\Psi$m but no cytochrome c release. It also induces SET complex nuclear translocation and activation leading to single strand DNA damage (Zhao, et al. 2007). Recently, it has been shown that GzmK induces mitochondrial damage by cleaving Bid and by inducing MOMP. Further investigations are needed to understand whether GzmK triggers cell death pathways similar to GzmA or more like GzmB.

Finally GzmM is the only, among the other Gzms, that cuts after Met or Leu residues. To date, its role in cell death induction is controversial. Kelly et al., have proposed that GzmM induces a caspase independent cell death pathway without any mitochondrial features involvement (Kelly, et al. 2004). On the other hand, Fan et al.,

have shown that GzmM induces a caspase dependent apoptotis with similar characteristic to that induced by GzmB (Lu, et al. 2006). Again, extra research needs to be done to verify the contribution of GzmM in cell death pathway (Chowdhury and Lieberman 2008).

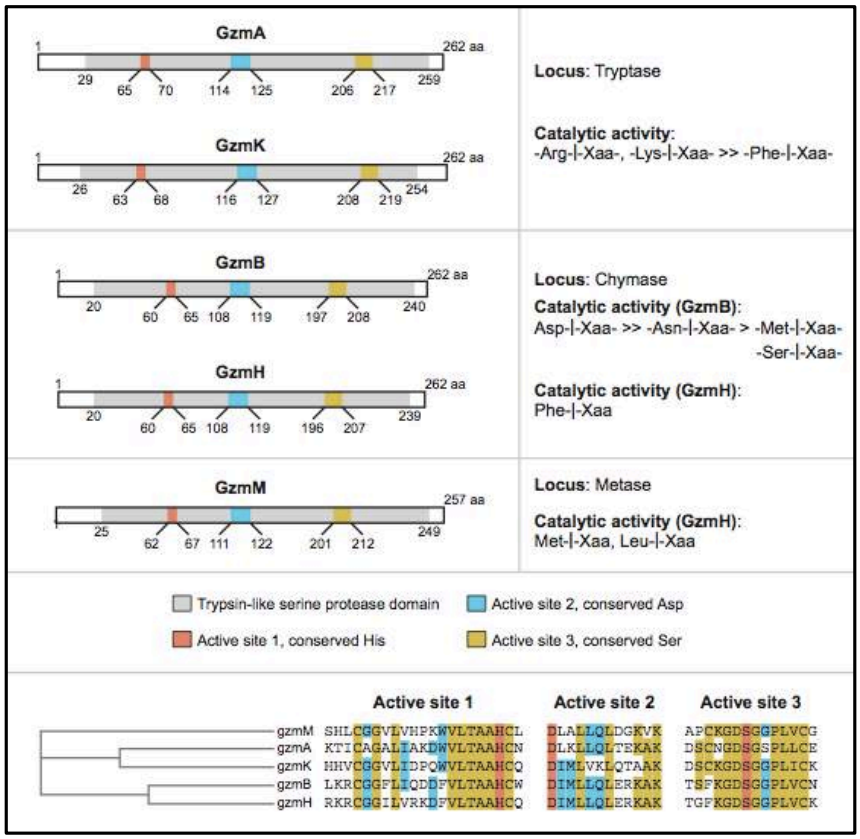

Figure 11: Human vs mouse Granzymes. Human and mouse Gzms originate from 3 different clusters. Gzm A and GzmK are encoded on chromosome 5 (13 mouse), GzmB and GzmH on chromosome 14 (GzmB and GzmC 14 mouse) and GzmM on chromosome 19 (10 mouse) (D. Chowdhury and J. Lieberman, 2008).

2.3.3 Granzyme B cell death pathway

Granzyme B (GzmB) belongs to the family of the serine proteases, mainly located in the cytotoxic granules of cytotoxic T lymphocytes (CTL) and natural killer (NK) cells. GzmB, together with the pore forming protein perforin (PFN), is released into

the immunological synapse localized between effector cells and target cell. Later on, PFN triggers GzmB delivery into the cytosol of the target cell to induce apoptosis (Figure 7 and 10) (Trapani, et al. 2000), (Lord, et al. 2003), (Thiery, Keefe and Boulant, et al. 2011).

The human GzmB gene (GZMB) was mapped on chromosome 14q11.2 referred as chymase locus (Salvesen, et al. 1987) (Klein, et al. 1989). GZMB gene is made of five exons and four introns, which cover 3.2 kb in length (Haddad, et al. 1990). GZMB promoter includes binding sites for many transcriptor factors such as Ikaros, NFAT (nuclear factor of activated T cells) and activator protein-1 (AP-1) (Wargnier, et al. 1995). A distal region contains NF-κB binding sites involved in GzmB transcription in NK cells (Huang, et al. 2006). GzmB is mainly express in CTLs and NK cells. However recent findings show that GzmB is also expressed in chondrocytes, keratinocytes, Sertoli cells, just to mention a few, as well as in certain cancer cell types (Rousalova and Krepela 2010).

GzmB directly cleaves the pro-apoptotic protein Bid to activate the mitochondrial cell death pathway. GzmB-induced Bid truncation favors Bax and Bak polymerization, activates MOMP and cytochrome c release. These events, followed by the apoptosome formation, will induce the caspases amplification loop. It is worth noting that, so far, human and mouse GzmB have been used indiscriminately in different experimental approaches generating controversial results. Human and mouse GzmB share many of the caspase substrates such as tubulin, lamin B, PARP-1, NuMa, DNA-PKs and can cleave other substrates similarly to caspase-6, -8 and -9. Human GzmB is able to recognize and cleave after the aspartic acid residue contained in the tetrapetide motif IEPD while, mouse GzmB specifically cleaves after IEFD. However, human and mouse GzmB display significant sequence variations, that contribute to

the different substrates specificity, and ultimately to disparate cell death phenotype. Indeed, human GzmB efficiently cleaves human or mouse Bid and ICAD to induce mitochondrial cell death pathway or DNA damage cell death, respectively. This is not the case for mouse GzmB suggesting that mouse GzmB-induced cell death is less dependent on the Bid pathway (Casciola-Rosen, et al. 2007). Furthermore, DNA fragmentation and cell death induced by human GzmB are poorly restricted in presence of caspase inhibitors. Differently, mouse GzmB-cell death pathway is strongly inhibited by the identical inhibitors (Pardo, et al. 2008). Dissipation of the transmembrane potential ($\Delta\psi m$), mitochondrial outer membrane permeabilization (MOMP), ROS propagation and pro-apoptotic proteins release from the mitochondria, are all hallmarks of GzmB mitochondrial pathway.

GzmB is a unique serine protease, which, similarly to caspase, cleaves after aspartic acid residues. Among other substrates, GzmB directly cleaves and activates the key executioner caspase-3 triggering caspase-dependent apoptosis. However, GzmB initiates also cell death in a caspase independent manner.

GzmB specifically interacts with downstream substrates such as ICAD, DNA-PK, tubulin, lamin B, NuMa and PARP-1 to induce caspase-independent cell death. Much emphasis has been put on the MOMP, leaving unclear whether ROS is critical for GzmB mediated apoptosis. We found that in contrary to the common view of ROS as bystander, ROS production in GzmB cell death pathway is an important step that in synergy with MOMP enhances cell death (Figure 12).

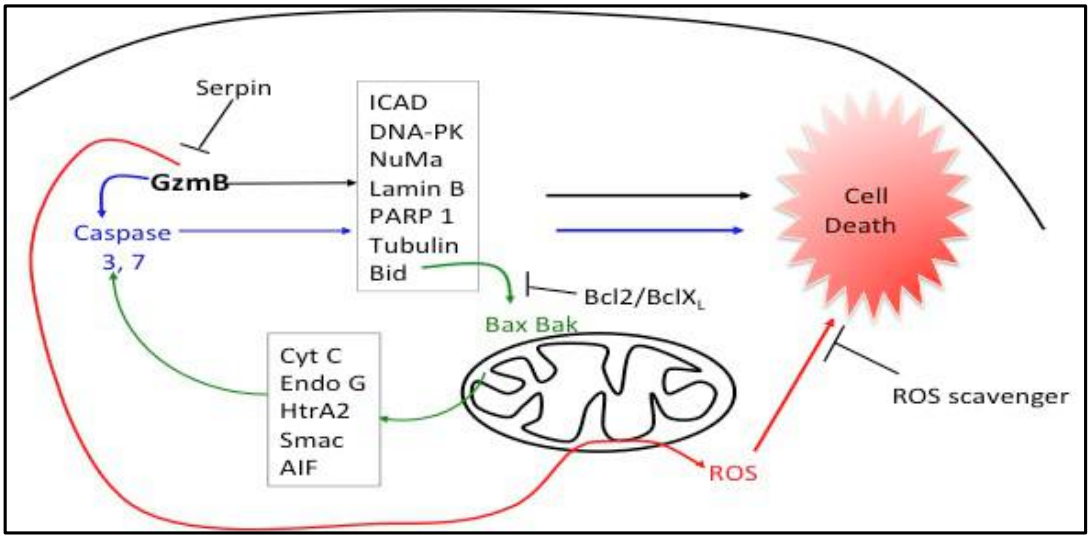

Figure 12: Granzyme B cell death pathways. GzmB directly activates effector caspase -3 and -7 resulting cell death. GzmB induces cell death independently of the caspases (cleaves many of the known caspase substrates). GzmB induces mitochondrial damage independently of the caspases (directly cleavage of Bid) resulting in MOMP. GzmB also acts on the mitochondria in a not well characterized pathway independently of cytosolic factors to induce ROS and cell death.

2.4 Mitochondria

Mitochondria are the most important determinants in the balance between death and life. For long, the main mitochondrial function has been attributed to its capacity to supply energy to the cell in the form of ATP. However it is now recognized that mitochondria contribute critically to many different physiologically processes such as cellular differentiation, calcium signalling, cell cycle control, ER-mitochondria tethering and cell death (McBride, Neuspiel and Wasiak 2006). All these events are triggered directly by mitochondria and mitochondrial-derived molecules. Indeed, when mitochondrial functions are altered, a wide spectrum of diseases are triggered, such as the neurodegenerative diseases Parkinson, Alzheimer and amyotrophic lateral sclerosis (Krieger and Duchen 2002), (Schon and Manfredi 2003) as well as diabetes,

cardiomyophathy (Zhang, Mott, et al. 2003), sepsis (Cairns 2001) and many age-related disease (Hekimi and Guarante 2003). Interestingly, a pivotal role of mitochondria in apoptosis induction has emerged. Up to date, many researchers have pointed out the role of mitochondrial outer membrane permeabilization (MOMP) as a principal mechanism involved in mitochondria-induced cell death pathway (see previous section) (Martinou and Green 2001). Our findings unequivocally consolidate the central position of mitochondria as a key players in the GzmB cell death pathway.

2.4.1 Origin and Function

After the discovery of mitochondria at the end of the 1800s, many scientists have observed a tight correlation between these organelles and bacteria. L. Margulis asserted that mitochondria originate from bacteria that fused with early eukaryotic cells in a symbiotic cooperation (Margulis 1970). The peculiar characteristic of the mitochondrial DNA (mtDNA) provides an additional support to this theory. In fact, mtDNA lacks introns and is a circular double stranded plasmid of approximatively 16.5 kb, that closely resembles the bacterial DNA. Moreover, mitochondria divide and replicate in a proper way that is autonomous and separated from the nuclear division (Kiefel, Gilson and Beech 2004). Finally, the shape, size and double membranes are all togerther characteristics which corroborate the endosymbiontic theory. About 99% of proteins building mitochondria are encoded in the nuclear genome. The messengers from those genes are translated in the cytoplasm and the resulting mitochondrial preproteins are then imported into the organelles through special target sequence (Calvo, et al. 2006). mtDNA encodes only for 13 subunits of the electron transport chain associated with oxydative phosphorylation (OXPHOS)

and electron flux, 2 rRNAs genes (16S and 12S rRNAs), as well as the 22 tRNAs implicated in the translation of proteins encoded in the mtDNA. Mitochondria play a central role in the generation of almost all the energy required by our body produced by oxidative phosphorylation along the respiratory chain. Mitochondrion performs functions in the cellular metabolic processes through many biochemical processes such as pyruvic acid and lipid oxidation, tricarboxylic acid cycle, electron flow, OXPHOS and apoptosis (Wallace 2005).

2.4.2 Structure and cristae remodelling

In the middle of the 1900s with the development of electron microscopy (EM) technique, Sjöstrand and Palade started to look at the ultrastructure of the cells giving rise to a new mitochondrial picture. Indeed, mitochondria had the appearance of double membrane organelle: the mitochondrial outer membrane (OMM) and the inner membrane (IMM) which delimited the intermembrane space (IMS). Another soluble and electondense area called the matrix was observed inside the mitochondria. The IMM-associated long invaginations were called cristae (Palade 1952). The mitochondrial membrane shape was coupled to the different mitochondrial metabolic phase. Indeed, Hackenbrock showed that changes in osmosis or metabolytes resulted in the detachment of the IMM from the OMM. However, the matrix turned into a condensed conformation and the IMM and the OMM fused only in few and specific “contact sites” (Hackenbrock 1966). In situ, the mitochondrial matrix becames bigger, IMS shortened and the space between cristae and OMM decreased in an orthodox conformation. Only in 2001, by the combination of EM tomography and 3D reconstruction, cristae were recognized as a different and unique structures inside the

mitochondria, appearing more like little pockets (28 nm in diameter) connected to IMS (Perkins, et al. 2001). Accordingly with Hackenbrock, is now accepted that cristae numbers and morpholgy affects the diffusion of ions and compounds involved in oxidative phosphorylation generating different ATP production according to different conditions (Perotti, Anderson and Swift 1983), (D'Herde, et al. 2001). Furthermore, the involvement of cristae morphology has been associated with the distribution of cytochrome c in the intermembrane and intracristal space (Bernardi and Azzone 1981), (Scorrano, et al. 2002). Consequenctly, the mitochondrial critae morphology is now recognized as a critical determinant for cell death. Indeed, concomitantly to MOMP, tBid triggers cristae junction opening by destabilizing OPA 1 (optic atrophy 1) oligomers, resulting in extensisve cytochrome c release and cell death. Moreover, since mitochondrial cristae also house the respiratory chain complexes, proper cristae morphology is critical for the maintenance of optimal respiratory chain orgainzation and function (Cogliati, et al. 2013).

Mitochondria continually undergo changes in shape; their morphology moves from little spheres shape to elongated and interconnected tubules (Bereiter-Hahn and Voth 1994). This dynamic morphology, results from a tightly regulated balence between fusion and fission events (Figure 13). In mammals, mitochondrial fission relies on a GTPase dynamin related protein, termed DRP1 (Dnm1 in yeast). Another mitochondrial outer membrane protein FIS 1 (mitochondral fission 1 protein), is thought to recrute DRP1 in order to emphasize structural changes during mitochondrial fission. Indeed, it has been shown that DRP1 and FIS1 physically interact *in vitro* (Yoon, et al. 2003) but wether this interaction is necessary to induce mitochondrial fragmentation, is still controversial. However, to induce fission, DRP1 is phosphorylated at Serine 616 by Cdk1 and dephosphorylated at Serine 637 by the

Ca^{2+}-dependent phosphatase calcineurin (Chang and Blackstone 2007), (Jahani-Asl and Slack 2007), (Taguchi, et al. 2007). These two events result in DRP1 activation. Upon activation DRP1 translocates to the organelle to induce fission (Cereghetti, et al. 2008). On the other hand, MFN1 (mitofusin 1) and MFN2 (mitofusin 2) and their coiled coil domain are implicated in mitochondrial fusion (Koshiba, et al. 2004). Mitofusins are two GTPases related proteins founded in the mitochondrial outer membrane and therefore contribute to the mitochondrial outer membrane fusion while OPA-1 mediates the fusion of the mitochondrial inner membrane (Chen, et al. 2003).

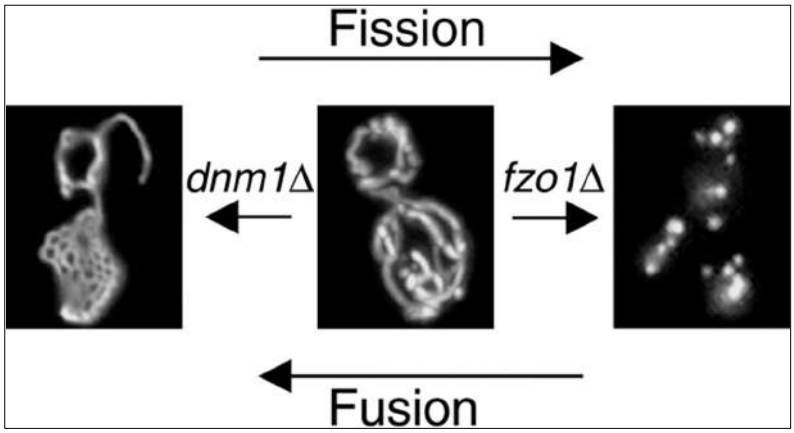

Figure 13: Mitochondrial fusion and fission. Physiological tubular mitochondrial network in WT yeast cells (middle). Fused mitochondria are observed in Dnm1p GTPase $^{-/-}$ cells (left); fragmented mitochondria are observed in Fzo1p GTPase $^{-/-}$ cells (fzo1Δ) (right). Mozdy A et al., J Cell Biol 2000.

2.4.3 Tim Tom Complex

99% of the mitochondrial proteins are encoded in the nuclear genome. This vast majority of proteins translated in the cytosol reach the mitochondria by means of their pre-sequences or targeting signals. To date, two different mitochondrial import signals have been distinguished: cleavable pre-sequence, which are preferentially conducted to the matrix, mitochondrial inner membrane and intermembrane space,

and internal sequence directed to the outer and inner mitochondrial membrane. The first external barrier to be crossed is the mitochondrial outer membrane; it contains the receptor TOM 70, 20 and 22, which, together with the pore forming channel TOM 40 (Abe, et al. 2000), (Becker, et al. 2005), represent the translocase of the outer membrane (TOM) complex. Subsequently, proteins continue their route across the inter membrane space by using the translocase of the inner membrane (TIM) complex and its channel Tim 23. The second class of mitochondrial-directed proteins contains an internal signal sequence, which allows them to be directed to the mitochondrial inner membrane as it is the case for the ATP/ADP carrier proteins. Carrier proteins first interact with the receptor TOM 70, with the channel TOM 40 (Wiedemann, et al. 2003) and finally with TIM 22 complex which will favor their insertion into the inner membrane. Recently, the mitochondrial intermembrane space import has been also characterized. Indeed, precursor proteins directed to the intermembrane space first interact with the TOM complex and then with the MIA 40 complex (Chacinska, et al. 2004) (Figure 14).

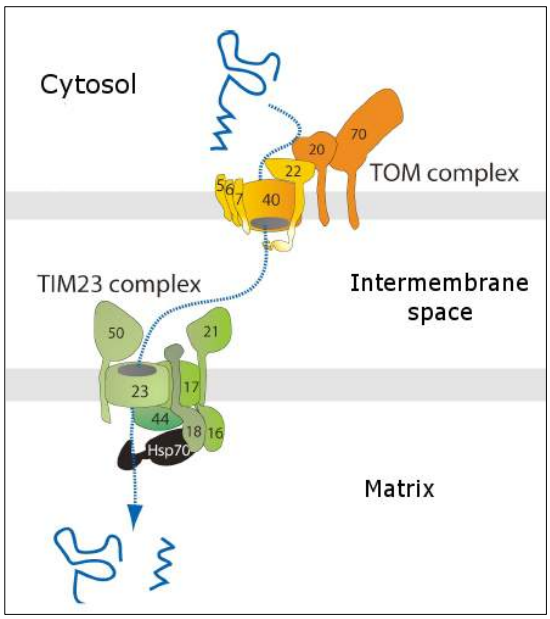

Figure 14: TIM TOM complex. Mitochondrial protein are imported into the mitochondrial by using a complex machine. Translocase outer membrane (TOM) brings mitochondrial protein from the cytosol to the mitochondrial intermembrane space and Transolcase inner membrane (TIM) brings them to the matrix. http://www.lucasbrouwers.nl/blog/2010/02/evolving-molecular-machines/.

2.4.4 Mitochondrial Respiratory Chain (OXPHOS complexes)

The first step in the energy production takes place in the cytoplasm during glycolysis and responds for only 5% of the cellular energy demand. The most important energy source is the mitochondrial electron transport chain (ETC). It consists of four electron carriers complexes which favor the transition of high energy electrons from NADH or $FADH_2$ to the final acceptor Oxygen (O_2) coupling electron transport with energy transfer and storage in the final form of ATP. The respiratory chain complexes are organized in order to transfer the electrons from the higher oxidative state complex to the lower, avoiding energy dispersion. Indeed, electrons from NADH are delivered to CoQ by Complex I activity (NADH dehydrogenase). Electrons are also transferred directly from succinate to CoQ, by Complex II (succinate dehydrogenase). Then, electrons flow from the reduced CoQ to cytochrome c *via* Complex III (ubiquinone-

cytochrome *c* reductase). Complex IV (cytochrome *c* oxidase) transfers electrons from cytochrome c to the final acceptor oxygen. The free energy derived from the electron flow along the respiratory chain is stored as a proton gradient in the intermembrane space that is used by the ATP synthase to produce ATP from ADP and Pi (Figure 15).

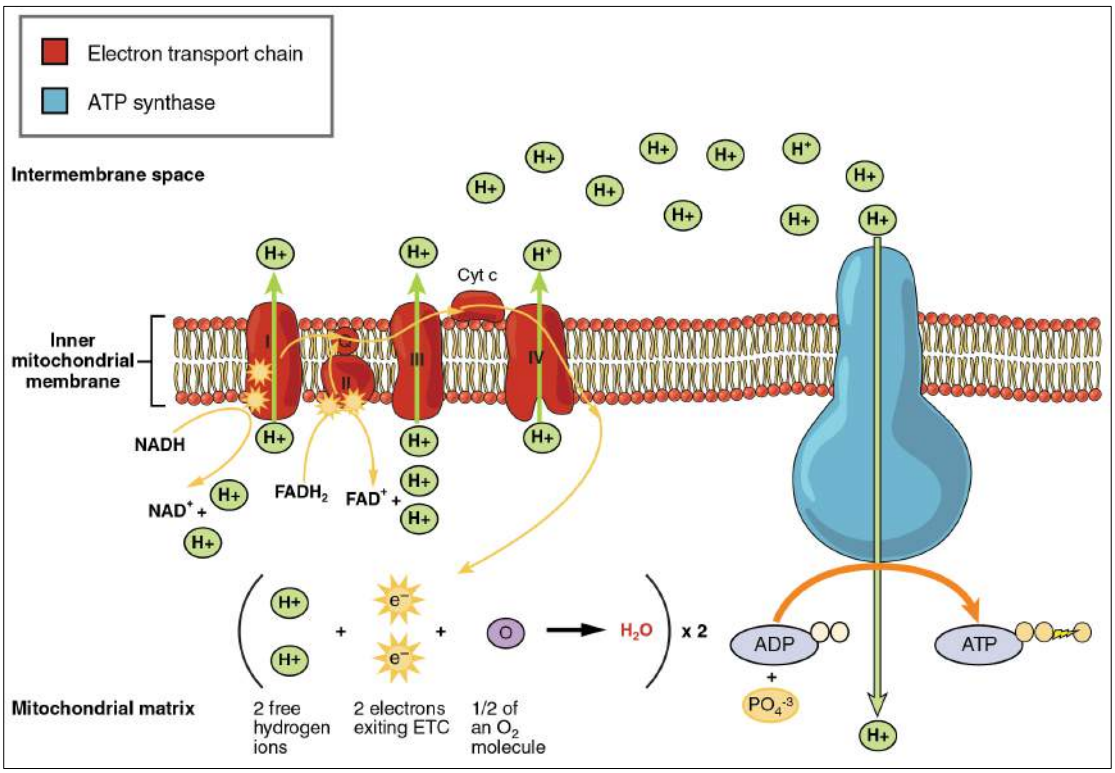

Figure 15: OXPHOS complexes. Electron transport chain consists of four electron carriers who favor the transition of the electrons to the final acceptor oxygen. It is coupled to pump H^+ out of the mitochondrial matrix and generate ATP (Physiology text book).

2.4.5 Mitochondrial Complex I: biogenesis and function

NADH:Ubiquinone oxidoreductase complex I is a 1 MDa complex, made of 45 subunits, 7 of which encoded in the mtDNA (hydrophobic subunits ND1-ND6 and ND4L). The complexity of this large holoenzyme and its primary role in the electron transfer in mitochondria and plasma membrane of various bacteria, has led many

researchers to focus on the identification of its assembly and 3D structure. Bacterial complex I, which contains 14 essential subunits sufficient for its function, has been used as model to understand mitochondrial complex I biogenesis. Based on these structural studies, complex I has been depicted as L-shaped in which the hydrophilic peripheral arm and the hydrophobic inner membrane embedded arm of 200 Å each, are connected in a tight point (Sazanov, et al. 2000). The bacterial homologous and essential subunits have been divided in three different modules, N, P and Q each of them with a different role. Complex I is considered the entry gate for the electron transport chain. The N module or "electron input module" consists of 3 subunits, NDUFV1, NDUFV2 and NDUFS1. The 51 kDa subunit NDUFV1 accepts electron from NADH. The electrons, then flow through the NDUFV1 bound FMN prostetic group to reach its iron-sulfur cluster N3. The electrons will move to other iron-sulfur clusters N4 and N5 in the 75 kDa NDUFS1 subunit. The Q module or "electron output module" is made of four nuclear DNA (nDNA) encoded subunits (NDUFS2, NDUFS3, NDUFS7 and NDUFS8), which accept electrons from the N module to pass through other iron-sulfur clusters N6a and N2 which finally releases them to the ubiquinone. The P module, which represents the embedded mitochondrial arm, is the site where the protons are translocated into the intermembrane space. It consists of seven mtDNA-encoded subunits. The remaining thirty nDNA-encoded subunits called "supernumerary" might have a role in the assembly and stability of complex I (Brandt 2006). The 45 subunits of mitochondrial complex I together with its dual genetic origin make complex I assembly a complex and poorly understood process. Taking advantage of BN-page, which preserve the associated complexes in their native conformation and based on patients with complex I deficiency (either in mtDNA or nDNA encoded subunits), it was shown that human complex I assembly relies on a

larger number of intermediates modules which fit together in a highly coordinated manner (Figure 16). Importantly, many diseases such as lethal infantile mitochondrial disease, myopathy or neurodegenerative disorder in adults, have been involved in mutations in genes encoding both nuclear and mitochondrial complex I subunits (Kirby, et al. 1999).

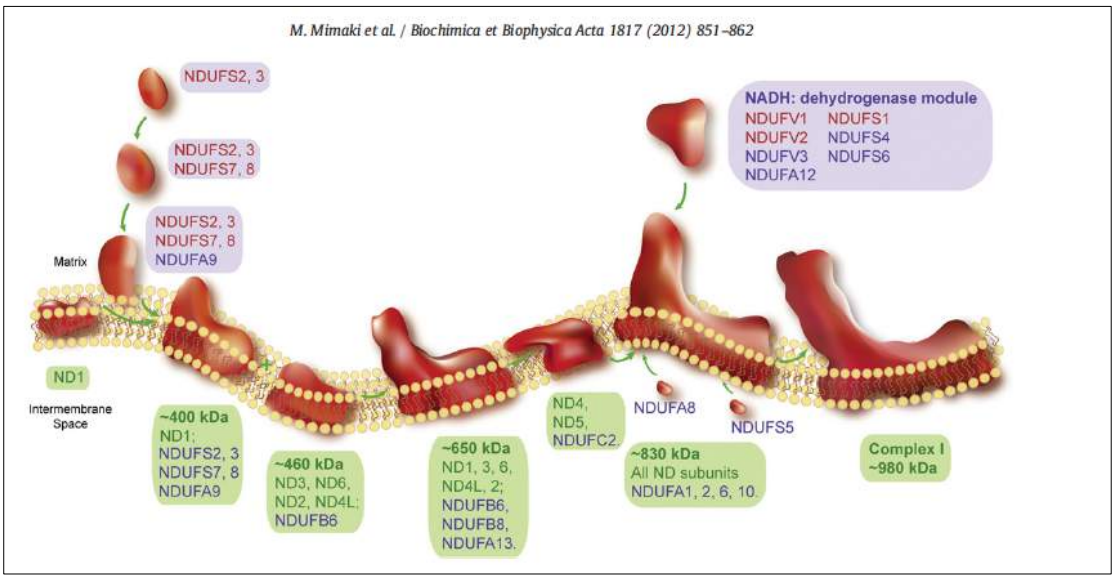

Figure 16: Human complex I assembly model. NDUFS2 and NDUFS3 are the core subunits which form a small hydrophilic complex further enlarged by NDUFS7, NDUFS8 and NDUFA9 hydrophylic subunits. Together with ND1 (mtDNA-encoded subunit) ND1, forms a ~ 400 kDa assembly intermediate which becomes a ~ 650 kDa complex with ND3, ND6, ND2, ND4L and NDUFB6. With the addition of the N module and remaining subunits mature complex I is assembled. Red: core subunits, blue: other nDNA-encoded subunits green: mtDNA-encoded-subunits. Masakazu Mimaki et al., 2012).

2.4.6 Mitochondrial Complex II: subunits and assembly

Succinate dehydrogenase complex II is the smallest OXPHOS complex, consisting of four nDNA encoded subunits. Complex II catalyzes the oxidation of succinate into fumarate in the Tricarboxylic acid cycle (TCA) and it is involved in the electrons transfer from $FADH_2$ to ubiquinone. Its assembly mechanism is still unclear.

However, studies conducted in yeast and other animal models, suggest that complex II assembly may start with the cytochrome b and SDHAF1 (succinate dehydrogenase complex assembly factor 1) recruitment (Ghezzi, et al. 2009). Three iron-sulfur clusters (Fe-S) and one FAD molecule, identified as the catalytic and soluble complex II portion, complete complex II assembly picture.

2.4.7 Mitochondrial Complex III: subunits and assembly

Cytotchrome c reductase complex III is made of ten nuclear encoded subunits and one mtDNA encoded subunit cytochrome b. Blue-natitve gel analysis suggest that complex III functions as a homodimer. Three subunits (cytochrome b, cytochrome c_1 and the Rieske 2Fe-2S protein) form the catalytic subunits being involved in the mitochondrial electrons transfer. The core proteins (Core 1 and 2) together with the remaining seven small subunits define the entire complex. Recently, Zara et al. have postulating that the initial precomplex requires the association of cytochrome b with cytochrome c_1, the two core proteins (Core1 and 2), the two small proteins (Qcr7p and Qcr8p) and the chaperone protein Bcs1p. This precomplex is thought to incorporate the remaining small subunits (Qcr6p, Qcr9p, Qcr10p) and the Rieske 2Fe-2S protein resulting in the mature final complex (Zara, Conte and Trumpower 2009).

2.4.8 Mitochondrial Complex IV: subunits and assembly

Cytochrome c oxidase complex IV is the last complex of the OXPHOS system. It is made of thirteen subunits among which three are mtDNA encoded (COX 1, 2 and 3). COX IV assembly requires the sequential association of three different intermediates

(S1, S2 and S3). COX 1, which carries the heme A groups (a and a3), is the first protein to be inserted into the mitochondrial inner membrane, followed by other two subunits COX 4 and COX 5A. Consequently, COX 2 with its copper center (CuA and CuB), ensures the S2 intermediate association with COX 3 giving rise to the S4 monomeric complex. Furthermore, the ten nuclear-encoded subunits not yet characterized, seem to contribute to the complex IV assembly and its dimerization (COX 6A, COX 6B and COX 5B) (Fernandez-Vizarra, Tiranti and Zeviani 2009).

2.4.9 Mitochondrial ATP synthase: subunits and assembly

Mitochondrial ATP synthase (complex V) is required for the phosphorylation of ADP in ATP through the energy originated from the proton-motive force in the respiratory chain. This complex is mainly described in two portions: the hydrophilic F1 and hydrophobic FO portion, interconnected by two other proteins (Futai, Noumi and Maeda 1989). F1, with its nuclearly encoded 5 subunits (three α, three β, and one γ, δ and ε) is located in the mitochondrial matrix housing complex V catalytic activity. On the other hand, FO with its eight subunits (a, b, c, d, e, f, g, and A6L) is deeply seated in the mitochondrial inner membrane allowing proton flux in the F1 portion by a rotary exercise (Stock, Leslie and Walker 1999). Complex V assembly takes place in three different steps. Importantly, it has been shown that complex V exists as a dimer *in vivo* and *in vitro* and this conformation has been associated with the stabilization of the mitochondrial cristae morphology (Paumard, Vaillier and Coulary 2002), (Campanella, Casswell and Chong 2008), (Strauss, et al. 2008). However until now the F1-FO portion implicated in complex V dimerization has not been identified yet.

2.4.10 Supercomplexes

Nowadays, the texts books picture of the linear respiratory chain have been challenged. Single complexes irregularly embedded in the mitochondrial inner membrane, have been replaced by a more dynamic and organized system. Using FRAP (fluorescence recovery after photobleaching) technique and electrophoretic relaxation, it was proposed a “random collision model” known also as “fluid model”. In the fluid model the mitochondrial complexes randomly diffuse in the inner membrane allowing the casual electron transfer. However this random collision model was also challenged by the observation of enzymatic activity in isolated complex I-III units (Hatefi 1978) or complex II-III complexes, suggesting unit probably interaction also in the natural membrane. Using electron microscopy analysis, it was further suggested a supermolecular complex organization, where the electron carriers and the ATP synthase are assembled in a big complex of 1.8-1.9 x 10^6 molecular weight. This idea gave rise to a new model called “solid model”, where the OXPHOS proteins assemble in a more compact and organized manner named supercomplex (Figure 17). The study of protein-protein interaction and function under native conditions, the use of non-ionic detergents and Blue Native electrophoresis (BN-Page), became an important tool to study OXPHOS association (Schagger 1995). To prove the supercomplex existence, different organisms were used as a model. Bovine mitochondria displayed an association between monomeric complex I, dimeric complex III and one to four molecule of complex IV ($I+III_2+IV_{1-4}$) called “respirasome” in the presence of dimeric ATP synthase (Schagger and Pfeiffer 2000). Furthermore, the respiratory chain organization seen as one single functional unit was supported by flux control experiment (Boumans, et al. 1998), (Bianchi, et al. 2004),

by the instability of one OXPHOS protein due to point mutation in another subunit (Acin-Perez, et al. 2004) (Diaz, et al. 2006) and by electron microscopy (EM) images, where the redox components appeared closely associated (Dudkina, et al. 2005). It is worth noticing that complex II does not take part in this supercomplex organization maybe because of its role in TCA cycle. Altogether these findings highlight the importance of the supercomplex organization. First of all, the OXPHOS proteins assembly will favor the electrons transfer that, as proposed in the substrates channeling model, will be faster and more efficient. The higher molecular organization is also involved in the determination of the mitochondrial inner membrane ultrastructure, as well as in its capacity to insert proteins. Moreover, supercomplex assembly is involved in the stabilization of all the single components, especially for Complex I, which was shown to be destabilized by complex III and IV mutations. Today the old and the new model have been fused together to give rise to a hybrid model where the single complexes and the supercomplexes coexist in a dynamic manner.

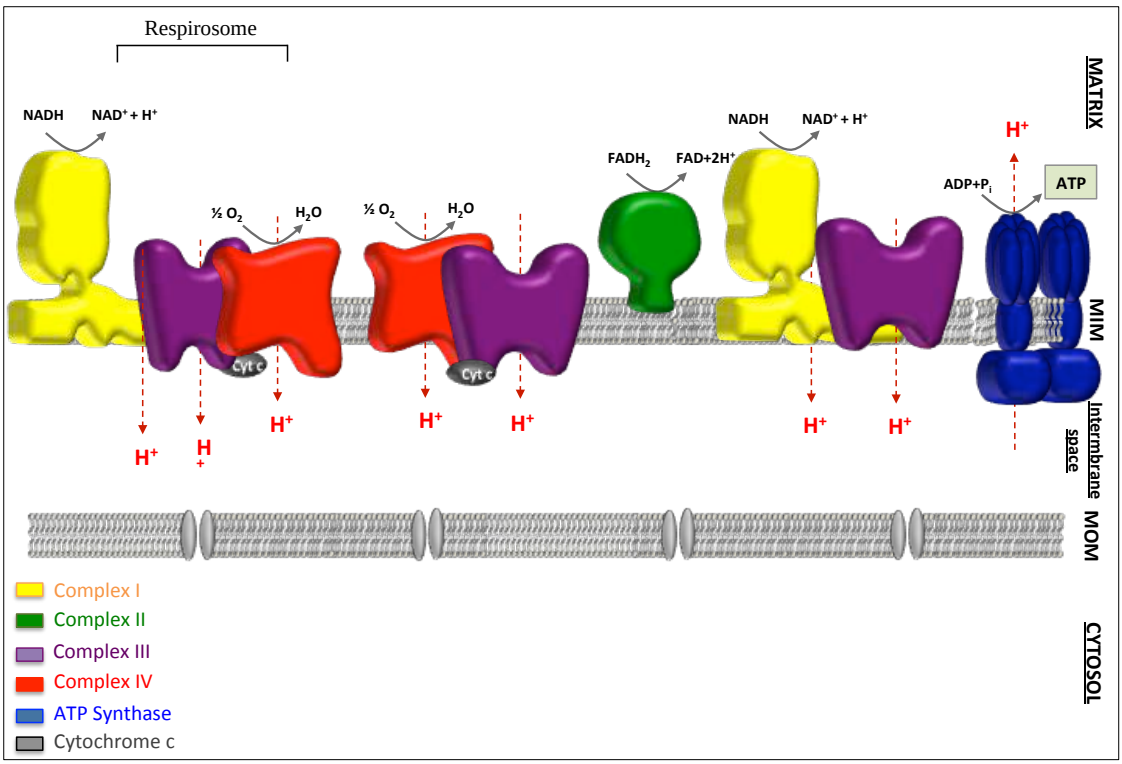

Figure 17: OPHOS Supercomplex organization. The monomeric electron transport chain subunits are organized in supermolecules complexes: CI+CIII+CIV (Respirasome), CIII+CIV, CI+CIII. CII is not part of the supercomplexes. ATP synthase is in from of dimer.

2.4.11 Reactive Oxygen Species

In spite of the conventional mitochondrial role as cellular “power station”, in recent years is emerged a new fascinating mitochondrial picture as Pandora’s vase, an intracellular container essential not only for the life but also for the cell death. Indeed, in the last decade mitochondria have been implicated not only in physiological but also in pathological conditions including Parkinson’s and Alzheimer’s disease, atherosclerosis, heart attack and aging, just to mention some. Therefore, it is not surprising that mitochondria can generate molecules able to react with lipids (Rubbo, et al. 1994), polysaccharides (Kaur and Halliwell 1994), DNA (Richter, Park and

Ames 1998) and proteins (Stadtman and Levine 2000) in order to demolish the cell. Even though these molecules, called reactive oxygen species (ROS), can be generated exogenously (radiation, chemicals) and endogenously from different cell compartments (endoplasmic reticulum, cytoplasm, peroxisome, lysosome, microsome and plasma membrane), it is now accepted that the dominant ROS source is the mitochondrion, especially mitochondrial complex I and III (Brand, et al. 2009). Also called “free radicals”, reactive oxygen species exist individually, contain one or more electron unpaired and are very reactive compounds (Figure 18). These species originate when one electron is transferred to molecular oxygen, giving rise to the superoxide anion radical ($O_2^{\cdot -}$), hydrogen peroxide (H_2O_2), and hydroxyl radical ($HO^{\cdot}$), meaning one, two or three electron transfer. The superoxide anion radical is considered the harbinger of almost all reactive species, whereas $HO^{\cdot}$ the most dangerous because the most long live and therefore most reactive. The oxidoreductase centers in the mitochondrial electron transport chain are thought to be the first place from where electrons escape and reduce molecular oxygen in order to produce ROS (Andreyev, Kushnareva and Starkov 2005). Importantly, mitochondrial complex I has been marked as the main ROS producer, based on its FMN (flavin mononucleotide), iron-sulphur clusters, ubiquinone Q-binding site and mitochondrial encoded N2 protein. Indeed, either complex I activity blockage at the level of the NADH-substrate, or the use of succinate as complex II substrate, have been shown to favor ROS generation. The former obviously arrests from the onward electron flow and the second favors the back flow from complex II to complex I (Ross, et al. 2013). Despite this, mitochondria have adopted many mechanisms to eliminate and to control ROS. First of all, all cells possess a family of enzymes called superoxide dismutases (SODs), important to keep superoxide at a low level by converting it in H_2O_2. In

particular, the mitochondrial matrix, expresses a manganese-containing SOD (Mn SOD), able to dismute the superoxide from the matrix (Fridovich 1998). In the mitochondrial intermembrane space, low pH, cytochrome c and a different SOD containing copper and zinc (CuZnSOD) are all mechanisms that monitor the $O_2^{\cdot -}$ levels. Glutathione peroxidase and phospholipid-hydroperoxide glutathione peroxidase are involved in the hydrogen peroxide degradation and in the lipid peroxide reduction, respectively. In peroxisomes and heart mitochondria, catalase oxidizes phenols, formic acid, formaldehyde and alcohol by using H_2O_2. Ubiquinol and vitamin E also contribute to maintain low ROS levels in cells. However, it is precisely from the unbalance between ROS production and antioxidant defense that oxidative stress is triggerd, leading to many diseases and ultimately to cell death (Turrens 2003).

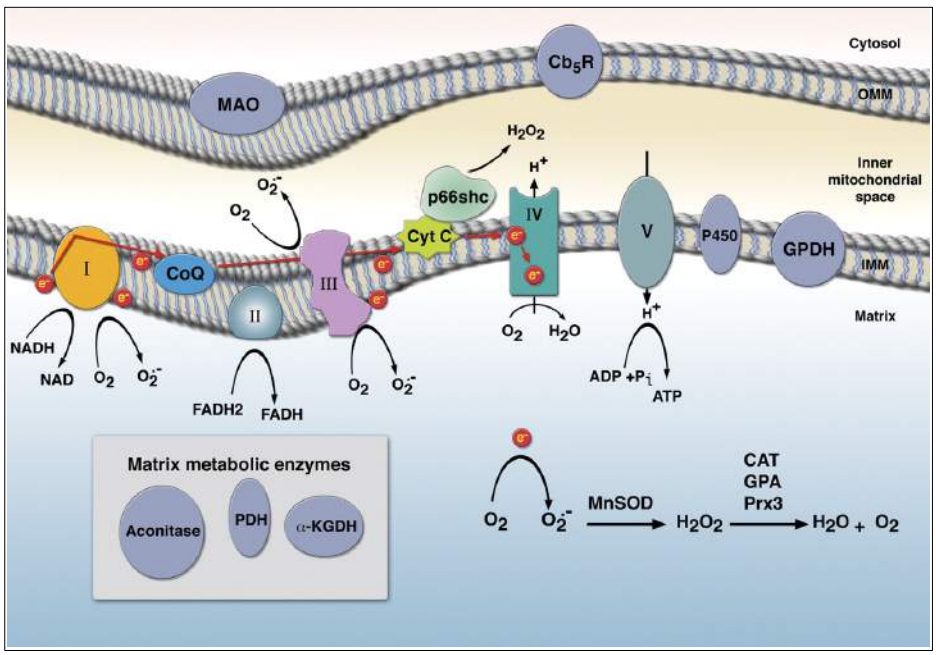

Figure 18: Mitochondrial ROS generation. Reactive oxygen species originates mainly from complex I and complex III. Other sources of ROS consists of enzymes in the outer mitochondrial membrane such as monoamine oxidase (MAO) and cytochrome b5 reductase (Cb5R), inner membrane such as glycerol-3-phosphate dehydrogenase (GPDH) and cytochrome P450. (Lin and Beal, 2006; Brand, 2010).

2.5 Aim of my thesis

Cytotoxic T Lymphocytes (CTLs) kill their target cell predominantly via the cytotoxic granule pathways where the pore forming protein perforin (PFN) and a family of serine proteases called Granzymes (Gzms) are released from the cytototxic granules into the target cells. Among all the Gzms, GzmA and GzmB are the best characterized. GzmA induces cell death in a ROS dependent manner altering mitochondrial complex I subunit NDUFS3; ROS production will cause the SET complex translocation in the nucleus in order to induce DNA damage and finally cell death. Evolution has developed many tools to eradicate malignant cells, among which, our lab has focused on Granzyme B-induced cell death. GzmB-induced cell death can occur both in a caspase dependent or independent manner.

Knowing that GzmA and GzmB are mainly involved in cyototxic granule pathway, we reasoned that GzmB, similarly to GzmA, could induce cell death in a ROS dependent manner. Therefore, we aimed to investigate the caspase independent pathway where GzmB targets directly mitochondria in order to induce cell death and ROS production. Therefore, I proposed to characterize the:

- Molecular mechanism involved in GzmB-induced ROS.
- Effects of GzmB on mitochondrial complex I activity.
- Significance of GzmB disruption of complex I for ROS production and cell death.

Chapter 3
MATERIAL AND METHODS

3.1 Perforin and Granzyme B treatment

K562 cells were washed three times in PBS and resuspended in cell buffer containing HBSS, 10 mM HEPES [pH 7.2], 0.4% BSA, 3 mM CaCl2. (2×10^4 cells in 60 ul final volume). GzmB was added at 50nM, 150 nM and 450 nM as indicated and PFN was added at a sublytic dose (10% of cell death). The cells were incubated at 37°C for 1 hour. When indicated the cells were preincubated with Tiron 100 μM, zVAD+DEVD 100 μM for 30 minutes at R.T. Cell death was measured with staining with annexin V and PI and analyzed by flow cytometry as described. ROS production was measured by adding HE 2 μM just before flow cytometry analysis.

For immunostaining 2×10^4 MEF WT and MEF Bax Bak DKO cells were plated on 10 mm glass cover-slips in a 48-well plate. The cells were incubate with 300ul DMEM w/o FBS + 100 nM of Mitotracker for1 hour at 37°C. After three washes with serum free medium, DMEM was added and incubated 1 hour at 37°C. After wash with HBSS the cells were treated with GzmB 450 nM and PFN at a sublytic dose and

incubated for 1 hour at 37°C. Then the cells were fixed with 4% PAF for 30 min. and stained with anti cytochrome c-Alexa 488 (BD Pharmingen) for 1h.

3.2 Citotoxicity assay (^{51} C release)

2×10^6 EL4 target cells were incubated with 0.5 µg/ml LCMV gp33 peptide for 1 hour in the presence of 100 µCi/ml Na251CrO4 at 37°C. After washing, 2×10^3 target cells were preincubated or not for 15–30 minutes at 37°C in triplicate microtiter wells with Tiron or D147 ROS inhibitors. Cells were then mixed with indicated P14 or P14GzmB$^{-/-}$ effector cells at effector:target ratio 50/1 in 100 µl K10 medium and incubated at 37°C for 6 hour. After centrifugation at 760 × g for 5 min, 45 µl supernatant was counted on a TopCount (Packard Instrument Company). Specific release was defined as ([cpm − spontaneous release]/[total release − spontaneous release]) × 100.

3.3 Isolated mitochondria assay

For all assays, mitochondria were freshly isolated from mouse liver as described (Susin, et al. 2000). Mitochondria (2.5 mg/ml protein) were incubated with or without S100 (cytosolic factor) (1 mg/ml) plus GzmB or GzmA at indicated concentrations in 60 µl of mitochondrial buffer (220 mM sucrose, 68 mM mannitol, 10 mM KCl, 5 mM KH2PO4, 2 mM MgCl2, 0.5 mM EGTA, 5 mM succinate, 2 mM rotenone, 10 mM HEPES, pH 7.2) for 30 minutes at 37°C. ROS production was mesured by adding HE

2 μM before flow cytometry analysis as above. When indicated Valynomicin 16 nM and O-phenanthroline 2μM was added 15 minutes prior GzmB treatment.

For proteomic analysis purified mouse liver mitochondria were treated with buffer or human GzmA (0.3 μM) or human GzmB (0.3 μM) for 10 minutes and resolved by 2D gel electrophoresis and silver staining. One spots that was disappearing after GzmB treatment corresponding to missing proteins in the GzmB-treated sample, were excised and characterized by mass spectrometry.

Isolated mitochondria treated with GzmA 1μM for 5 min at 37 °C solubilized with Lauryl Malthoside or Digitonin and assessed by Blue Native gel and in gel activity assay as indicated in the paper for GzmB.

Chapter 4 RESULTS

Granzyme B disrupts respiratory chain complex I to induce ROS-dependent cell death.

Guillaume Jacquemin [#], Daniela Margiotta [#], Atsuko Kasahara, Esen Yonca Bassay, Michael Walch, Jerome Thiery, Judy Lieberman and Denis Martinvalet.

[#]Authors contributed equally to this work

My contribution to this paper was to investigate the molecular mechanism by which GzmB disrupts mitochondrial complex I. Indeed, I focused on GzmB cleavage of three mitochondrial complex I subunits - NDUFV1, NDUFS2 and NDUFS1 - in K562 cell lines and in intact purified mitochondria. I showed that GzmB cleaves these three subunits in a caspases independent and valynomicin dependent manner, highlightening the importance of an intact m to get GzmB inside the mitochondria in order to cleave its substrates (Figure 1D, 2A). I verified that GzmB enters

mitochondria to reach its substrates by flow cytometry and WB analysis of isolated mitochondria (Figure 5F and 5G). I also investigated the MOMP involvement in GzmB cell death pathway. I showed that GzmB induces Cyotochrome c and Endo G release only in the presence of cytosolic factors (S100) whereas it cleaves NDUFS1 regardless of S100. It suggests that MOMP is not required for GzmB cleavage of complex I substrates (Figure 3A). I also investigated MOMP in Bax Bak DKO cells, which do not undergo MOMP (Figure 3B). I observed that GzmB induces cell death and ROS production also in these cell lines, highlightenig that ROS and MOMP could be two independent events which cooperate in order to better kill target cells. I was able to show that by cleaving its substrates, GzmB alters mitochondrial function by decreasing oxygen consumption and by reducing mitochondrial complex I and III activity within 1 minute of GzmB addition (Figure 6A-C). Furthermore, I investigated the role of GzmB in the ETC organization and showed that GzmB tilts the balance from monomeric complexes to an accumulation of supercomplexes $I+III_2$ (Figure 6D-G). I showed that GzmB also alters mitochondrial morphology by detaching cristae from the mitochondrial membrane (Figure 6H). Although the functional significance of GzmB-induced cristae detachment need further study, I demonstrated that GzmB induces cell death mainly by affecting mitochondrial respiration, electron transport activity and mitochondrial morphology. Altogether these mechanisms could favor electrons transfer when complex I function is compromised and help to explain how GzmB induces ROS dependent cell death. My contribution to this work was also to participate in the identification of GzmB substrates in Ctl:target cell conjugation and by using tagged version of GzmB substrates (Figure 1E-H). I also participate in the identification of GzmB-induced cell death in MOMP independent manner, in Bax

Bak DKO cells (Figure 3E-F) and GzmB-induced DNA oligonucleosomal fragmentation in a ROS dependent manner (Figure 4G-H).

Granzyme B disrupts respiratory chain complex I to induce ROS-dependent cell death.

Guillaume Jacquemin[1#], Daniela Margiotta[1#], Atsuko Kasahara[1], Esen Yonca Bassay[1], Michael Walch[2], Jerome Thiery[3], Judy Lieberman[4] and Denis Martinvalet*[1].

[1]CMU, Faculté de Médecine, Université de Genève, Genève Suisse

[2]Departement de Médecine, Unité d'Anatomie, Université de Fribourg, Fribourg, Suisse

[3]INSERM U753, Gustave Roussy Cancer Campus, Villejuif, France

[4]Program in Cellular and Molecular Medicine, Boston Children's Hospital, Harvard Medical School, Boston MA USA

[#]Authors contributed equally to this work

*Correspondence should be addressed to DM (Denis.Martinvalet@unige.ch)

4.1 Abstract

Cytotoxic T Lymphocytes (CTLs) and Natural Killer cells (NKs) are closely involved in the elimination of unwanted cells, meaning either cancer or pathogen-infected cells. In this work we focused on the cytotoxic granule pathway where Granzyme B (GzmB) a serine proteases and perforin (PFN) a pore forming protein, are released from the killer cell's cytotoxic granules into the target cells cytoplasm to kill them. GzmB and caspase, trigger cell death by inducing a mitochondrial ROS production, a transmembrane potential dissipation and mitochondrial outer membrane permeabilization (MOMP). Here, we showed that GzmB-induced cell death is a mitocentric event where GzmB without caspase and MOMP requirement, enter into the mitochondria, cleaves three complex I subunits NDUFV1, NDUFS2 and NDUFS1 leading to mitochondrial ROS production. Furthermore we showed that GzmB-induced complex I subunits cleavage plus GzmB-induced mitochondrial ROS production are two phenomena essential for mitochondrial alteration as demonstrated by complex I and III activity reduction, mitochondrial respiration decrease and loss of mitochondrial cristae junction. GzmB-uncleavable mutants forms of complex I subunits revealed that GzmB-dependent ROS production facilitated apoptogenic factors release from the mitochondria, increased DNA fragmentation and lysosomal fracture. Therefore, our data identify unequivocally a role for GzmB mediated mitocentric ROS production in apoptosis.

4.2 GranzymeB induces cell death in a ROS dependent and caspase independent manner

To understand whether ROS production is essential in GzmB-induced cell death pathway, we treated K562 cells with a sublytic dose of PFN plus GzmB. ROS production was assessed by HE and cell death by Annexin V/PI staining in flow cytometry analysis (FACS). The reaction between $O_2^{\cdot -}$ and HE resulted in ethidium formation. Ethidium binds to the DNA and the fluorescence emitted is detected by FACS. Annexin V belongs to a family of phospholipids binding proteins which bind to phosphatidilserin (PS) with high affinity and in a Ca^{2+} dependent manner. Indeed, an early event in apoptosis is the flipping of PS from the inner side to the outer plasma membrane side. After apoptotic stimuli, PS will therefore be exposed to the extracellular environment and recognized by Annexin V. If Annexin V is conjugated to a fluorescent tracer such as fluorescein isothiocyanate (FITC), cell death can be measured by FACS. Early apoptotic events and late stage apoptosis that involves impairment of the plasma membrane will be discriminated by adding, propidium iodide (PI) or 7-Amino-Actinomycin (7-AAD), two impermeable fluorescent dyes. Therefore, in our model, cells permeable to PI will represent necrotic cells (PI^+ Annexin V-$FITC^-$) whereas early apoptotic cells, when plasma membrane integrity is preserved, will exclude PI resulting in PI^- Annexin V-$FITC^+$ staining. Late apoptotic cells will be positive for both annexin V and PI staining. We observed that GzmB efficiently induces apoptotic cell death that is correlated with the extent of ROS production. The superoxide scavenger Tiron and *N*-acetyl-L-cysteine (NAC), a glutathione precursor, are two compounds well known for their antioxidants property (Ling, et al. 2003). When we used Tiron and NAC to specifically scavenge ROS, we

observed a decrease in apoptosis, suggesting that in our cellular model ROS production contributes significantly to GzmB-induced cell death (Figure 19 A and B). Furthermore, we showed that, human GzmB-induced ROS production is only sensitive to GzmB specific inhibitor and ROS scavenger Tiron, whereas pan caspase inhibitor cocktails zVAD+DEVD which irreversibly inhibits the caspases, has no effect on GzmB-induced ROS dependent cell death (Figure 20). These findings were also reproduced in a more physiological approach where WT CTLs expressing all the Gzms were used to kill their target cells in a CTL:cell target conjugation. Indeed, as shown in Figure 19 C, CTLs kill efficiently their targets, and this is efficiently inhibited by ROS scavangers. Altogether, these results suggest that GzmB induces ROS production in a dose dependent manner, that GzmB-induced ROS can be abrogated by superoxide scavengers and that ROS are involved not only in GzmB cell death pathway but also for the other Gzms, highlighting the importance of ROS as a determinant factor for cell vulnerability which finally lead to cell death.

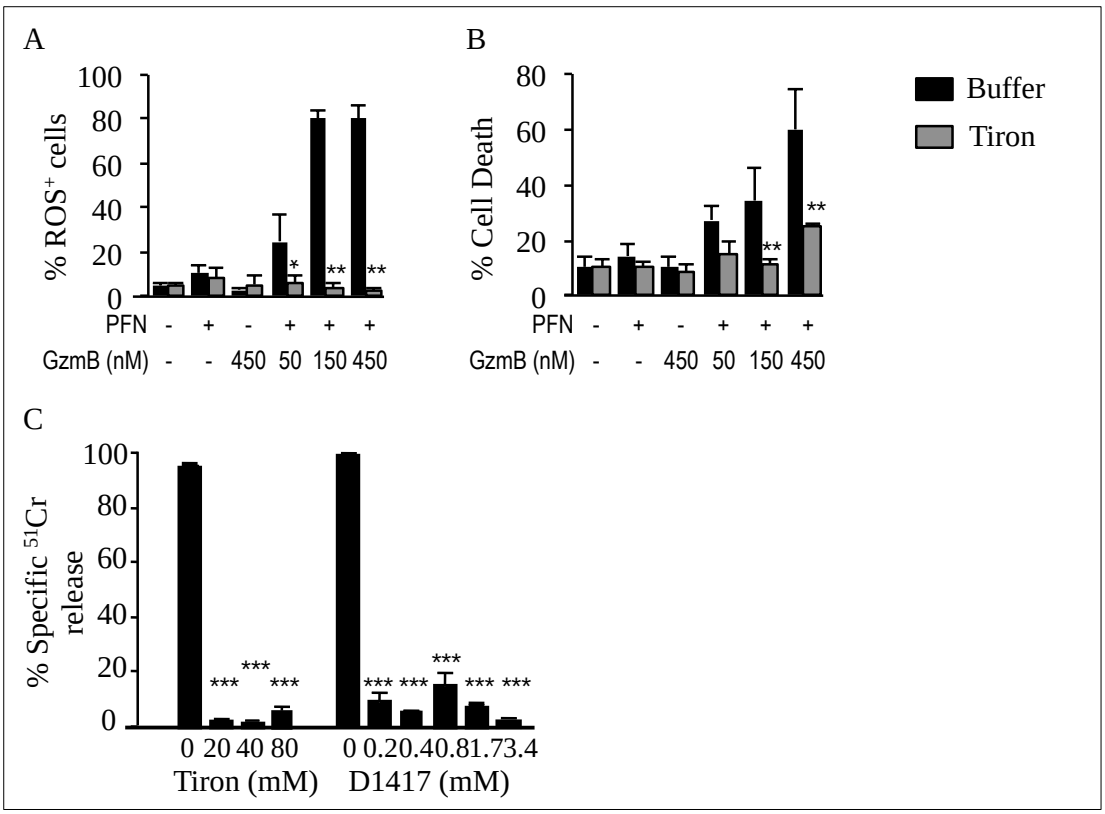

Figure 19: GzmB induces cell death in a ROS dependent manner. K562 cells preincubated or not with the ROS scavenger Tiron, were treated with sublytic dose of PFN plus GzmB. (A) ROS production was followed by dihydroethidium (HE) and (B) cell death by Annexin V/PI staining and flow cytometry analysis. (C), K562 cells were used as target cells for WT CTL expressing all the Granzymes in a ^{51}Cr release assay. Mean +/- SEM of at least 3 independent experiments is shown, *p<0.05, **p<0.01, ***p<0.001.

.

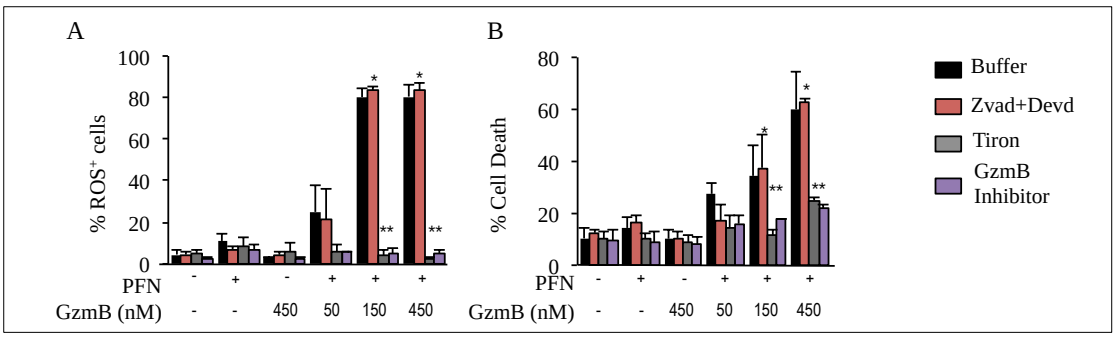

Figure 20: GzmB induces cell death in a caspases independent manner. K562 cells preincubated or not with different inhibitors as indicated were treated with sublytic dose of PFN plus GzmB. (A) ROS production was followed by dihydroethidium (HE) and (B) cell death by Annexin V/PI staining and flow cytometry analysis. Mean +/- SEM of at least 3 independent experiments is shown, *p<0.05, **p<0.01.

4.3 Granzyme B induces ROS from the mitochondria

We next investigated the source of ROS in GzmB/PFN treated cells. To this end, purified mouse liver mitochondria were treated or not with GzmA or GzmB and the samples were tested for ROS production by using dihydroethidium (HE) staining. Indeed, we observed that similar to GzmA treatment, GzmB induces a massive ROS production directly from isolated mitochondria, since addition of cytosolic factors (S100) has no effects on it (Figure 21). This result suggests that like GzmA, GzmB acts directly on the mitochondria to induce ROS. To further validate mitochondria as the primary source of ROS after GzmB treatment, we took advantage from cells ρ^0 cells. These cells are established by long-term treatment with low levels of ethidium bromide. They lack mtDNA and oxygen utilization, produce less ROS, have reduced activity in CI and CIV and therefore rely on glycolysis for their energy supply (King and Attardi 1989). To study mitochondrial functions we generated K562 ρ^0 cells which have almost complete loss of mtDNA (Figure 22 A). GzmB plus PFN treatment shows that pseudo ρ^0 cells are insensitive to ROS increase and cell death, supporting the role of mitochondria as primary source of ROS production in this pathway (Figure 22 B and C). Besides the electron transport chain, it has been shown that nicotinamide adenine dinucleotide phosphate oxidase (NOX), xanthine oxidase (XO) and cytochrome P450 monooxygenases contribute to ROS production from inside the cell (Block and Gorin 2012). To further clarify the origin of GzmB-induced ROS, we used Mef $Nox1^{-/-}$ and $Nox4^{-/-}$ deficient cells, as they lack the main NADPH oxidase machinery. Upon GzmB and PFN treatment we observed the similar extent of ROS production and cell death compared to the WT cells (Figure 23). Also we did not check for XO and P450, we could not exclude a role for ROS production. However

our data confirm the mitochondria as the primary source of ROS in this pathway and exclude a role for the NOX. We next investigated the molecular mechanism how GzmB induces ROS production in mitochondria.

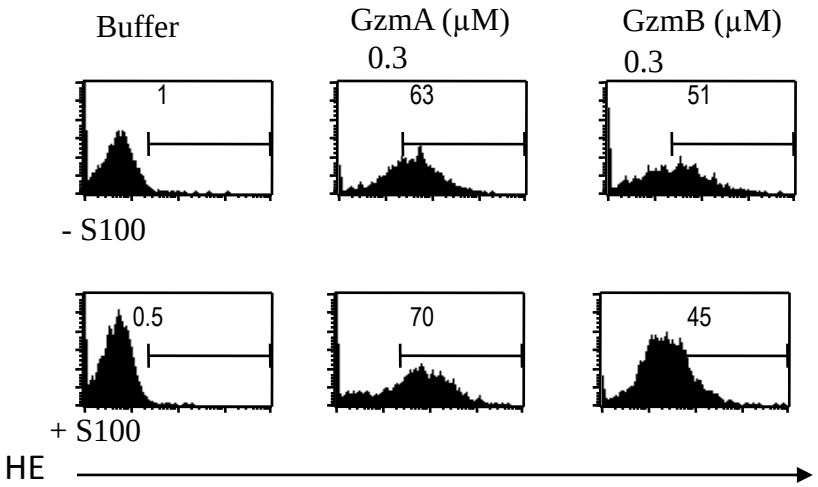

Figure 21: GzmB induces mitocentric ROS production. Purified mouse liver mitochondria were treated with Buffer, 0.3 µM of human GzmA or GzmB in the presence or absence of cytosolic factors S100 and ROS production was measured by HE staining.

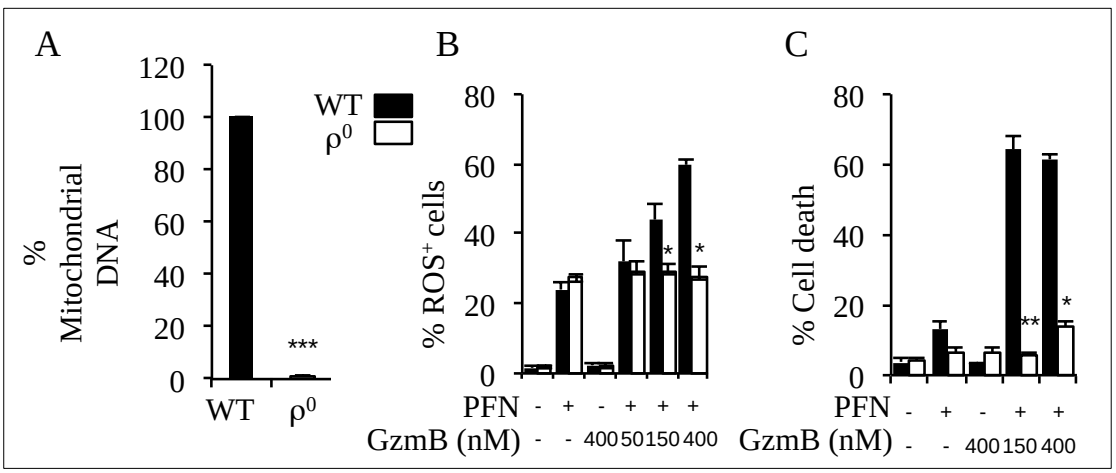

Figure 22: GzmB needs an intact ETC to induce ROS and cell death. K562 ρ^0 cells cultured in DMEM plus ethidium bromide (250 ng/ml), sodium pyruvate (110 µg/ml) and uridine (50 µg/ml) were treated with GzmB and PFN and ROS and cell death was measured by Mito SOX staining and Annexin V/PI respectively. Mean +/- SEM of at least 3 independent experiments is shown, *p<0.05, **p<0.01, ***p<0.001.

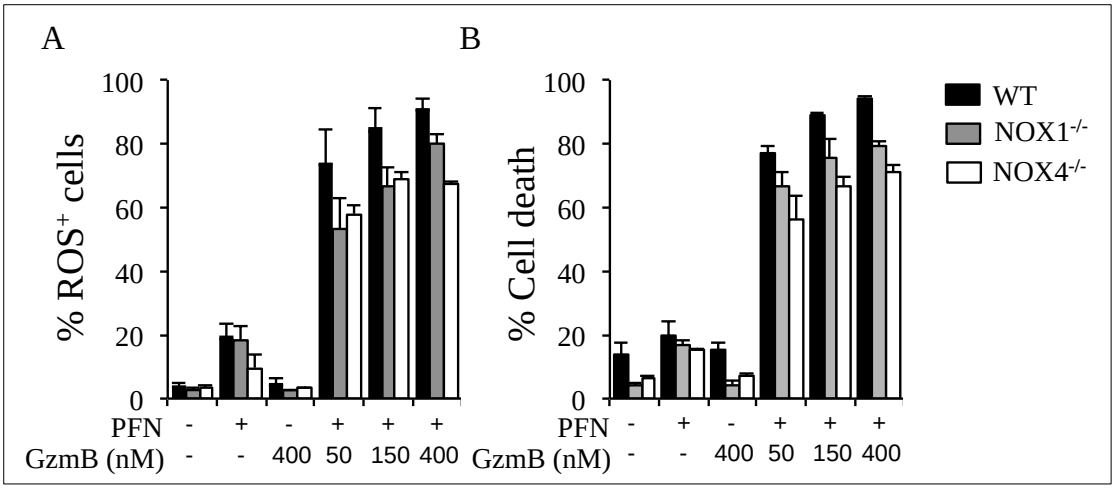

Figure 23: GzmB induces ROS and cell death in NOX1 and NOX4 KO cells. $Nox1^{-/-}$ and $Nox4^{-/-}$ MEF cells were treated with GzmB plus PFN and ROS production (A) and cell death (B) was measured by MitoSOX and AnnexinV/PI staining, respectively. Mean +/- SEM of at least 3 independent experiments is shown.

4.4 Granzyme B cleaves three mitochondrial complex I subunits

4.4.1 GzmB cleaves NDUFV1 a mitochondrial complex I subunit

To characterize the molecular mechanism by which GzmB induces ROS dependent cell death, we used an organelle proteomic approach as was done to characterize the GzmA cell death pathway (Martinvalet, et al. 2008). Purified intact mitochondria were treated with GzmB and GzmA, as control. The treated samples were resolved in 2D SDS-PAGE. The spot of interest, meaning the spot that was disappearing after GzmB treatment, was analyzed by mass spectrometry (Figure 24 A). With this approach we identified NDUFV1, the 51 kDa mitochondrial complex I subunit, as a putative GzmB target. In order to validate NDUFV1 as a physiologically relevant GzmB target, we looked at its fate in K562 cells treated with GzmB and PFN. Figure 24 B shows that GzmB plus PFN treatment induces dose and time dependent cleavage of NDUFV1 with a similar kinetic as the GzmB-induced cleavage of PARP-

1. Moreover, caspase inhibitor has only a minor effect on GzmB-induced NDUFV1 cleavage, whereas specific GzmB inhibitor prevents its degradation. These data suggests NDUFV1 as a physiologically relevant GzmB substrate. NDUFV1 carries the NADH binding site and its disruption could represent the first electron transfer leaking point in the electron transport chain, which could reasonably increase ROS production. Therefore, we investigated in more detail the GzmB effects on mitochondrial complex I.

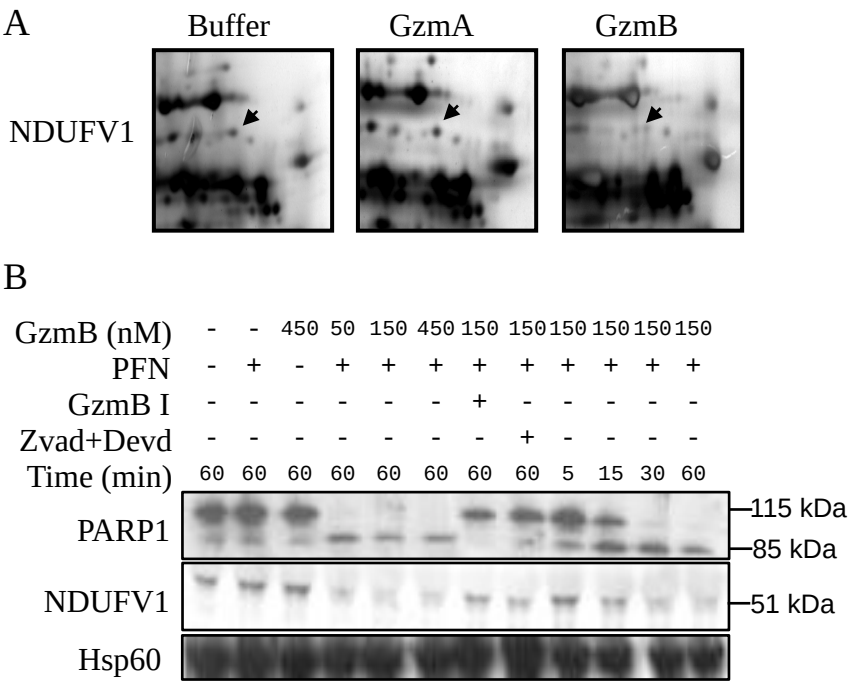

Figure 24: GzmB induces ROS production from mitochondria and targets NDUFV1. (A) Purified mouse liver mitochondria were treated with either GzmA or GzmB and samples were resolved in 2D gels and the spot of interest characterized by mass spectrometry. (B) K564 cells preincubated or not with GzmB specific inhibitor and zVAD+DEVD caspase inhibitor, were treated with sublytic dose of PFN and GzmB and the fate of NDUFV1 was followed by WB. GzmB induces a dose- and time-dependent cleavage of NDUFV1 similarly to GzmB-induced PARP1 cleavage.

4.4.2 GzmB cleaves NDUFV1, NDUFS2 and NDUFS1

GzmA and Caspase-3 have been reported to damage mitochondrial complex I by cleaving NDUFS3 (Martinvalet, et al. 2008) and NDUFS1 (J.-E. Ricci, et al. 2004), respectively. In this study we found that GzmB targets the complex I subunit NDUFV1, suggesting that all this three cell death pathway converge at the level of mitochondrial complex I in order to induce ROS dependent cell death. Furthermore, Walch and colleagues have recently showed that GzmB cleaves bacterial complex I subunits (Walch et al. 2014 *Cell* in press). Therefore, we investigated putative GzmB mitochondrial complex I targets by using a bioinformatics approach. Mammalian complex I consists of 45 subunits with a MW of about 1 MDa (Carroll, et al. 2006). To focus on the functional core subunits for complex I, we took advantage of the bacterial complex I, a simpler version with only 14 subunits that are all essential for complex I function. Indeed, we compute the primary sequence of the 15 human homologs of the bacterial complex I subunits against 240 reported GzmB cleavage sites deposited on the web tool CutDB. We focused on the putative GzmB substrates with the highest fidelity score for cleavage by GzmB. Indeed, by using the prediction site tool, we identified NDUFV1 (51 kDa), NDUFS2 (42 kDa), NDUFS1 (75 kDa), NDUFS3 (30 kDa), NDUFS7 (20 kDa) and NDUFA13 all subunits of the human complex I as 99% confidence GzmB targets (Table 1).

Rank	Position	Site	N fragment	C fragment	Frequency score	Similarity max score	Similarity max site	Average score	Specificity	
1	346 to 353	VDAE.ALVA	38.5 kD	40.9 kD	0.275	47.368	VDEDALTL	13.011	>99%	
2	344 to 351	GLVD.AEAL	38.3 kD	41.1 kD	0.148	45.000	FMVDNEAI	6.643	>99%	
3	395 to 402	EEAD.VVLL	43.7 kD	35.8 kD	0.137	47.222	AEADAIIQ	6.847	>99%	
4	451 to 458	ILQD.IASG	50.0 kD	29.5 kD	0.097	56.410	IVPDIAVG	5.474	>99%	
5	190 to 197	AGVD.DLGT	21.2 kD	58.3 kD	0.090	48.571	SSVDILAT	4.391	>99%	
6	359 to 366	NRVD.SDTL	39.9 kD	39.5 kD	0.058	39.024	NEADSLTY	2.272	>99%	NDUFS1
7	34 to 41	VFVD.GQSV	3.9 kD	75.5 kD	0.049	42.105	VEVDGSIM	2.061	>99%	
8	548 to 555	LGAD.GGCI	60.2 kD	19.3 kD	0.034	53.488	LGKDGGLD	1.825	>99%	
9	392 to 399	AGVE.EADV	43.4 kD	36.1 kD	0.027	50.000	IEVDESDV	1.331	>99%	
10	361 to 368	VDSD.TLCT	40.1 kD	39.3 kD	0.025	47.368	VDEDALTL	1.189	>99%	
11	654 to 661	VRYD.DIEG	71.8 kD	7.6 kD	0.019	53.846	VGVDSVEG	1.011	>99%	
Rank	**Position**	**Site**	**N fragment**	**C fragment**	**Frequency score**	**Similarity max score**	**Similarity max site**	**Average score**	**Specificity**	
1	253 to 260	LRLD.ELEE	29.3 kD	23.2 kD	1.372	50.000	VRADILED	68.595	>99.9%	
2	356 to 363	IKVD.DAKV	41.2 kD	11.3 kD	0.137	60.525	VKVDSKKM	8.298	>99%	NDUFS2
3	443 to 450	MLAD.VVAI	50.7 kD	1.8 kD	0.058	54.286	VVTDLIAV	3.159	>99%	
Rank	**Position**	**Site**	**N fragment**	**C fragment**	**Frequency score**	**Similarity max score**	**Similarity max site**	**Average score**	**Specificity**	
1	115 to 122	VNAD.EGEP	13.2 kD	37.6 kD	0.414	58.537	VKADDLEP	24.226	>99.9%	
2	337 to 344	MDFD.ALVQ	36.9 kD	13.9 kD	0.138	52.778	AEADAIIQ	7.303	>99%	NDUFV1
3	335 to 342	VLMD.EDAL	36.7 kD	14.1 kD	0.067	43.590	VQGDIDAI	2.91	>99%	
Rank	**Position**	**Site**	**N fragment**	**C fragment**	**Frequency score**	**Similarity max score**	**Similarity max site**	**Average score**	**Specificity**	
1	187 to 194	ILTD.IGFE	21.6 kD	8.7 kD	0.089	47.368	ILTDAGKV	4.206	>99%	NDUFS3
2	255 to 262	EAGD.KKPD	29.6 kD	0.7 kD	0.016	54.762	DSVDAKPD	0.885	>99%	
Rank	**Position**	**Site**	**N fragment**	**C fragment**	**Frequency score**	**Similarity max score**	**Similarity max site**	**Average score**	**Specificity**	
1	34 to 41	VATD.GPSS	3.8 kD	19.8 kD	0.018	47.222	ISNDSASS	0.869	>95%	NDUFS7
2	65 to 72	AKLD.DLVN	6.9 kD	16.6 kD	0.016	47.500	NELEDLID	0.747	>95%	
Rank	**Position**	**Site**	**N fragment**	**C fragment**	**Frequency score**	**Similarity max score**	**Similarity max site**	**Average score**	**Specificity**	
1	91 to 98	LEEE.AIIM	10.9 kD	5.8 kD	0.022	58.333	VEEDSILI	1.26	>99%	NDUFA13
2	87 to 94	LREN.LEEE	10.4 kD	6.3 kD	0.004	47.500	IQDDSEEE	0.173	>95%	

TABLE 1: Putative GzmB cleavage sites of human complex I subunits. The protein sequences encoding for the human orthologs of the 15 subunits of the bacterial complex I were computed against 264 identified GzmB cleavage sites deposits on web tool CutDB using the prediction tool Site Prediction.

In order to validate these subunits as putative GzmB targets we used 721.221 cells; this cell line was preferred to K562 because better targets for YT Indy. 721.221 overexpressing tagged versions of NDUFS1 and NDUFS2 were treated with GzmB and PFN resulting in a decrease in NDUFS1 and NDUFS2 full length forms as detected by immunoblot (Figure 25 A and B). This result suggest that GzmB specifically attacks mitochondrial ETC complex I by cleaving NDUFV1, NDUFS2, NDUFS1, 3 subunits of this complex. Importantly, GzmB-induced complex I subunits cleavage in target cells was also observed during killer cells attack (Figure 26). Target cells overexpressing the TAG version of GzmB substrates were put in contact with the effector cells YT Indy and the fate of these target were followed by WB,

suggesting that complex I disruption is a physiological event during immune mediated target cell death.

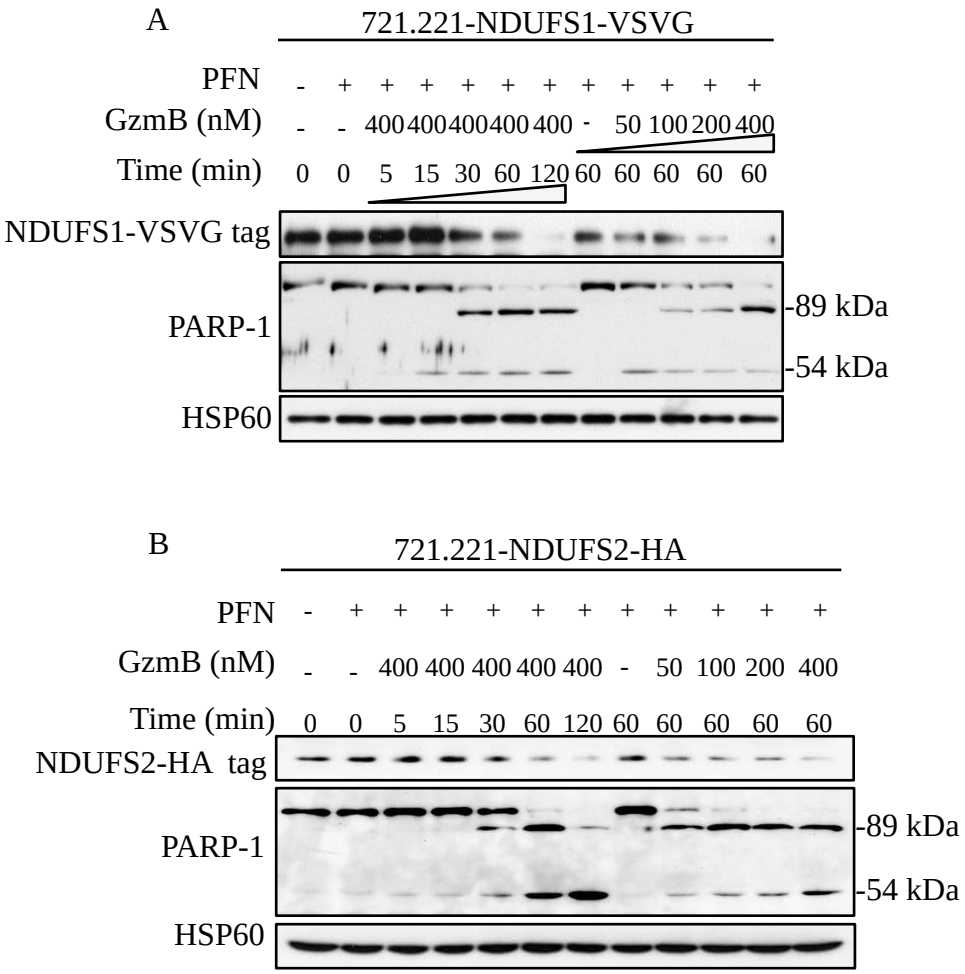

Figure 25: GzmB cleaves the mitochondrial subunits NDUFS1 and NDUFS2. 721.221 overexpressing NDUFS1-VSVG (A) and NDUFS2-HA (B) were treated with sublytic dose of PFN and GzmB and the fate of NDUFS1 and NDUFS2 was followed by WB. GzmB induces a time and dose dependent cleaveage of NDUFS1 and NDUFS2 similar to GzmB-induced PARP1 cleavage. Hsp60 serves as a loading control.

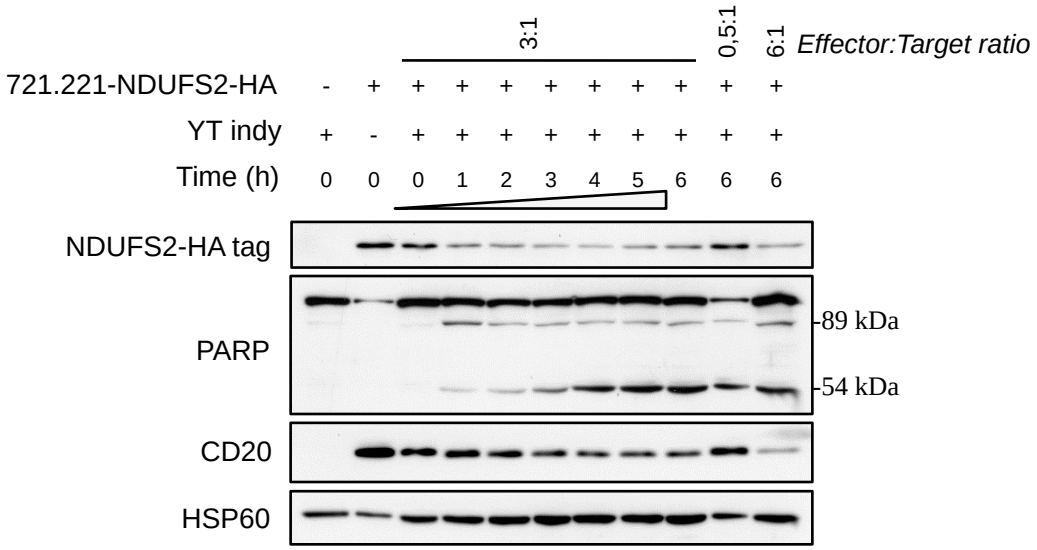

Figure 26: GzmB cleaves the mitochondrial subunits NDUFS2 in a cell target cell/Ctl conjugation. 721.221 overexpressing NDUFS2-HA were put in contact with the effetcor cells YT Indy and the fate of the TAG-NDUFS2 was followed by WB. Loading control Hsp 60.

4.4.3 Granzyme B cleaves NDUFV1, NDUFS2 and NDUFS1 in intact mitochondria in a valinomycin dependent manner.

GzmB induces ROS directly from mitochondria and cleaves NDUFV1, NDUFS2 and NDUFS1, the three mitochondrial complex I subunits. We reasoned that to investigate in more detail GzmB-induced complex I subunit cleavage we had to purify intact mitochondria as source of ETC complexes without any other cytosolic factors.

When purified mitochondria were treated with GzmB, we detected rapid NDUFV1, NDUFS2 and NDUFS1 cleavage in a dose dependent manner already after one minute of GzmB treatment (Figure 27). Protein cleavage was indicated by decreasing intensity of the full-length forms and also by the appearance of cleavage products.

The size of the cleavage fragment combined with the bioinformatics data allowed us to determine the putative GzmB cleavage sites (Figure 28).

To test our hypothesis that ΔΨm is essential for GzmB uptake into mitochondria and subsequent mitochondrial substrate cleavage, wee used the neutral ionophore Valinomycin. It allows K^+ to cross the mitochondrial membrane disrupting the mitochondrial membrane potential (ΔΨm). Valinomycin inhibits GzmB-induced complex I subunits cleavage suggesting that ΔΨm is important for GzmB entry into the mitochondria to cleave its targets. Although, GzmB entry into the mitochondria is out of the scope of my thesis, it is important to note that it has been shown that GzmA enters mitochondria in a ΔΨm dependent manner to induce ROS and cell death (Martinvalet, et al. 2008).

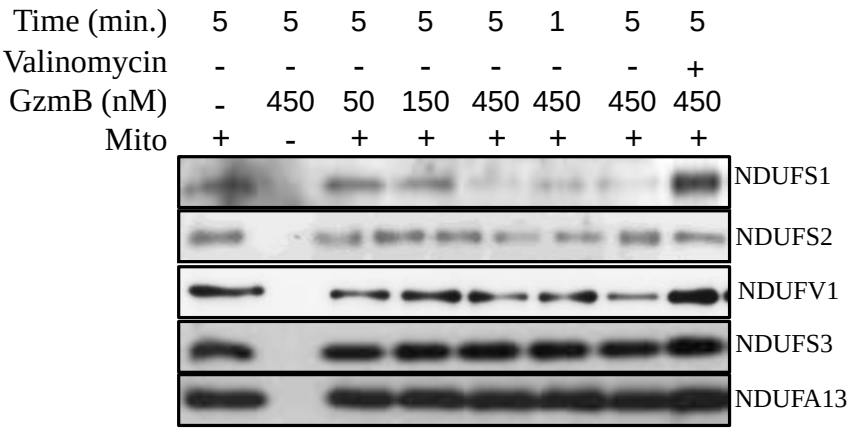

Figure 27: GzmB cleaves NDUFS1, NDUFS2 and NDUFV1 inintact mitochondria in valinomycin dependent manner. Purified mouse liver mitochondria were treated with GzmB, in the absence or presence of Valinomycin. GzmB cleaves NDUFS1, NDUFS2 and NDUFV1 in a dose dependent manner and in absence of Valinomycin whereas NDUFS3 and NDUFA13 are not cleaaved.

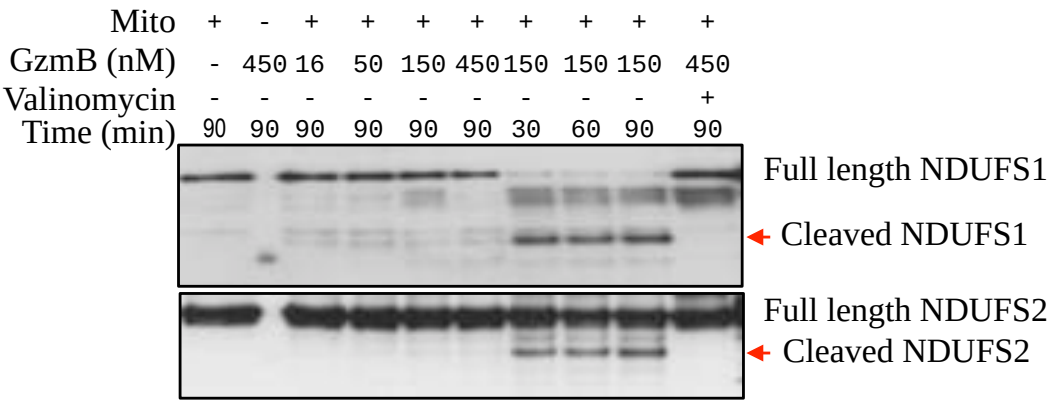

Figure 28: GzmB cleaves NDUFS1 and NDUFS2 in intact purified mitochondria showing a putative cleavage product. Purified mouse liver mitochondria were treated with GzmB, in the absence or presence of Valinomycin. GzmB induce a dose- and time-dependent cleavage of NDUFS1 and NDUFS2.

In agreement with that, it was demonstrated that GzmB targets HAX-1 a mitochondrial protein involved in mitochondrial membrane potential, supporting the role of GzmB activity inside the mitochondria (Han, et al. 2010). To further prove GzmB-induced NDUFS1 and NDUFS2 cleavage as a direct event, we inhibit the mitochondrial AAA ATP-dependent proteases by using the heterocyclic organic compound o-phenanthroline that was demonstrated to specifically inhibit AAA proteases (Ishihara, et al. 2006). GzmB still cleaves NDUFS1 and NDUFS2 in the presence of o-phenanthroline suggesting that these mitochondrial proteases are not involved in GzmB-induced cleavage (Figure 29).

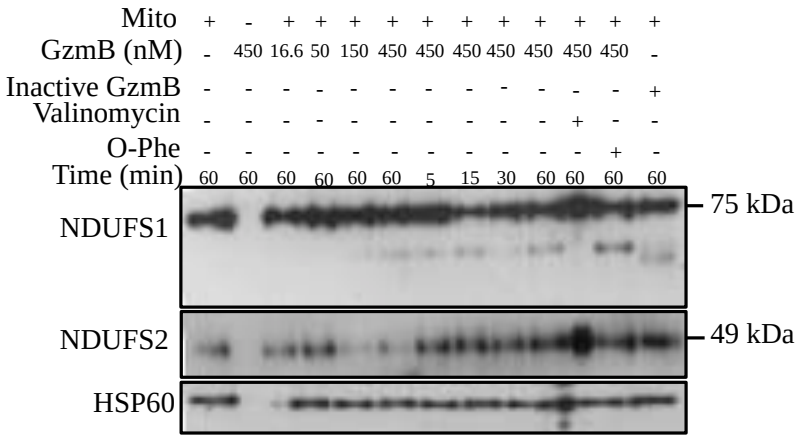

Figure 29: GzmB directly cleaves NDUFS1 and NDUFS2 in intact mitochondria independenlty of the mitochondrial AAA ATP-dependent proteases. Mouse liver mitochondria treated with GzmB and preincubated with Valinomycin, Inactive GzmB, or Phenantrolne show that GzmB cleaves NDUFS1 and NDUFS2 in the presence of mitochondrial inhibitors proteasis o-phenanthroline whereas Valinomycin and Inactive GzmB inhibit this cleavage.

As state earlier MOMP and apoptogenic factor release are important for GzmB cell death pathway. Therefore, we next investigated whether GzmB-induced mitocentric ROS is dependent or not on the MOMP using Bax Bak double (D) KO cells, which do not undergo cytochrome c release and MOMP after GzmB treatment (Figure 30 A and B).

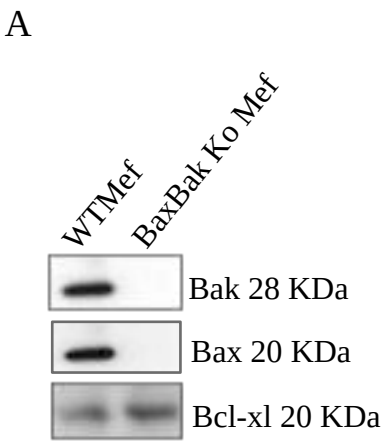

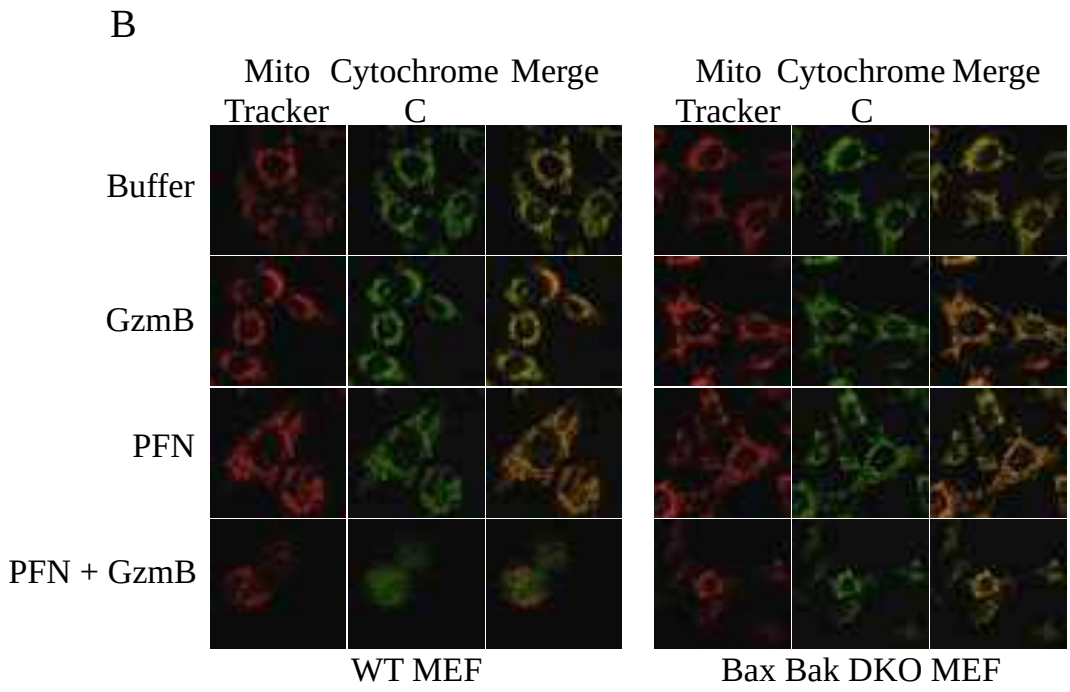

Figure 30: GzmB induced cytochrome c release in WT MEF but not in Bax Bak DKO MEF. (A) Phenotype of Bax Bak doubles KO cells. (B) WT or Bax Bak DKO MEF cells were treated with PFN and GzmB and Cytochrome C release was followed by immunostaining.

When MEF $Bax^{-/-}$ $Bak^{-/-}$ cells were treated with GzmB and PFN, we observed that GzmB still induces potent ROS production and cell death although to a lower extent as compared to the MEF WT cells (Figure 31) suggesting that ROS production and MOMP could be two independent events that synergize in order to kill target cell more efficiently.

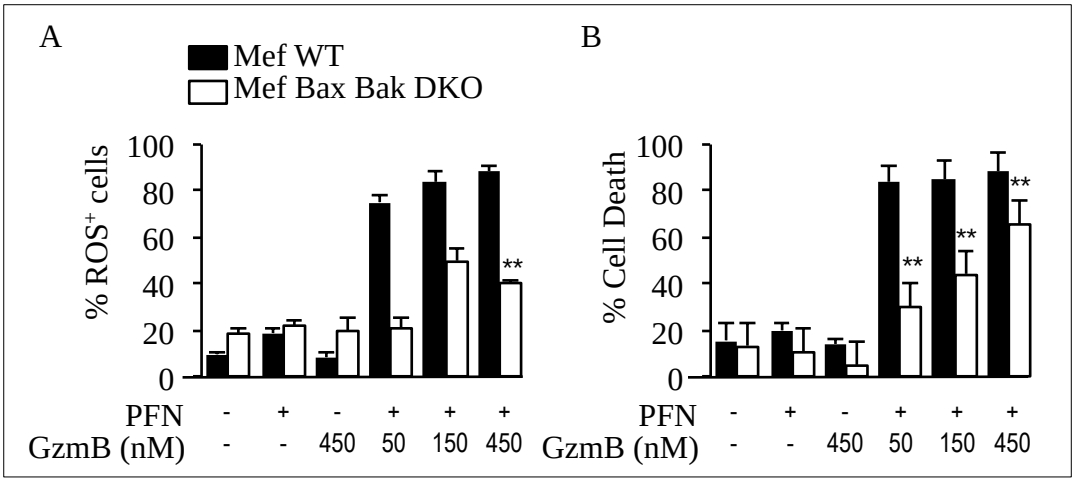

Figure 31: GzmB induces ROS and cell death in WT MEF and Bax Bak DKO MEF. Wild type MEF or Bax Bak double knockout MEF were treated with a sublytic dose of PFN plus GzmB. (A) ROS production was followed by dihydroethidium (HE). (B) Cell death was followed by Annexin V + PI staining. Mean +/- SEM of at least 3 independent experiments is shown, *p<0.05, **p<0.01.

Consequently, we looked at the GzmB-induced cleavage of NDUFV1, NDUFS2 and NDUFS1 in Bax Bak DKO cells. When we overexpressed tagged version of the GzmB targets, we found that GzmB mediated cleavage of complex I subunits was not affected by the absence of Bax and Bak as compared to wild-type cells suggesting that GzmB-induced mitochondrial substrate cleavage is independent of MOMP (Figure 32).

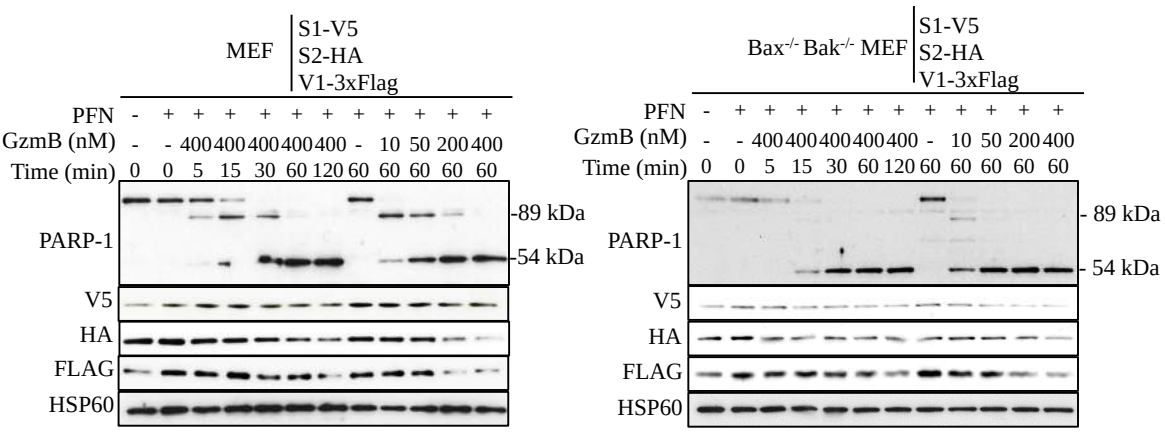

Figure 32: GzmB cleaves NDUFV1, NDUFS2 and NDUFS1 in MEF WT and Bax Bak DKO MEF. MEF WT and MEF Bax Bak DKO cells were treated with sublytic dose of PFN and GzmB and the fate of the overexpressed TAG version of NDUFV1, NDUFS2 and NDUFS1 was followed by WB with the respectively TAG. GzmB induces a dose- and time-dependent cleavage of these subunits similarly to GzmB-inducd PARP1 cleavage in both cell lines.

To further confirm the independence of GzmB-induced mitochondrial substrate cleavage and the mitochondrial outer membrane permeabilization, we looked at the apoptogenic factor release from mitochondria and NDUFS1 cleavage upon GzmB treatment in presence or absence cytosolic factors (S100). For this purpose, purified mouse liver mitochondria were treated with GzmB and apoptogenic factor release as well as NDUFS1 cleavage was followed by immunoblot. Endo G and cytochrome c were only release in presence of cyotosolic factors while complex I subunit cleavage was observed regardless of the addition of S100 (Figure 33). These results consolidate our model that GzmB cleaves NDUFV1, NDUFS2 and NDUFS1 independently from MOMP and both ROS and MOMP synergy to trigger cell death.

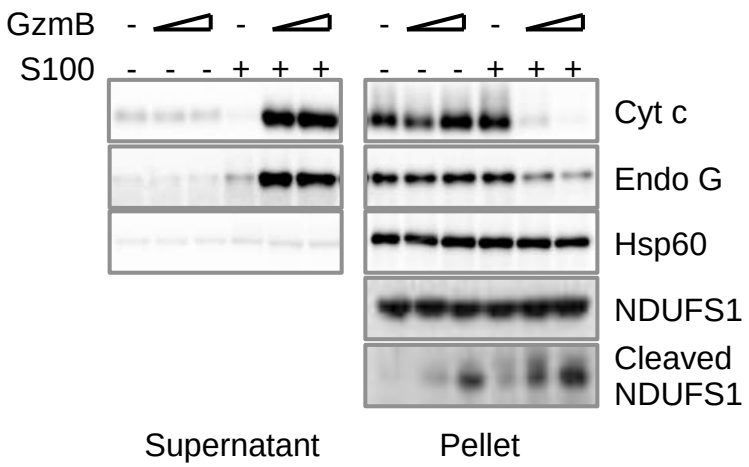

Figure 33: GzmB cleaves NDUFS1 in MOMP independent manner. Purified mitochondria treated with GzmB show GzmB-induced NDUFS1 cleavage indipendently of MOMP. Apoptogenic factors release (Endo G and Cyt c) occurs only after addition of cytosolic factors (S100).

4.4.4 GzmB directly cleaves NDUFV1, NDUFS2 and NDUFS1

So far our findings suggest that GzmB directly acts on the mitochondria by targeting three mitochondrial complex I subunits in order to induce ROS production and cell death. To further investigate the GzmB cleavage of NDUFV1, NDUFS2 and NDUFS1, we expressed and purified recombinant version of the putative GzmB substrates to study whether they are directly cleaved by GzmB. Recombinant proteins are widely used to address the direct interaction of proteins. However, the choice of the appropriate vector, the host where the recombinant protein will be expressed and the tag used are all important factors that must be taken in account for the optimization of expression and to get the highest yield of recombinant proteins while favoring the downstream step of purification. Therefore, we used different strategies to express the recombinant version of NDUFV1, NDUFS2 and NDUFS1. As shown in Figure 34, recombinant NDUFV1, NDUFS2 and NDUFS1 are directly cleaved by GzmB while NDUFS3, NDUFS7 and NDUFA13 are not cleaved.

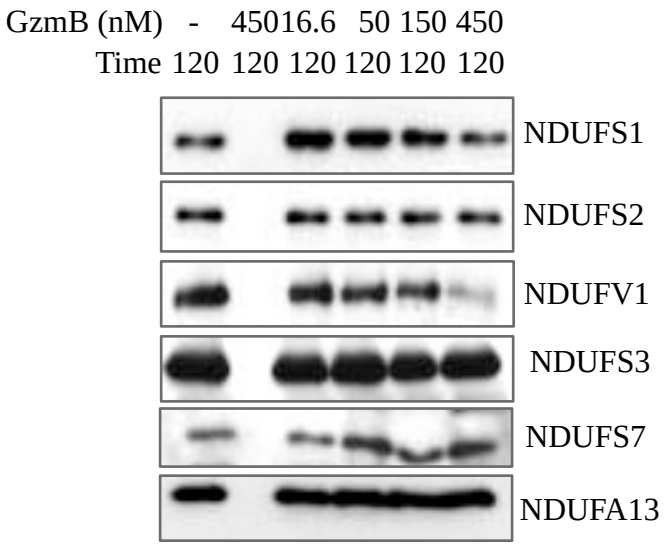

Figure 34: GzmB directly cleaves recombinant NDUFV1, NDUFS2 and NDUFS1. Recombinant protein treated with different dose of GzmB were incubated at 37°C for 2h. GzmB cleaves recombinant human NDUFS1, NDUFS2, and NDUFV1 in a dose dependent manner.

Moreover, recombinant human NDUFV1 expressed with a C terminal His tag, was cleaved by GzmB at concentration as low as 150 nM. This cleavage yielded a 37 kDa C-terminal fragment that corresponds to the predicted cleavage site at position D118 (Figure 35 A). GzmB induced dose dependent cleavage of NDUFS2 with a N-terminal 36 kDa cleavage product that mapped the predicted cleavage site D317 (Figure 35 B). Because of the amount of the cleavage products that were detected only by WB, we could not excise these bands for mass spectrometry analysis to characterize the cleavage sites. Therefore, we used *in vitro* transcription translation with ^{35}S-Methionine labeling based on a cell free extract to produce wild type NDUFV1, NDUFS1 and NDUFS2 or uncleavable D-A mutant version at the putative GzmB cleavage site. Using this approach we found that GzmB cleaved NDUFV1 at positions D118, D338/D340, NDUFS2 at position D317 and NDUFS1 at the position D364 (Figure 35C).

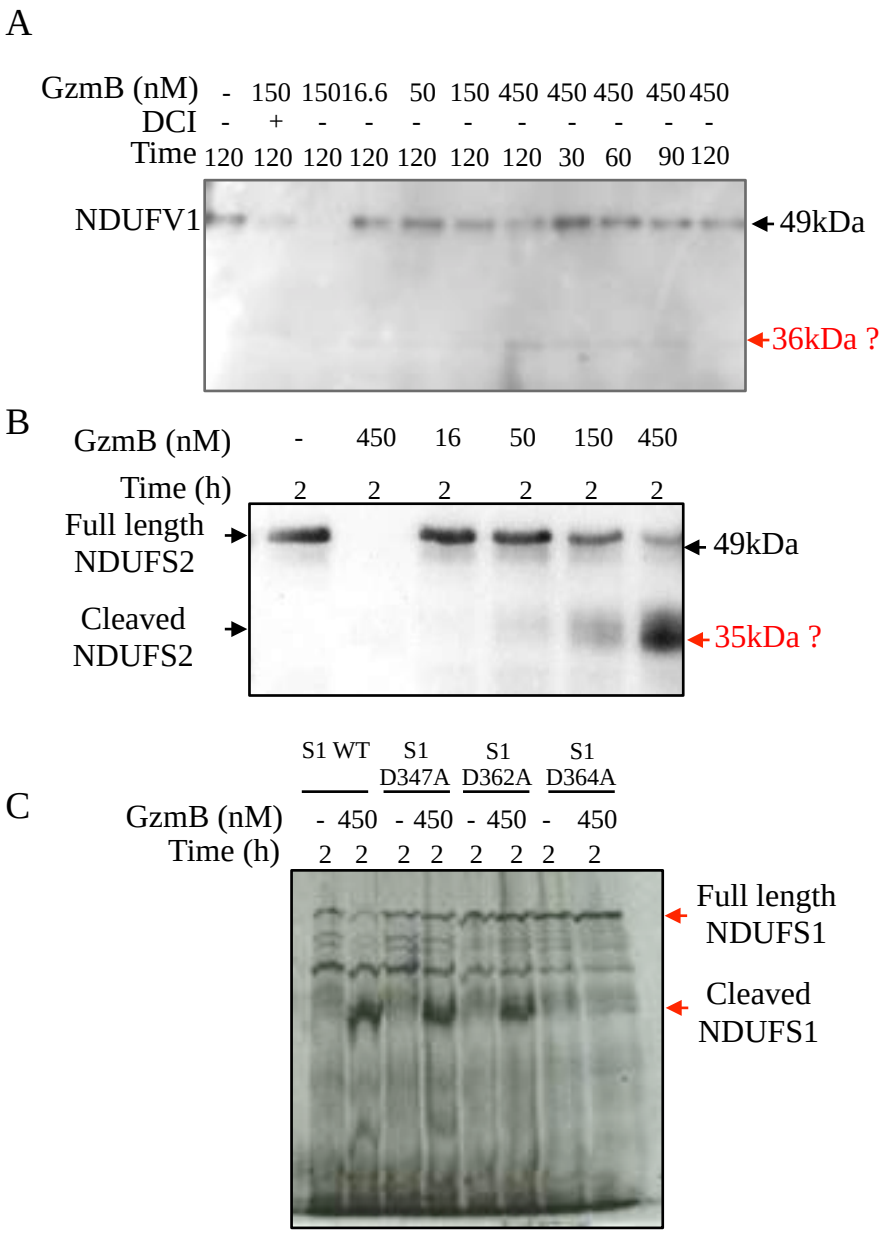

Figure 35: GzmB directly cleaves recombinant His tagged-NDUFV1 and NDUFS2 and 35S-Methionine NDUFS1. C terminal His-tagged NDUFV1 and NDUFS2 treated with GzmB show a putative cleavage site for NDUFV1 (A) and NDUFS2 (B) by using anti His antibody. (C) GzmB induces NDUFS1-^{35}S-Methionine labelled at the position D 364.

Together these results demonstrate that GzmB directly cleaves NDUFV1, NDUFS2 and NDUFS1.

4.4.5 GzmB-uncleavable NDUFV1, NDUFS2 and NDUFS1 inhibit GzmB-induced ROS dependent apoptosis

We next investigated the significance of GzmB cleavage of complex I subunits for this pathway by the use of GzmB uncleavable mutants. We reasoned that the overexpression of GzmB-uncleavable mutants should inhibit GzmB-induced ROS and cell death. We simultaneously overexpressed wild type NDUFV1, NDUFS2 and NDUFS1 or GzmB-uncleavable mutants in K562 cells that were treated with GzmB and PFN and assessed ROS production and cell death. As expected, GzmB-uncleavable mutants showed a decrease in ROS production and cell death without any effect after caspases inhibition (Figure 36 A and B). This strongly confirms that among the others branches, the GzmB cell death pathway, relies on mitochondrial ROS production and these ROS are mainly produced inside the mitochondria after GzmB mediated NDUFV1, NDUFS2 and NDUFS1 cleavage.

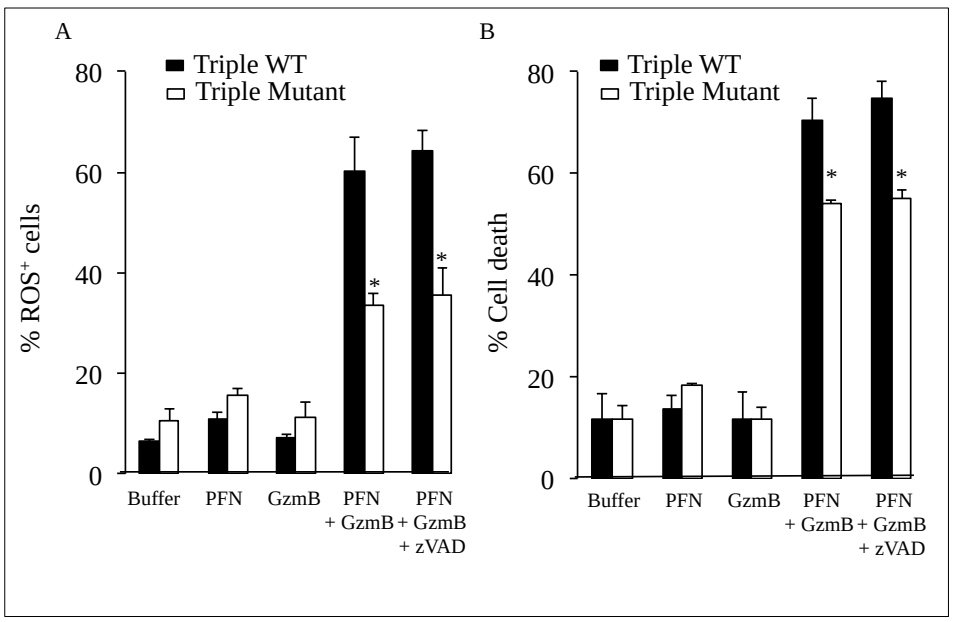

Figure 36: GzmB induces ROS and cell death dependently of GzmB-induced NDUFV1, NDUFS2 and NDUFS1 cleavage. K562 stably expressing native (Triple WT) or GB-uncleavable (Triple mutant) NDUFV1, NDUFS1 and NDUFS2 treated with PFN and GzmB [400nM] and pre incubated with zVAD where indicated, were assessed for mitochondrial ROS by MitoSOX staining (A) and for cell death (B) by annexin-PI staining and flow cytometry. Mean +/- SEM of at least 3 independent experiments is shown *p<0.05, **p<0.01.

4.5 Effect of GzmB-induced mitochondrial ROS:

4.5.1 Cytochrome c, Endo G and Smac release

Upon cell death stimuli, cytochrome c is released into the cytosol where it binds to Apaf-1 to induce apoptosome formation and cell death (Petrosillo et al 2003, 2004). Similarly, Endo G is released from mitochondria to promote apoptosis by inducing DNA damage (Kim et al 2008). Importantly, the mitochondrial apoptogenic factor release has been correlated with the ROS production from the same organelle (Simon, Haj-Yehia and Levi-Schaffer 2000).

Therefore, we investigated whether mitochondrial ROS generated after GzmB treatment could affect the apoptogenic factor release. After GzmB and PFN treatment, U937 cells were fractionated in their cytosolic and mitochondrial component and the release of Cytochrome c, Endo G and Smac were assessed by western blotting. GzmB induces apoptogenic factors release from mitochondria that was delayed by NAC pretreatment or by the overexpression of GzmB-uncleavable mutants form of NDUFV1, NDUFS2 and NDUFS1 (Figure 37 A and B respectively).

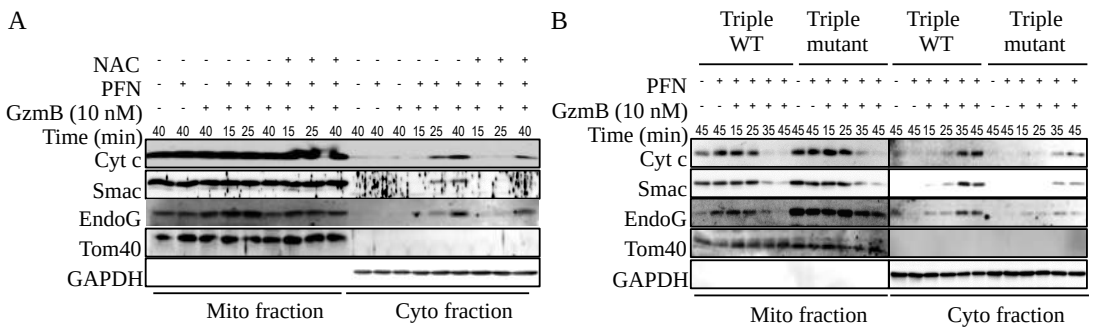

Figure 37: GzmB needs ROS to release apoptogenic factors into the cytosol. (A) U937 cells, treated with Pfn and GzmB and pretreated with NAC as indicated, were fractionated into cytosol (Cyto) and mitochondria (Mito). Release of Cyt c, Smac and EndoG were assessed by immunoblot. Loading and fractionation controls: Tom40 and GAPDH. (B) K562 stably expressing native (Triple WT) or GB-uncleavable (Triple mutant) NDUFV1, NDUFS1 and NDUFS2 were treated as in (A).

4.5.2 DNA fragmentation

GzmB can directly activate DNA damage by cleaving ICAD/DF45 the inhibitor of CAD/DFF40. Activated CAD/DFF40 together with Endo G will then induce oligonucleosomal DNA fragmentation (Thomas, et al. 2000). Since ROS potentiate Endo G release from the mitochondria, we hypothesized that GzmB-induced ROS enhances DNA fragmentation and, consequently, cell death. Agarose gel electrophoresis analysis confirmed that GzmB induces extensive oligonucleosomal DNA fragmentation in U937 cell line. More importantly, DNA fragmentation in U937 cells treated with GzmB plus PFN in the presence of the ROS scavenger NAC was decreased especially at earlier time points (Figure 38 A and B). Moreover, the overexpression of GzmB-uncleavable mutants form of NDUFV1, NDUFS1 and NDUFS2, which decreases GzmB-induced ROS generation, protected from GzmB-mediated DNA fragmentation similarly to the antioxidant treatment (Figure 38 C) indicating an enhancing and accelerating role of ROS in this process. All together these findings support an important contribution of GzmB-induced ROS to DNA damage and cell death.

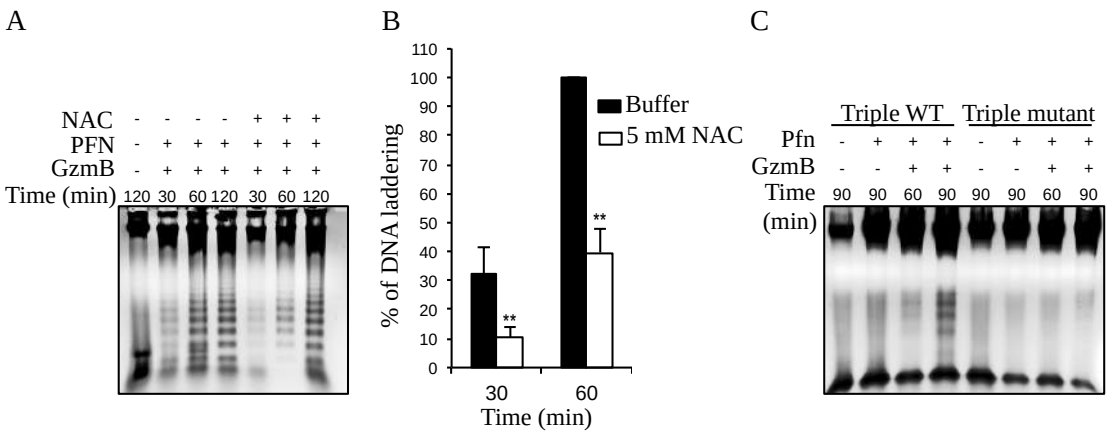

Figure 38: GzmB induces oligonucleosomal fragmentation in U937 and 721.221 cells in a ROS dependent manner. (A-B) GzmB and PFN treatment induce oligonucleosomal DNA fragmentation in U937 cells. Scavenging ROS with NAC pretreatment protect the cell from GzmB-induced DNA fragmentation. (C) GzmB-uncleavable mutants overexpression inhibit GzmB-induced DNA damage. The mean +/- SEM of 3 independent experiments. *p<0.05, **p<0.01.

4.5.3 Lysosomal permeabilization

The lysosomal membrane permeabilization (LMP) is involved into the proteases release into the cytosol and therefore contributes to the cell death features. Recently, a connection between mitochondrial ROS production and LMP was demonstrated. Following TNF treatment, ROS are involved in lysosomal membrane perturbation leading to its permeabilization in a process that is dependent on caspase 9 (Huai, et al. 2013). Therefore, we tested whether GzmB-induced mitochondrial ROS also affect lysosomal membrane integrity and therefore increase cell death extent. U937 cells, treated with GzmB and PFN, were stained with the Lysosenser green dye. The dye measures the lysosome acidic pH. It is fluorescent in intact lysosome and deems in compromised lysosome where the pH becomes basic as the lysosomal membrane is damaged. GzmB plus PFN treatment induces a Lysosenser green fluorescence decrease after 30 min of treatment suggesting that GzmB also triggers lysosome

membrane permeabilization. Interestingly, in the presence of the antioxidant NAC, the Lysosensor green fluorescence was maintained as an indication that scavenging ROS preserve the lysosomal membrane integrity (Figure 39 A). Accordingly, the overexpression of GzmB-uncleavable complex I subunits weakens lysosomal membrane rupture suggesting that GzmB-induced ROS contribute to the lysosomal membrane rupture (Figure 39 B).

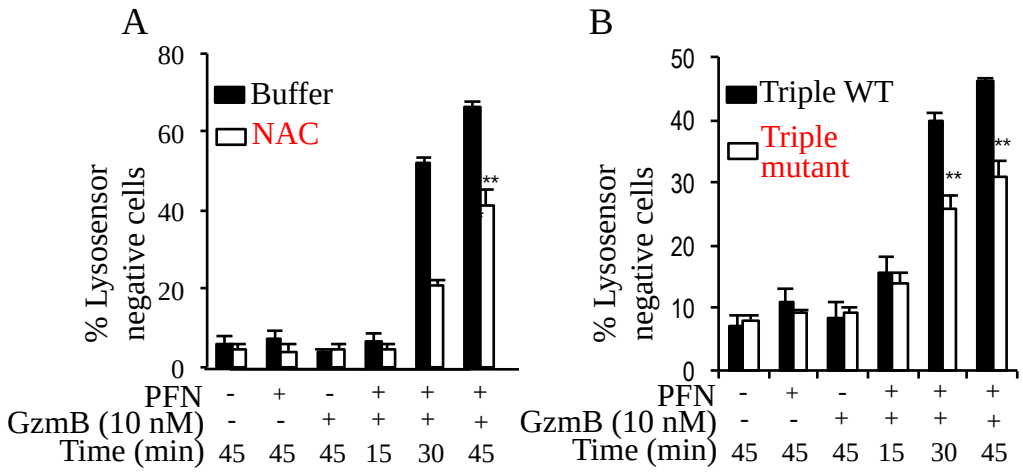

Figure 39: GzmB triggers lysosomal membrane permeabilization in a ROS dependent manner. U937 cells treated with 5 mM NAC as indicated, were stained with Lysosensor which only fluoresces in lysosomes that maintain acidic pH. (A) GzmB-induced lysosomal membrane permeabilization is inhibited by scavenging ROS (NAC) or (B) by overexpressing triple mutant complex I subunits in K562 cells. The mean +/- SEM of 3 independent experiments *p<0.05, **p<0.01.

DNA fragmentation and lysosome membrane permeabilization, in addition to the apoptogenic factor release from mitochondria, allow the conclusion that GzmB-induce ROS potentiate GzmB-induced cell death.

4.5.4 GzmB alters Oxygen consumption

Given the importance of GzmB-induced ROS in mitochondrial cell death, we want to investigate the effect of GzmB on mitochondrial respiration. Purified mitochondria were stimulated with glutamate/malate or succinate and oxygen consumption was measured using a Clark electrode. Within one minute of GzmB addition we observed a drastic change in the slope of oxygen consumption indicating a reduction in mitochondrial oxygen consumption (Figure 40). Importantly, NADH generated by glutammate/malate will give electrons to complex I and $FADH_2$ generated by succinate, will fuel complex II. Both of them will sustain the electron flow to complex III. In this scenario, GzmB-induced mitochondrial respiration loss, suggests that dismantling of complex I at the level of NDUFV1, NDUFS2 and NDUFS1 is only the tip of the iceberg and that GzmB is rather detrimental for the mitochondrial function.

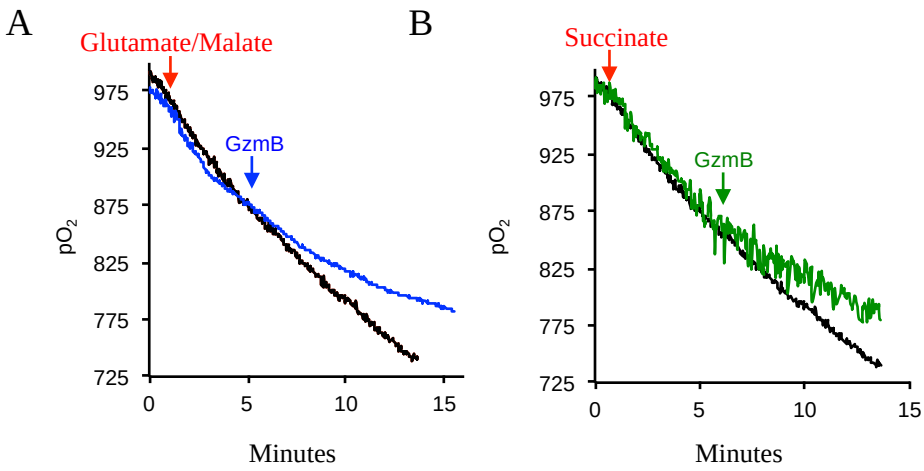

Figure 40: GzmB induces loss of mitochondrial respiration. Purified mouse liver mitochondria in respiration buffer were stimulated with glutamate/malate (A) or succinate (B) and O_2 consumption was measured using a Clark electrode. Data are representative of at least 3 independent experiments.

4.5.5 GzmB alters mitochondrial complex I and III activity

To further investigate the significance of GzmB-induced complex I subunits cleavage on the function of the electron transport chain (ETC) complexes, purified intact mitochondria were treated or not with GzmB before solubilization with lauryl maltoside (LM) containing buffer, which preserves the native and active form of the ETC complexes for in-gel activity assays (Nijtmans et al. 2002) (Smet et al. 2011). ETC complexes were then resolved by blue native gel electrophoresis (BN-gel). As shown in Figures 41 A and B, GzmB induces a dose-dependent inhibition of complex I activity within 1 min of GzmB treatment. This alteration is specific since complex IV or V function is not affected (Figure 41 A-E). Surprisingly, when we measured complex III activity, we found that GzmB also rapidly inhibited complex III activity, although to a lesser extent than complex I (Figure 41 D). However, our main focus on GzmB-induced mitochondrial complex I alterations leave an open question about GzmB targeting mitochondrial complex III.

A

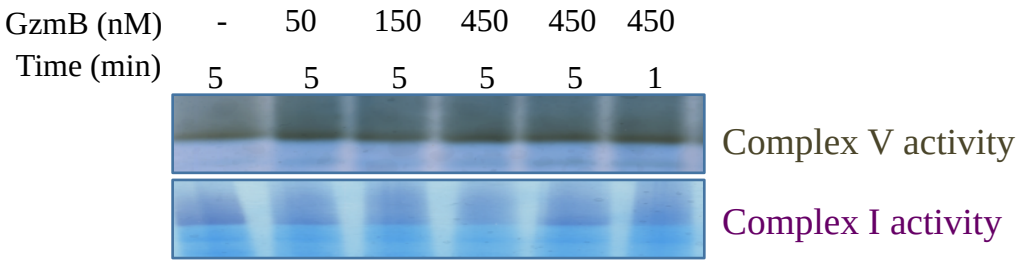
GzmB (nM) - 50 150 450 450 450
Time (min) 5 5 5 5 5 1
Complex V activity
Complex I activity

B

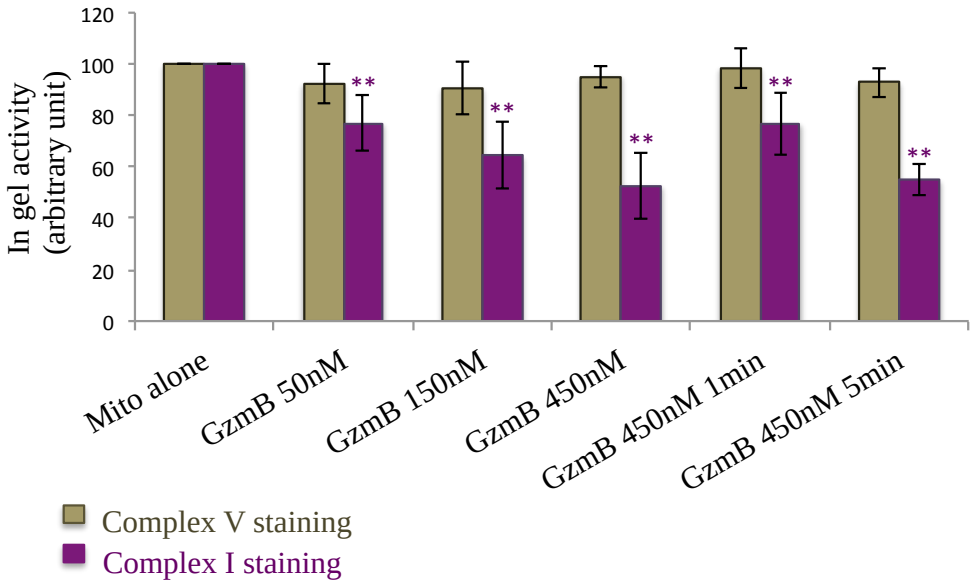
In gel activity (arbitrary unit)
120
100
80
60
40
20
0
**
Mito alone
GzmB 50nM
GzmB 150nM
GzmB 450nM
GzmB 450nM 1min
GzmB 450nM 5min
Complex V staining
Complex I staining

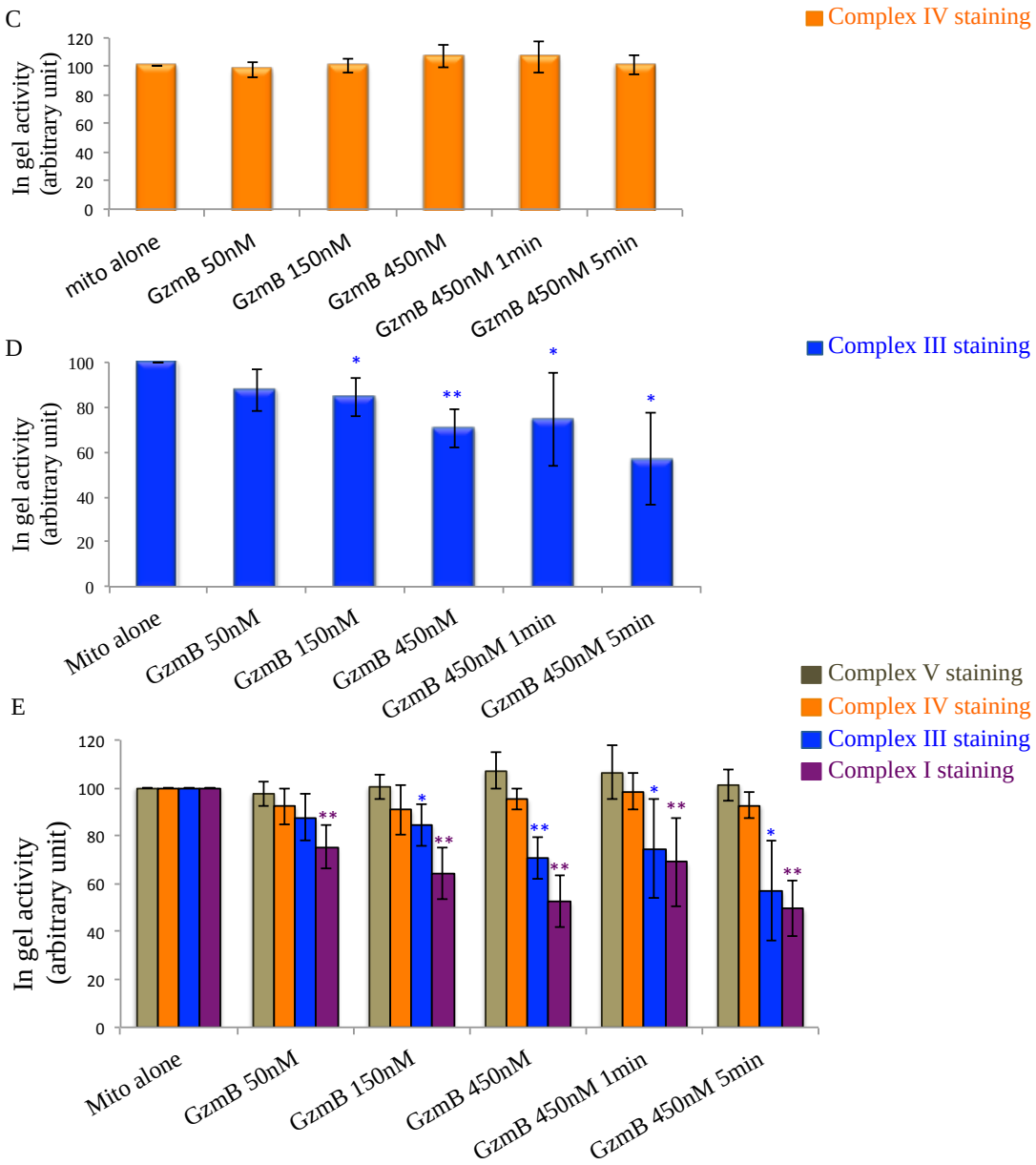

Figure 41: GzmB reduces mitochondrial complex I and III activity. Purified mouse liver mitochondria were treated or not with GzmB, resolved in monomeric ETC complexes by BN gel. In gel activity assays were used to follow complex I, III, IV and V activity. GzmB treatement reduces complex I and III activity (B and D) *p<0.05, **p<0.01.

More interesting, when we compared the activity of mitochondrial electron transport chain complexes after GzmA treatment, we observed that GzmA, alters both mitochondrial complexes I and III activity (Figure 42). All together, these findings highlight the importance of mitochondrial complex I and III disruption for ROS production and cell death, which seems a conserved mechanism between GzmA and GzmB.

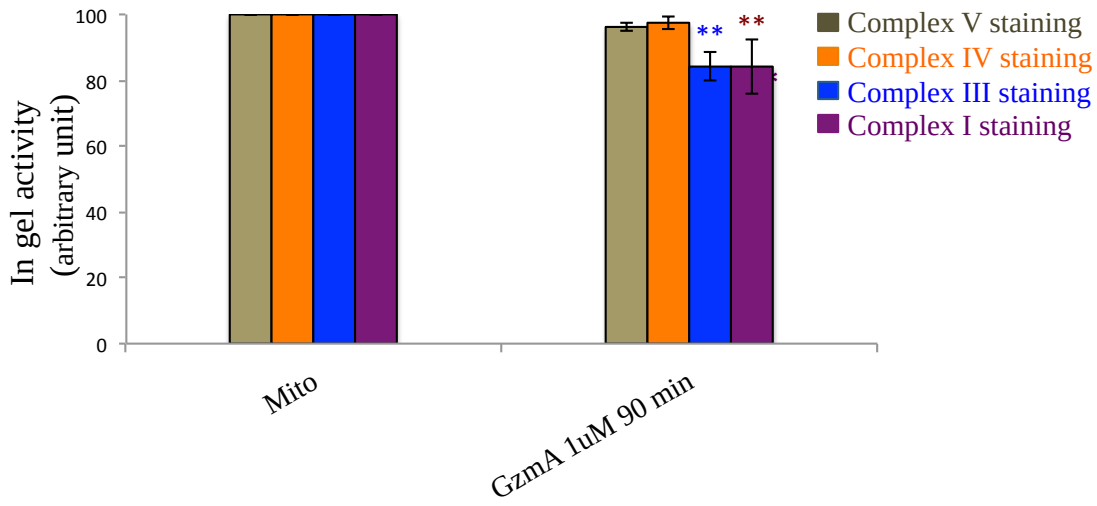

Figure 42: GzmA reduces mitochondrial complex I and III activity. Purified mouse liver mitochondria were treated or not with GzmA, resolved in monomeric ETC complexes by BN gel. In gel activity assays were used to follow complex I, III, IV and V activity. GzmA treatement reduces complex I and III activity. *p<0.05, **p<0.01.

4.5.6 GzmB alters ETC Supercomplexes

GzmB targets mitochondrial complex I via the cleavage of the subunits NDUFV1, NDUFS2 and NDUFS1; this cleavage alters the mitochondrial oxygen respiration and disrupts mitochondrial complexes I as well as, surprisingly, III function. Therefore, to further understand how GzmB induces ROS in order to kill its target cells, we focused

on the ETC organization to see whether GzmB treatment causes structural changes in the respiratory chain. Purified mouse liver mitochondria were treated or not with GzmB. The efficiency of GzmB treatment was assessed by following GzmB-induced NDUFS1 cleavage by WB (Figure 43 A). The samples were then solubilized either with lauryl maltoside (LM) or digitonin (D) containing buffers and resolved in BN-gel. Lauryl maltoside disrupts ETC complexes interaction leading to monomeric complexes resolution, whereas Digitonin, preserves both single and supercomplexes (SC) association. Finally, complex I and III activity was assessed by in gel activity assay from both monomeric complexes and SC (Figure 43 B and C). GzmB disrupts complex I and III activity in monomeric complexes (LM-solubilized samples) but not in supercomplex formation (D- solubilized samples) (Figure 40 D).

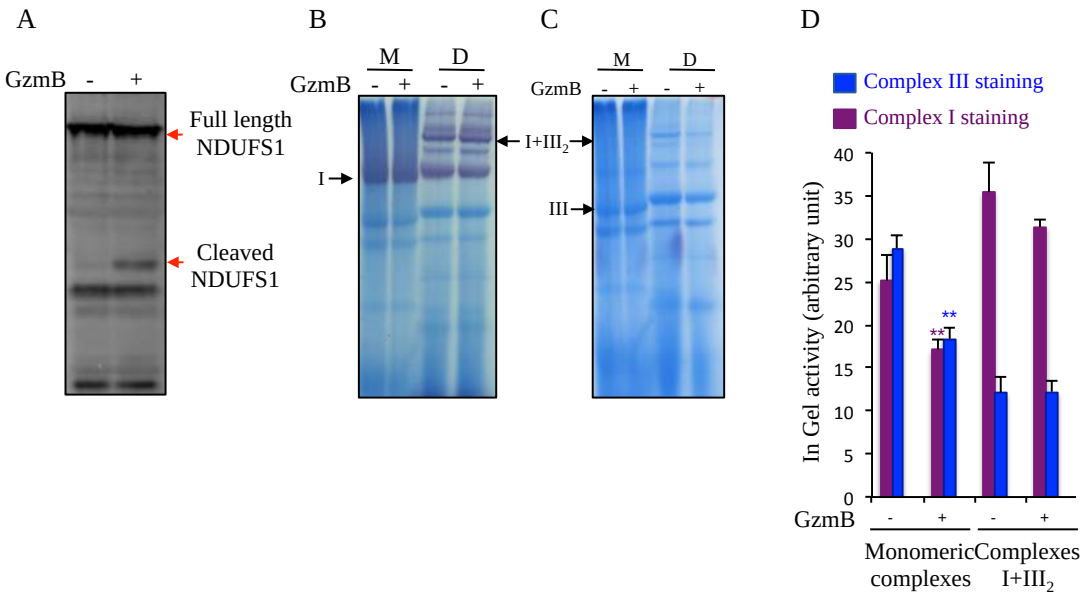

Figure 43: GzmB induces loss of complex I and III activity in monomeric ETC complexes. Purified mouse liver mitochondira were treated or not with GzmB. (A) GzmB cleaves NDUFS1 (B-C) Monomeric ETC complexes (M) and supercomplexes (D) were resolved by BN gel and analized by in gel activity assay. GzmB induces loss of CI and CIII activity from monomeric ETC but not from suopracomplexes$I+III_2$. (D) The mean +/- SEM of at least 3 independent experiments. *p<0.05, **p<0.01.

To further investigate whether GzmB stabilizes complex I and III inside the ETC supercomplexes, the samples were analyzed by western blotting. Obviously, GzmB induces NDUFV1, NDUFS2 and NDUFS1 cleavage in monomeric ETC mitochondria complexes, whereas three tested complex III subunits were unaffected (UQCRC1, UQCR2 or UQCRS1) (Figure 44 A). Surprisingly, GzmB induces an accumulation of NDUFV1, NDUFS2, NDUFS1 as well as of NDUFSA13 and NDUFS3 subunits in Digitonin solubilized mitochondria, suggesting an increase in $I+III_2$ supercomplexes formation (figure 44 B). However, the level of complex I and III activity in SC was unchanged after GzmB treatment. GzmB-induced stabilization of the mitochondrial supercomplexes $I+III_2$ that has same activity levels inside the SC $I+III_2$, suggests that GzmB induces loss of mitochondrial complex I and III specific activity also from the supercomplexes. All together these findings suggest that GzmB-induced NDUFV1, NDUFS2 and NDUFS1 cleavage stabilize the supercomplexes formation. This result implies that GzmB may alter the equilibrium between monomeric complexes and supercomplexes. It is possible that supercomplexes accumulation could be a compensatory mechanism to elevate GzmB-induced ROS production and complex I dysfunction by facilitating mitochondrial electron flow.

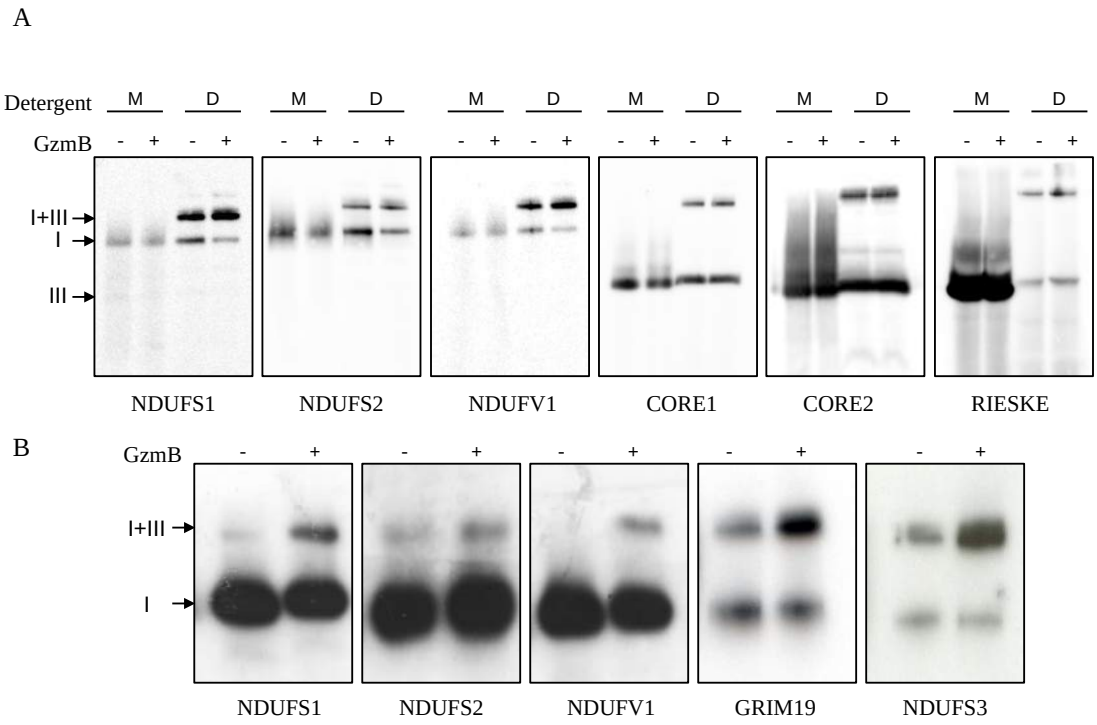

Figure 44: GzmB induces loss of complex I and III activity inside the supercomplexes. (A and B) Purified mouse liver mitochondira were treated or not with GzmB. Monomeric ETC complexes (M) and supercomplexes (D) were resolved by BN gel and analized by WB. GzmB induces accumulation of supercomplex $I+III_2$.

GzmB action on the respiratory chain function lead us to analyze mitochondrial cristae morphology since it plays a critical role in the ETC organization (Cogliati et al., 2013). Therefore, mitochondria treated or not with GzmB were analyzed by Electron microscopy. Surprisingly we observed cristae detachment from the outer mitochondrial membrane rather than opening, after GzmB treatment (Figure 45). However, even though GzmB-induced cristae remodeling is out of the scope of this thesis, it still fits our proposed model. Indeed, cristae opening disrupt supercomplexes organization whereas in our model GzmB stabilizes the supercomplexes formation. Therefore, GzmB could preserve supercomplexes organization by detaching cristae from the mitochondrial outer membrane rather than opening them. However, to

understand the significance of GzmB-induced this morphological and functional aspect needs further investigations.

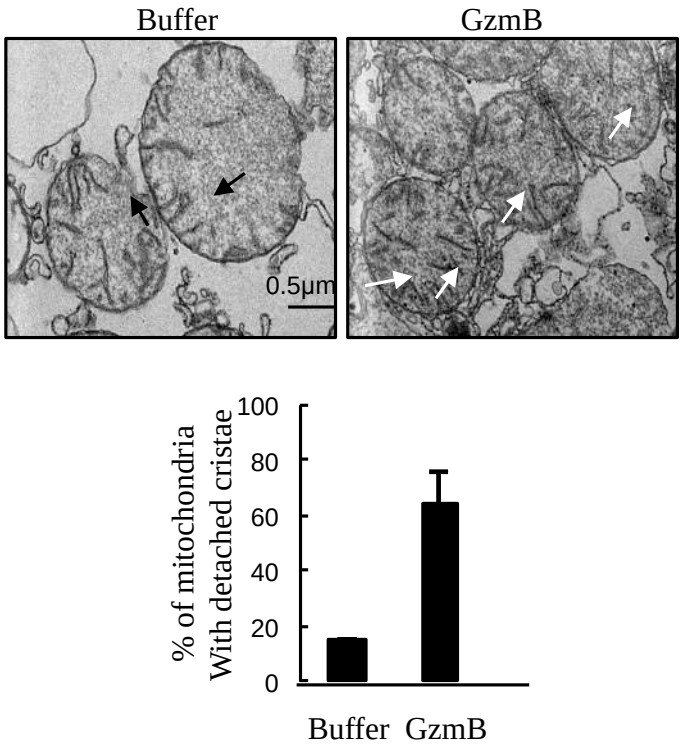

Figure 45: GzmB induces detachment of cristae from the mitochondrial outer membrane. Mitochondria were treated or not with GzmB and analyzed by electron mircroscopy. GzmB induces cristae ditach from mitochondria rather than opening.

Chapter 5
DISCUSSION

5.1 Discussion

We report here that Granzyme B induces a mitocentric ROS production that is required for cell death. As the key element of this novel pathway we propose GzmB-induced complex I dismantling (Figure 46).

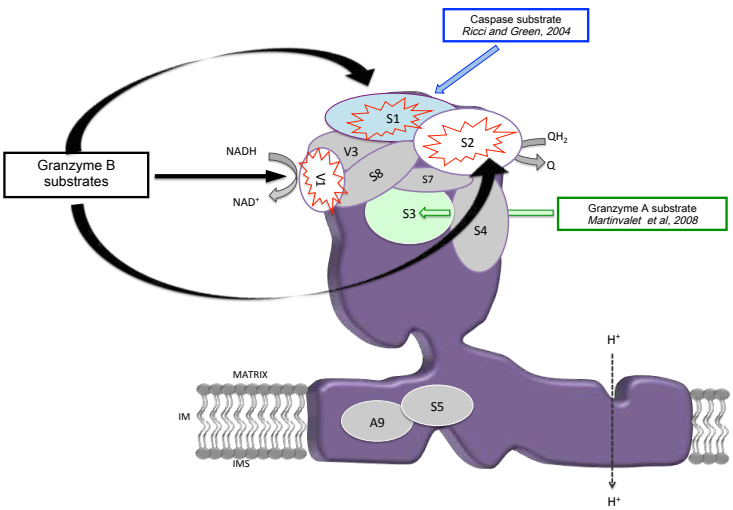

Figure 46: GzmB-induced complex I dismantling. GzmB cleaves the mitochondrial complex I subunits NDUFV1, NDUFS2 and NDUFS1. Similarly, GzmA cleaves NDUFS3 and Caspase 3 cleaves NDUFSc1 in the same complex I. All together these three different cell death pathways coverge at the level of CI, highlightening the role of GzmB-induced mitocentric ROS production by dismantling CI.

In fact, GzmB induces time and dose dependent cleavage of three mitochondrial ETC complex I subunits NDUFV1, NDUFS2 and NDUFS1 (Figure 24 and 25) in order to increase ROS production, independently of the caspases and largely independent of mitochondrial outer membrane permeabilization (MOMP) (Figure 36 and 33). In addition, GzmB-induced complex I dismantling was associated with a loss of mitochondrial respiratory functions. Within 5 minutes after GzmB treatment there was a significant inhibition of complex I and III activity (Figure 41), loss of mitochondrial respiration (Figure 40), detachment of cristae from the mitochondrial inner membrane (Figure 45) and modulation of the electron transport chain supercomplex organization (Figure 44). The involvement of the mitochondria as the source of ROS during GzmB-mediated cell death was further confirmed by the use of ρ^0 cells which lack mitochondrial DNA. After long culture in ethidium bromide, sodium pyruvate and uridine, K562 ρ^0 cells are depleted of mitochondrial DNA, and have reduced in oxygen consumption rate and mitochondrial complex I and complex IV activity. Therefore, ρ^0 cells energy production rely energetically mainly on glycolysis rather than oxidative phosphorylation (King and Attardi 1989). After GzmB treatment we observed that K562 ρ^0 cells were completely refractory to GzmB-induced ROS and cell death (Figure 22) supporting the role of mitochondria as primary source of ROS in this pathway. However it has been proposed that GzmB induces ROS by NADPH oxidase (NOX) enzyme activation in a caspase dependent manner and independently of the mitochondria (Pardo, et al. 2008). In this work Aguillo et al., have shown that GzmB-induced cell death was sensitive to apocynin (NADPH inhibitor) and was abrogated in mitochondrial DNA-depleted cells. They also observed a ROS-dependent phosphatidylserine (PS) exposure, which allows the engulfment of the target cell by mean of its antigen presentation to the phagocytes

(Pardo, et al. 2008). However, the mechanism of ROS-induced PS exposure has not been identified yet and the role of NADPH oxidase, as major ROS reservoir in GzmB-induced cell death, is controversial. Notably, we have shown that MEF deficient for NOX1 or NOX4 ($Nox1^{-/-}$ or Nox 4 $^{-/-}$ knock out) which lack the main component of the NADPH oxidase, were still susceptible to GzmB-induced both ROS and cell death excluding the NOXs from this pathway and supporting the role of a mitocentric ROS production rather than NOX oxidase (Figure 23). Altogether, our results strongly support the role of mitochondria in GzmB induced ROS production and cell death. Moreover the inhibition of GzmB-induced ROS and cell death in k562 ρ^0 cells highlights the fact that GzmB needs a functional respiratory chain to induce cell death and ROS production.

GzmB cleaves NDUFV1, which harbors the NADH binding site. Therefore, this is a direct indication that this action on complex I might affect the electron supply at the first step of the electron transport. Since the ρ^0 data suggested the necessity for an electron flow, the question of ROS production in this pathway is quite intriguing. One possible mechanism to justify ROS production could come from the reverse flow mode of electron transport. This reverse flow mode could be possible only considering the solid state organization of the respiratory chain. In fact, the most updated version of the ETC organization account for an equilibrium between single monomeric ETC (fluid model) and larger structure called supercomplexes (state model). The development of BN-gel technique led Schagger & K. Pfeiffer in 2000 to coin the word respirasome meaning the association of complex I, III and IV in a unique structure or supercomplex, a common feature found not only in bacteria but also in yeast, plants and mammals (Schagger and Pfeiffer 2000). The effective role and the functional consequence of respirasome are still under debate, but current

research is trying to address this issue. It has been proposed that the association of respiratory complexes into supercomplexes may enhance the activity and stability of complex I (Lenaz and Genova 2012), may be involved in optimizing metabolism substrates and reducing oxidative stress. It was recently shown that supercomplex assembly and disassembly is a dynamic process where the electrons have access to their substrates. (Lapuente-Brun, et al. 2013). This picture may be helpful to explain the functional significance of GzmB-induced mitochondrial complex I perturbation. In fact we observed that GzmB treatment favors the supercomplex organization of the respiratory chain (Figure 44), which in our model could account for the maintenance of an electron flow for ROS production. Another possible mechanism for ROS production could come from the exposure of the Fe-S clusters to ambient oxygen following GzmB cleavage. NDUFV1, NDUFS1 and NDUFS2 are all three Fe-S cluster containing subunits of complex I. The Fe-S centers are very reactive to surrounding oxygen and there localization in the heart of the protein body of complex I subunits, isolate them and prevent them from directly reacting with oxygen. Therefore it is reasonable to anticipate that GzmB by cleaving NDUFV1, NDUFS1 and NDUFS2 might expose their Fe-S centers allowing them to react with oxygen and consequently produce radical species. We have observed that GzmB cleaves those subunits inside complex I and inside supercomplex SC I+III_2 (Figure 44). This is in agreement with the topology of complex I. Beside the eccentric size of this 1 MDa complex, NDUFV1 and NDUFS1 are part of the electron entry site localized at the tip of the matrix protruding domain of complex I, which is well exposed to the solvent and therefore accessible to GzmB. Similar conclusion can be made for NDUFS2. Dimeric complex III associate with complex I to form suprercomplex SC I+III_2 by binding the membrane embedded domain of complex I opposite to the matrix

protruding domain. So, even in this configuration NDUFV1, NDUFS2 and NDUFS1 are still accessible to GzmB. Altogether our data give us a good picture of how GzmB triggers ROS production from the mitochondrial complex I.

GzmB alone does not trigger apoptogenic factor release from isolated mitochondria. Endo G and cytochrome c were released from mitochondria only in the presence of GzmB plus cytosolic factors (S100), most likely via the truncation of bid (Figure 33). Until now mitochondrial outer membrane permeabilization and the apoptogenic factors release have been considered essential in the execution of GzmB-mediated cell death. However it has been also shown that GzmB induces cell death in mouse cells genetically deficient for Bid, Bax and Bak mainly involved in MOMP (Han, et al. 2010) (Thomas, et al. 2001) (Heibein, et al. 1999) (MacDonald, et al. 1999). Here, we show that GzmB cleaves complex I regardless of the presence of S100, suggesting that GzmB does not need the MOMP to cleave complex I subunits. Further confirmation was given by the use of Bax Bak DKO cells. These cells do not undergo MOMP and therefore no cytochrome c is released (Figure 30). Interestingly, GzmB still induces ROS increase in these cells, yet to a lesser extent compared to wild-type cells (Figure 31). However, cleavage of NDUFV1, NDUFS2 and NDUFS1 was found to be of comparable efficiency in Bax Bak DKO and wild type MEFs (Figure 32). Together these results indicate GzmB-induced ROS is largely independent of mitochondrial outer membrane permeabilization (MOMP). Our work also indicates the significance of the ROS for apoptogenic factor release. Indeed, GzmB-induced ROS are necessary for proper release of Cyt c, Endo G and Smac from the mitochondrial intermembrane space into the cytosol. This synergistic action of the ROS for apoptogenic factor release could be explained by the ability of ROS to untether these factors from the mitochondrial intermembrane space by disrupting

electrostatic and/or hydrophobic interactions with cardiolipins. Accordingly, Petrosillo et al., have shown that cytochrome c binds the mitochondrial membranes by both electrostatic and hydrophobic interaction and that this interaction is destabilized in a ROS dependent manner (Petrosillo, Ruggiero and Paradies, Role of reactive oxygen species and cardiolipin in the release of cytochrome c from mitochondria 2003) (Petrosillo, Ruggiero and Pistolese, et al. 2004). Consequently, cytoplasmic cytochrome c released will trigger apoptosome formation, caspases-9 activation and cell death . Furthermore ROS enhance Endo G release from mitochondria which in turn may potentiate apoptotic DNA damage (Kim, et al. 2008).

Altogether suggesting that proper apoptogenic factor release requires at least two steps: Bid/Bax/Bak mediated MOMP and ROS that release the factors through the opening generated by the MOMP. Interestingly, GzmB directly cleaves NDUFV1, NDUFS1 and NDUFS2. NDUFV1, NDUFS1 and NDUFS2 are matrix subunit of complex I. This means that GzmB must find its way into the heart of the mitochondria to reach these substrates. As stated early GzmB acts on complex I independently of MOMP, indicating that GzmB does not penetrate the mitochondria through the opening providing by the breach of the outer mitochondrial membrane, taking place during MOMP. How GzmB enters the heart of these double membrane organelles is an opened question. Bioinformatics analysis indicates that GzmB does not have a canonical N-terminal mitochondrial matrix targeting sequence. We have also confirmed that GzmB requires an intact mitochondrial membrane potential to enter the organelles. Indeed the protonophore valinomycin inhibits GzmB entry into the mitochondria (Figure 27). The requirement for an intact membrane potential raises the question of the hierarchy between MOMP and ROS production. Since MOMP also result in loss of membrane potential, GzmB must enter mitochondria that do not

undergo MOMP or access the organelle before MOMP takes place. This later hypothesis stresses even more the importance of the ROS pathway during GzmB cell death pathway. Definitely more work is needed to understand the hierarchy of these events: GzmB mitochondrial import, ROS production, MOMP, apoptogenic factor release and caspase-3 activation.

DNA fragmentation is a key feature of apoptosis. It is the result of the combined action of CAD and Endo G among other DNAses being activated during apoptotic cell death. GzmB-induced ROS production is also necessary for oligonucleosomal DNA fragmentation. This was expected since the ROS favor Endo G release from the mitochondria. However the extent of inhibition of DNA fragmentation suggests that ROS is also necessary for CAD action. We observed that anti-oxidant or over expression of GzmB-uncleavable complex I subunits do not alter ICAD cleavage however they severely compromised DNA laddering (Figure 38). One possible explanation for this observation is that ROS might also enhance nucleocytoplasmic shuttling of CAD and Endo G. Here again more work is required to understand how ROS contribute to GzmB-induced DNA fragmentation. Interestingly, we have also demonstrated that GzmB-mediated ROS favor the late endosome permeabilization in order to seal the death sentence. It is possible that ROS by reacting with the lipid destabilized this highly explosive cellular compartment to mediate the leakage of the deadly lysosomal enzymes.

GzmA and caspase 3 also directly attack complex I to cleave NDUFS3 and NDUFS1, respectively. This indicates that three cell death pathways, GzmA, caspases-3 and GzmB, converge at the level of complex I to induce ROS dependent cell death. Moreover, in a recent study by Walch et al., it was demonstrated that GzmB uses a similar mechanism of ROS induction to kill bacteria (Walch et al. 2014 *Cell* in press).

In this work, it was shown that granulysin, a prokaryotic membrane disrupting protein only expressed in human killer cells, delivers GzmA and GzmB into bacteria resulting in the cleavage of the bacterial complex I subunits and ROS-dependent bacterial death. Taken together these results unravel an unexpected central role for complex I disruption and ROS production during cell death. Indeed, these results depict complex I as a novel point of crosstalk of three cell death pathways. Moreover, the conservation of this process across two animal phyla suggests that contrary to the common understanding of ROS as bystander, there is a conserved biochemical pathway dedicated to the production of ROS during cell demise that is centered on the dismantling of the respiratory chain complex I. This is in agreement of the critical role of complex I for energy and ROS production. I think that putting the ROS at their rightful place in the field of cell death will definitely open new avenues of investigation to dissect their mode of action. It is logical to anticipate that targeting complex I and/or ROS could also be novel strategy to harness the oxidative stress arm of cell death for therapeutic intervention aiming either at increasing or dampening apoptosis depending of the pathological conditions.

5.2 Conclusion

Granzyme B-induced cell death has been shown to occur in a caspases -dependent and -independent manner. The aim of this study was to investigate the molecular mechanism by which GzmB induces cell death in a novel pathway by targeting directly the mitochondria in order to induce ROS production. During this thesis we confirmed GzmB-induced caspase independent and dependent cell death pathway and we identify a novel mitocentric GzmB-induced ROS dependent apoptotic pathway. By using bioinformatics, proteomic and cellular approaches we identify three mitochondrial complex I subunits to be direct targets of GzmB. We show that GzmB induces:

- Mitocentric ROS production by directly cleaving three mitochondrial complex I subunits (NDUFV1, NDUFS2 and NDUFS1) in a valinomycin-sensitive and caspases and MOMP-insensitive manner.
- ROS-enhanced cytochrome c, Endo G and Smac release, DNA fragmentation and Lysosomal permeabilization.
- Functional changes in mitochondria by reducing Oxygen consumption, mitochondrial complex I and III activities by altering the supercomplex organization and by detaching cristae from the mitochondrial outer membrane.

Our data demonstrate that GzmB acts preferentially at the level of mitochondria in order to induce ROS-dependent cell death. GzmA directly cleaves NDUFS3 and caspase 3 cleaves NDUFS1, two other mitochondrial complex I subunits. All together suggests that three cell death pathways converge at the level of the same

mitochondrial complex I in order to induce target cell death more efficiently. GzmB-substrates cleavage, leads to electron leakage for ROS production. Deregulation of complex I and III activities, reduction in oxygen respiration, cristae remodeling as well as unbalance between monomeric electron transport chain and supercomplex are all new feature of GzmB-mitochondrial pathway to destroy target cells (Figure 47).

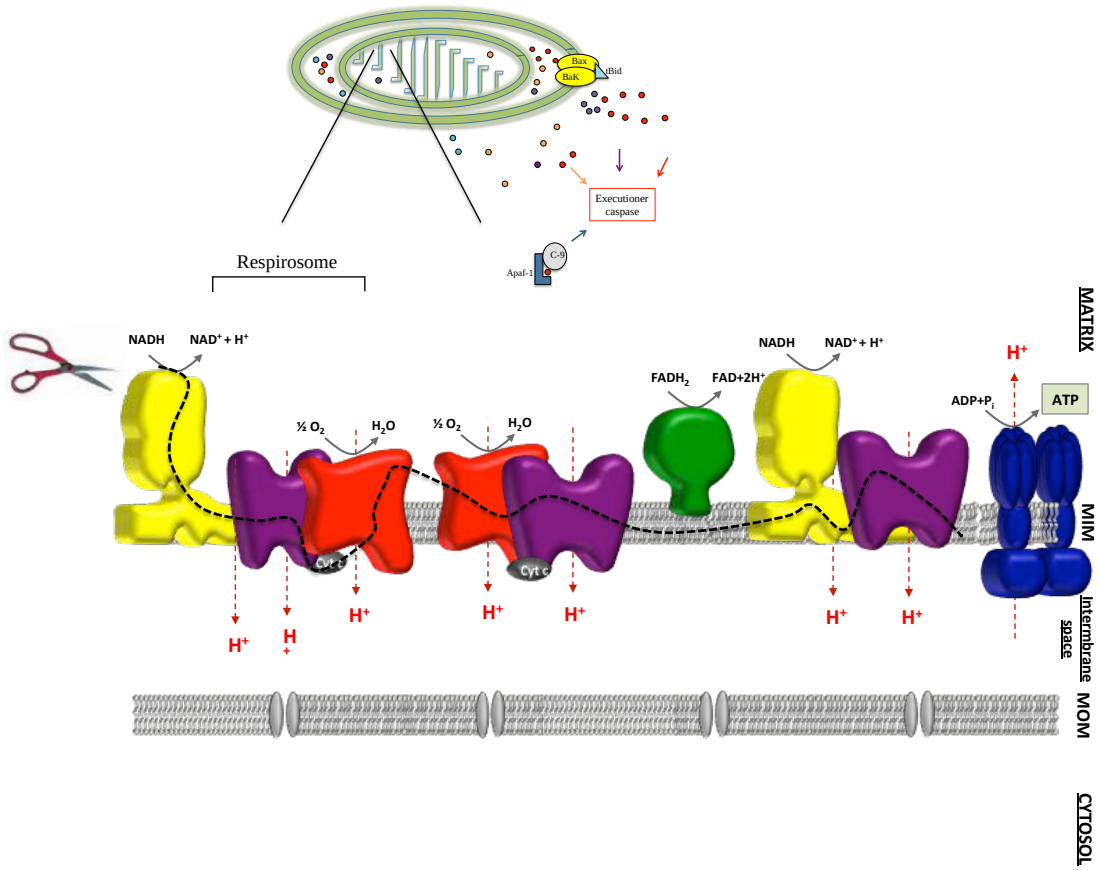

Figure 47: GzmB-induced mitocentric ROS dependent pathway. GzmB induces mitocentric ROS production by cleaving three mitochondrial complex I subunits. GzmB reduces oxygen respiration, and mitochondrial complex I and III activity. GzmB alters mitochondrial ETC organization by stabilizing the supercomplex. GzmB-induced ROS from complex I contribute to apoptogenic factor release and cell death.

5.3 Perspective

Mitochondria pictured as Pandora's vase, which plays a central role in the life as well as in the death of the organism, have been designated as the main ROS producers particularly from complex I and III. In this thesis we have carried out a large-scale of bioinformatics, proteomics and cellular studies in order to clear up the role of GzmB in cell death. This has led to the discovery of a novel apoptotic pathway where GzmB primarily and directly affects mitochondria, mainly complex I and III, in order to induce a massive ROS production and cell death. However, the mechanism by which ROS contribute to GzmB-induced cell death, the putative GzmB effects on mitochondrial complex III and cristae remodeling, as well as GzmB entry into the mitochondria, are all aspects that need more elucidation.

The main role of ROS in GzmB-induced cell death pathways has been extensively demonstrated here, pointing out the mitochondrial complex I as a source of ROS production. It will be significant to establish the precise amount and composition of ROS after GzmB treatment by *in vivo* electron spin resonance (ESR), which will detect unpaired electrons. Furthermore, it will be also important to check ROS-induced protein carbonylation, proteins and lipids oxidation after GzmB treatment.

Here we showed that GzmB reduces complex III activity. Although we could not find any GzmB targets at the level of complex III (GzmB did not cleave UQCRB, UQCRC1, UQCRC2 and UQCRFS1), we cannot exclude that GzmB induces other complex III subunits cleavage. This can be assessed by following the fate of the other mitochondrial complex III subunits after GzmB treatment in cell loading experiments or with overexpressed tagged proteins, by WB.

GzmB induces cristae detachment from the mitochondrial membrane. Mitochondrial cristae morphology is critical for cell death. It has been shown that tBid destabilizes the fusion protein OPA1, leading to cristae opening, cytochrome c release and cell death. Moreover, the correct cristae morphology is important to preserve the optimal ETC organization and function (Cogliati, et al. 2013). Therefore, cell lacking for fission (DRP1) or fusion proteins (OPA1) will be treated with GzmB and ROS production, cell death and apoptogenic factor release will be assessed by MitoSOX, Annexin V/PI staining and western blotting.

GzmB enters into the mitochondria to cleave NDUFV1, NDUFS2 and NDUFS1, three mitochondrial complex I subunits. Since GzmB, similarly to GzmA, lacks the classical mitochondrial import sequence, the mechanism how it enters into the mitochondrial remains unclear is part of our laboratory research. A preliminary investigation on this direction has been carried using the yeast deficient for TOM (Tom 70, Tom 22 and Tom 20) and, being TOM part of the canonical import machinery, it allows us to exclude TOM involvement in GzmB entry into the mitochondria. By using a combination of immune precipitation (IP) and mass spectrometry analysis will be possible to identify the putative mitochondrial GzmB receptor. This candidate will be further tested by using yeast genetic approach and by gene knock down (KD) experiments. Cells expressing low levels of the putative GzmB receptor will be treated with GzmB. We expect that GzmB entry into the mitochondrial will be inhibited and GzmB-induced NDUV1, NDUFS2 and NDUFS1 cleavage, ROS production, apoptogenic factors release and cell death will be assessed as discussed above.

To conclude, our work characterizes a novel cell death mechanism and confirms GzmB as a molecular player that by destroying mitochondrial complex I and by

generating a massive ROS production from this organelle could serve as a potential therapeutic target in many pathological conditions and aging.

Chapter 6
BIBLIOGRAPHY

Abbas, AK, and AH Lichtman. "Cellular and Molecular Immunology." 5th ed. (2003).

Abe, Y, et al. "Structural basis of presequence recognition by the mitochondrial protein import receptor tom 20." *Cell* 100 (2000): 551-560.

Acin-Perez, R, et al. "Respiratory complex III is required to maintain complex I in mammalian mitochondria." *Mol.Cell.*, 2004: 805-815.

Adams, JM, and S Cory. "The Bcl-2 protein family: arbiters of cell survival." *Science* 281 (1998): 1322-1326.

Andreyev, AY, Kushnareva, and AA Starkov. "Mitochondrial metabolism of reactive oxygen species." *Biochemistry (Mosc)*, 2005: 200-14.

Arnoult, Damien, Brigitte Gaume, Mariusz Karbowski, Juanita C.Sharpe, Francesco Cecconi, and Richard Youle. "Mitochondrial release of AIF and EndoG requires caspase activation downstream of Bax/Bak-mediated permeabilization." *The EMBO Journal* 22 (2003): 4385-4399.

Ashkenazi, A. *Nat Rev Cancer* 2(6) (2002): 420-30.

Ashkenazi, A, and VM Dixit. "Death receptors: Signaling and modulation." *Science* 281 (1998): 1305-8.

Ashkenazi, A, P Holland, and SG Eckhardt. "Ligand-based targeting of apoptosis in cancer: the potential of recombinant human apoptosis ligand 2/tumor necrosis factor-related apotosis-inducing lignad rhApo2L/TRAIL." *J Clin Oncol* 26 (2008): 3621-3630.

Balaji, KN, N Schaschke, W Machleidt, M Catalfamo, and PA Henkart. "Surface cathepsin B protects cytotoxic lymphocytes from self-destruction after degranulation." *J. Exp. Med.*, 2002: 493-503.

Becker, L, et al. "Preprotein translocase of the outer mitochondrial membrane: reconstituted Tom40 forms a characteristic TOM pore." *J Mol Biol* 353 (2005): 1011-1020.

Benedict, M.A., Y Hu, N Inohara, and G Nunez. "Expression and functional analysis of Apaf-1 isoforms. Extra Wd-40 repeat is required for cytochrome c binding and regulated activation of procaspase-9." *J. Biol. Chem* 275 (2000): 8461-8468.

Bereiter-Hahn, J, and M Voth. "Dynamics of mitochondria in living cells: shape changes, dislocations, fusion, and fission of mitochondria." *Microsc Res Tech.* 27, no. 3 (1994): 198-219.

Bernardi, P, and GF Azzone. "Cytochrome c as an electron shuttle between the outer and inner mitochondrial membranes." *J Biol Chem* 256 (1981): 7187-7192.

Bianchi, C, ML Genova, G Parenti Castelli, and G Lenaz. "The mitochondrial respiratory chain is partially organized in a supercomplex assembly: kinetic evidence using flux control analysis." *J Biol Chem* 279 (2004): 36562-36569.

Block, K, and Y Gorin. "Aiding and abetting roles of NOX oxidases in cellular transformation." *Nat Rev Cancer* 12 (2012): 627-637.

Boumans, H, JA Berden, LA Grivell, and K van Dam. "Metabolic control analysis of the bc1 complex of Saccharomyces cerevisiae: effect on cytochrome c oxidase, respiration and growth rate." *Biohem J*, 1998: 877-883.

Brand, M, AJ Kowaltowski, NC De Souza-Pinto, RF Castilho, and AE Vercesi. "The sites and topology of mitochondrial superoxide production." *Free Radic Biol Med* 47 (2009): 333-343.

Brandt, U. "Energy converting NADH:Ubiquinone oxidoreductase." *Annu Rev Biochem.* 75 (2006): 69-92.

Bratton, SB, M MacFarlane, K Cain, and GM Cohen. "Protein complexes activate distinct caspase cascades in death receptor and stress-induced apoptosis." *Exp Cell Res* 256(1) (2000): 27-33.

Britton, Chance, and G.R. Williams. "A Method for the Localization ofSites for Oxidative Phosphorylation." *Nature* 176, no. 4475 (1955): 250-254.

Brunner, T, RJ Mogil, and D LaFace. "Cell- autonomous Fas (CD95)/Fas-ligand interaction mediates activation-induced apoptosis in T-cell hybridomas." *Nature* 373 (1995): 441-444.

Cain, Kelvin K, David G Brown, Claudia Langlais, and Gerald M Cohen. "Caspase activaton involves the formation of the apoptosome, a large (approximately 700 kDa) caspase-activating complex." *J. Biol. Chem* 274 (1999): 22686-22692.

Cairns, B. "Rude unhinging of the machinery of life: metabolic approaches to hemorrhagic shock." *Curr Opin Crit Care* 7 (2001): 437-443.

Calvo, S, et al. "Systematic identification of human mitochondrial disease genes through integrative genomics." *Nat Genet* 38 (2006): 576-582.

Cammann, K. "Ion-selective bulk membranes as models." *Top. Curr. Chem* 128 (1985): 219-258.

Cande, C, F Cecconi , P Dessen, and G Kroemer. "Apoptosis-inducing factor (AIF): key to the conserved caspase-independent pathways of cell death?" *J Cell Sci* 15 (2002): 4727-4734.

Cande, C, F Cecconi, and G Kroemer. "Apoptosis-inducing factor (AIF): key to the conserved caspase-independent pathways of cell death?" *J Cell Sci* 15 (2002): 4727-4734.

Carroll, J, I M Fearnley, J M Skehel, R J Shannon, J Hirst, and J.E. Walker. "Bovine complex I is a complex of 45 different subunits." *J. Biol. Chem* 281 (2006): 32724–32727 .

Casciola-Rosen, Livia, et al. "Granzyme B have distinct tetrapeptide specificities and abilities to recruit Bid Pathway." *The Journal of Biological Chemistry* 282, no. 7 (2007): 4545-4552.

Cereghetti, GM, et al. "Dephosphorylation by calcineurin regulates translocation of Drp1 to mitochondria." *Proc Natl Acad Sci* 105 (2008): 15803-8.

Chan, DC. "Dissecting mitochondrial fusion." *Dev. Cell* 11 (2006): 592-4.

Chang, CR, and C Blackstone. "Cyclic AMP-dependent protein kinase phosphorylation of Drp1 regulates its GTPase activity and mitochondrial morphology." *J Biol Chem* 282 (2007): 21583-21587.

Chen, H, SA Detmer, AJ Ewald, EE Griffin, and DC Chan. "Mitofusins Mfn1 and Mfn2 coordinately regulate mitochondrial fusion and are essential for embryonic development." *Journal of Cell Biology* 160 (2003): 189-200.

Cho, YS, et al. "Phosphorylation-driven assembly of the RIP1–RIP3 complex regulates programmed necrosis and virus-induced inflammation." *Cell* 137 (2009): 1112-1123.

Chowdhury, D, and J Lieberman. "Death by a thousand cuts: granzyme pathways of programmed cell death." *Annu Rev Immunol* 26 (2008): 389-420.

Cogliati, S, et al. "Mitochondrial cristae shape determines respiratory chain supercomplexes assembly and respiratory efficiency." *Cell* 155, no. 1 (2013): 160-71.

Cory , S, and JM Adams. "The Bcl2 family: regulators of the cellular life-or-death switch." *Nat Rev Cancer* 2, no. (9) (2002): 647-656.

Cryns, VL, et al. "Specific proteolysis of the kinase protein kinase C-related kinase 2 by caspase-3 during apoptosis. Identification by a novel, small pool expression cloning strategy." *J. Biol. Chem.* 272 (1997): 29449-29453.

Declercq, W, T Vanden Berghe, and P Vandenabeele. "RIP kinases at the crossroads of cell death and survival. ." *Cell* 138 (2009): 229-232.

Denault, JB, and GS Salvesen. "Capsases: keys in the ignition of cell death." *Chem Rev* 102(12) (2002): 4489-500.

D'Herde, K, et al. "Ultrastructural localization of cytochrome c in apoptosis demonstrates mitochondrial heterogeneity." *Cell Death Differ* 7 (2001): 331-337.

Diaz, F, H Fukui, S Garcia, and CT Moraes. "Cytochrome c oxidase is required for the assembly/stability of respiratory complex I in mouse fibroblasts." *Mol.Cell.Biol.* 26 (2006): 4872–4881.

Du, C, M Fang, Y Li, L Li, and X Wang. "Smac, a mitochondrial protein that promotes cytochrome c-dependent caspase activation by eliminating IAP inhibition." *Cell* 102 (2000): 33-42.

Dudkina, NV, H Eubel, W Keegstra, EJ Boekema, and HP Braun. "Structure of a mitochondrial supercomplex formed by respiratory-chain complexes I and III." *Proc Natl Acad Sci*, 2005: 3225-9.

Dunai, Z, PI Bauer, and R Mihalik. "Necroptosis: biochemical, physiological and pathological aspects." *Pathol. Oncol. Res*, 2011: 791-800.

Dunai, Z, PI Bauer, and R Mihalik. "Necroptosis: biochemical, physiological and pathological aspects." *Pathol. Oncol. Res.* 14 (2011): 791-800.

Elmore, S. "Apoptosis: a review of programmed cell death." *Toxicol Pathol* 35 (2007): 495-516.

Fellows, Edward, Shirley Gil-Parrado, E. Jenne Deiter, and Florian C Kurschus. "Natural killer cell–derived human granzyme H induces an alternative, caspase-independent cell-death program." *Blood* 11 (2007): 544-552.

Fernandez-Vizarra, E, V Tiranti, and M Zeviani. "Assembly of the oxidative phosphorylation system in humans: what we have learned by studying its defects." *Biochim. Biophys. Acta.* 1793 (2009): 200-211.

Fischer, U, RU Janicke, and K Schulze-Osthoff. "Many cuts to ruin: a comprehensive update of caspase substrates." *Cell Death and Differentiation* 10 (2003): 76-100.

Fridovich, I. "The trail to superoxide dismutase." *Protein Science*, 1998: 2688–2690.

Froelich, C.J., et al. "New paradigm for lymphocyte granule-mediated cytotoxicity." *J. Biol. Chem*, 1996: 29073-29079.

Futai, M, T Noumi, and M Maeda. "ATP synthase (H+-ATPase): results by combined biochemical and molecular biological approaches." *Annu Rev Biochem* 58 (1989): 111-136.

Galluzzi, L, and G Kroemer. "Necroptosis: A Specialized Pathway of Programmed Necrosis." *Cell* 135 (2008): 1161–1163.

Galluzzi, Lorenzo, and Guido Kroemer. "Necroptosis: A specialized Pathway of Programmed Necrosis." *Cell* 135 (2008): 1161-1163.

Ghezzi, D, et al. "SDHAF1, encoding a LYR complex-II specific assembly factor, is mutated in SDH-defective infantile leukoencephalopathy." *Nat Genet* 41 (2009): 654-6.

Hackenbrock, CR. "Ultrastructural bases for metabolically linked mechanical activity in mitochondria. I. Reversible ultrastructural changes with change in metabolic steady state in isolated liver mitochondria." *J Cell Biol* 30 (1966): 269-297.

Haddad, P, et al. "Structural organization of the hCTLA-1 gene encoding human granzyme B." *Gene* 87 (1990): 265-271.

Han, Jie, Leslie A Goldstein, Wen Hou, Christopher J Froelich, Simon C Watkins, and Hannah Rabinowich. "Deregulation of Mitochondrial Membrane Potential by Mitochondrial Insertion of Granzyme B and Direct Hax-1 Cleavage." *The journal of biological chemistry* 285, no. 29 (2010): 22461-22472.

Hatefi, Y. "Preparation and properties of the enzymes and enzymes complexes of the oxydative phosphorylation system." *Methods Enzymol.* 53 (1978): 3.

Hegde , R, et al. "Identification of Omi/HtrA2 as a mitochondrial apoptotic serine protease that disrupts inhibitor of apoptosis protein-caspase interaction." *J. Biol. Chem.* 277 (2002): 432-438.

Hekimi, S, and L Guarante. "Genetics and the specificity of the aging process." *Science* 299 (2003): 1351-1354.

Holler, N, et al. "Fas triggers an alternative, caspase-8-independent cell death pathway using the kinase RIP as effector molecule." *Nat. Immunol* 1 (2000): 489-495.

Huai, J, et al. "TNFalpha-induced lysosomal membrane permeabilization is downstream of MOMP and triggered by caspase-mediated NDUFS1 cleavage and ROS formation." *Journal of cell science* 126 (2013): 4015-4025.

Huang, C, E Bi, Y Hu, and et al. "A novel NF-kappaB binding site controls human granzyme B gene transcription." *J. Immunol.* 176 (2006): 4173-4181.

Ishihara, N, Y Fujita, T Oka, and K Mihara. "Regulation of mitochondrial morphology through proteolytic cleavage of OPA1." *The EMBO Journal*, 2006: 2966-2977.

Itoh, N, et al. "The polypeptide encoded by the cDNA for human cell surface antigen Fas can mediate apoptosis." *Cell* 66 (1991): 233-243.

Jahani-Asl, A, and RS Slack. "The phosphorylation state of Drp1 determines its cell fate." *EMBO Rep* 8 (2007): 912-913.

Johnoson, Hillary C, Luca Scorrano, Stanley J Korsmeyer, and Timothy J Ley. "Cell death induced by granzyme C." *Blood*, 2003: 3093-3101.

Kabelitz, D, T Pohl, and K Pechhold. "Activation- induced cell death (apoptosis) of mature periph- eral T lymphocytes." *Immunol. Today* 14 (1993): 338-339.

Kamada, S, et al. "A cloning method for caspase substrates that uses the yeast two-hybrid system: cloning of the antiapoptotic gene gelsolin." *Proc. Natl. Acad.* 95 (1998): 8532-8537.

Kaufmann, SH, and WC Earnshaw. "Induction of apoptosis by cancer chemotherapy." *Exp Cell Res* 256, no. 1 (2000): 42-49.

Kaur, H, and B Halliwell. "Evidence for nitric oxide-mediated oxidative damage in chronic inflammation. Nitrotyrosine in serum and synovial fluid from rheumatoid patients." *FEBS Lett*, 1994: 9-12.

Keefe, D, et al. "Perforin triggers a plasma membrane-repair response that facilitates CTL induction of apoptosis." *Immunity* 23 (2005): 249-62.

Kelekar, A, and CB Thompson. "Bcl-2-family proteins: the role of the BH3 domain in apoptosis." *Trends Cell. Biol.* 8 (1998): 324-330.

Kelly, J.M, et al. "Granzyme M mediates a novel form of perforin-dependent cell death." *J. Biol. Chem* 279 (2004): 22236-22242.

Kerr, JF, AH Wyllie, and AR Currie. "Apoptosis: A basic biological phenomenon with wide-ranging implications in tissue kinetics." *Br J Cancer*, no. 26 (1972): 239-57.

Kiefel, BR, PR Gilson, and PL Beech . "Diverse eukaryotes have retained mitochondrial homologues of the bacterial division protein FtsZ." 2004.

Kiessling, R, Eva E Klein, and H Wigzell. "„Natural" killer cells in the mouse. I. Cytotoxic cells with specificity for mouse Moloney leukemia cells. Specificity and distribution according to genotype." *European Journal of Immunology* 5, no. 2 (1975): 112-117.

King, MP, and G Attardi. "Human cells lacking mtDNA: repopulation with exogenous mitochondria by complementation." *Science* 246 (1989): 500-503.

Kirby, D.M., M Crawford, M.A. Cleary, H.H. Dahl, X Dennett, and D.R. Thorburn. "Respiratory chain complex I deficiency: an underdiagnosed energy generation disorder." *Neurology* 52 (1999): 1255-1264.

Kischkel, FC, et al. "Cytotoxicity-dependent APO-1 (Fas/CD95)-associated proteins form a death-inducing signaling complex (DISC) with the receptor." *The EMBO Journal* 14, no. 22 (1995): 5579-88.

Klein, JL, TB Shows, B Dupont, and JA Trapani. "Genomic organization and chromosomal assignment for a serine protease gene (CSPB) expressed by human cytotoxic lymphocytes." *Genomics* 5 (1989): 110-117.

Koshiba, T, S.A. Detmer, J.T. Kaiser, H Chen, J.M. McCaffery, and D.C. Chan. "Structural basis of mitochondrial tethering by mitofusin complexes." *Science* 305 (2004): 858-862.

Krieger, C, and MR Duchen. "Mitochondria, Ca(2+) and neurodegenerative disease." *Eur J Pharmacol* 447 (2002): 177-188.

Lanier, LL. "Up on the tightrope: Natural killer cell activation and inhibition." *Nat. Immunol.* 9 (2008): 495.

Lapuente-Brun, E, et al. "Supercomplex Assembly Determines Electron Flux in the Mitochondrial Electron Transport Chain." *Science* 340, no. 6140 (2013): 1567-1570.

Law, Ruby, et al. "The structural basis for membrane binding and pore formation by lymphocyte perforin." *Nature letter researvh* 468 (2010).

Leist, M, and M Jaattela. "Four deaths and a funeral: From casapases to alternative mechanisms." *Nat Rev Mol Cell Biol* 2 (2001): 589-98.

Lenaz, Giorgio, and Maria Luisa Genova. "Supramolecular Organisation of the Mitochondrial Respiratory Chain: A New Challenge for the Mechanism and Control of Oxidative Phosphorylation." *Adv Exp Med Biol* 748 (2012): 107-144.

Li, LY, X Luo, and X Wang. "Endonuclease G is an apoptotic DNase when released from mitochondria." *Nature* 412 (2001): 95-99.

Li, P, and et al. "Cytochrome c and dATP-dependent formation of Apaf-1/caspase-9 complex initiates an apoptotic protease cascade." *Cell* 4 (1997): 479-489.

Li, P, et al. "Cytochrome c and dATP-dependent formation of Apaf-1/caspase-9 complex initiates an apoptotic protease cascade." *Cell* 4 (1997): 479-489.

LI, P, et al. "Cytochrome c and dATP-dependent formation of Apaf-1/caspase-9 complex initiates an apoptotic protease cascade." *Cell* 91, no. 4 (1997): 479-489.

Lieberman, Judy. "Cytotoxicity: new weapons in the arsenal." *Nature reviews immunology*, 2003.

Ling, YH, L Liebes, Y Zou, and R Perez-Soler. "Reactive oxygen species generation and mitochondrial dysfunction in the apoptotic response to Bortezomib, a novel proteasome inhibitor, in human H460 non-small cell lung cancer cells." *J Biol Chem*, 2003: 33714-23.

Liu, QA, and MO Hengartner. "The molecular mechanism of programmed cell death in C.elegans." *Ann NY Acad Sci* 887 (1999): 92-104.

Liu, Z, et al. "Structural basis for binding of Smac/DIABLO to the XIAP BIR3 domain." *Nature* 408 (2000): 1004-1008.

Lord, SJ, RV Rajotte, GS Korbutt, and RC Bleackley. "Granzyme B: a natural born killer." *Immunol Rev* 193 (2003): 31-38.

Lozzio, CB, and BB Lozzio. "Human chronic myelogenous leukemia cell-line with positive Philadelphia chromosome." *Blood*, 1975: 321-334.

Lu, H, et al. "Granzyme M Directly Cleaves Inhibitor of Caspase-Activated DNase (CAD) to Unleash CAD Leading to DNA Fragmentation." *The Journal of Immunology* 177, no. 2 (2006): 1171-1178.

Luo, X, I Budihardjo , H Zou, C Slaughter , and X Wang. "Bid, a Bcl2 interacting protein, mediates cytochrome c release from mitochondria in response to activation of cell surface death receptors." *Cell* 94(4) (1998): 481-90.

Malassagne, B., et al. "The superoxide dismutase mimetic MnTBAP prevents Fas-induced acute liver faillure in the mouse." *Gastroenterology* 121 (2001): 1451-1459.

Margulis, Lynn. "Origin of Eukaryotic Cells." *Yale University Press*, 1970.

Martinou, JC, and DR Green. "Breaking the mitochondrial barrier." *Nat Rev Mol Cell Biol*, 2001: 63-67.

Martins, L.M., et al. "The serine protease Omi/HtrA2 regulates apoptosis by binding XIAP through a reaper-like motif." *J. Biol. Chem.* 277 (2002): 439-444.

Martinvalet, D., P. Zhu, and J. Lieberman. "Granzyme A induces caspase-independent mitochondrial damage, a required first step for apoptosis." *Immunity* 22 (2005): 355-370.

Martinvalet, Denis, Derek M Dykxhoorn, Roger Ferrini, and Judy Lieberman. "Granzyme A Cleaves a Mitochondrial Complex I Protein to Initiate Caspase-Independent Cell Death." *Cell* 133 (May 16 2008): 681–692.

McBride, HM, M Neuspiel, and S Wasiak. "McBride HM, Neuspiel M, Wasiak S (2006). "Mitochondria: more than just a powerhouse". Curr. Biol. 16 (14): R551–60." *Curr. Biol.* 16 (2006): 551-560.

McNeil, P.L., and R.A. Steinhardt. "Plasma membrane disruption: repair, prevention, adaptation." *Annu. Rev. Cell. Dev. Biol.* 19 (2003): 697-731.

Meier, P, A Finch, and G Evan. "Apoptosis in development." *Nature* 407 (2000): 796-801.

Micheau, O, and J Tschopp. "Induction of TNF receptor I-mediated apoptosis via two sequential signaling complexes." *Cell* 114 (2003): 181-190.

Millard, PJ, MP Henkart, CW Reynolds, and PA Henkart. "Purification and properties of cytoplasmic granules from cytotoxic rat LGL tumors." *J Immunol* 132 (1984): 3197-3204.

Muller, F.L., Y Liu, and H van Remmen. "Complex III releases superoxide to both sides of the inner mitochondrial membrane,." *Journal of Biological Chemistry* 279 (2004): 49064-49073.

Mund, T, A Gewies, N Schoenfeld, MK Bauer, and S Grimm. "Spike, a novel BH3-only protein, regulates apoptosis at the endoplasmic reticulum." *Faseb J* 17, no. 6 (2003): 696-8.

Nagata, S. "Apoptosis by death factor." *Cell* 88 (1997): 355-365.

Naismith, JH, and SR Sprang. "Modularity in the TNF-receptor family." *Trends Biochem Sci* 23(2) (1998): 74-9.

Ngu, L.H., et al. "A catalytic defect in mitochondrial respiratory chain complex I due to a mutation in NDUFS2 in a patient with Leigh syndrome." *Biochimica et biophysica acta* 1822 (2012): 168-175.

Oltvai, ZN, CL Milliman, and SJ Korsmeyer. "Bcl-2 heterodimerizes in vivo with a conserved homolog, Bax, that accelerates programmed cell death." *Cell* 74 (1993): 609-619.

Palade, GE. "The fine structure of mitochondria." *Anat. Rec.* 114 (1952): 427-451.

Pardo, J, et al. "Granzyme B-induced cell death exerted by ex vivo CTL: discriminating requirements for cell death and some of its signs." *Ceel Death Differ.*, 2008: 567-579.

Perkins, GA, CW Renken, TG Frey, and MH Ellisman. "Membrane architecture of mitochondria in neurons of the central nervous system." *J Neurosci Res* 66 (2001): 857-865.

Perotti, ME, WA Anderson, and H Swift. "Quantitative cytochemistry of the diaminobenzidine cytochrome oxidase reaction product in mitochondria of cardiac muscle and pancreas." *J Histochem Cytochem* 31 (1983): 351-365.

Pinkoski, M.J., et al. "Entry and trafficking of granzyme B in target cells during granzyme B-perforin-mediated apoptosis." *Blood*, 1998: 1044-1054.

Piontek, GE, et al. "YAC-1 MHC class I variants reveal an association between decreased NK sensitivity and increased H-2 expression after interferon treatment or in vivo passage." *The Journal of Immunology* 135, no. 6 (1985): 4281-4288.

Pipkin, E Matthew, and Judy Lieberman. "Delivering the kiss of death: progress on understanding how perforin works." *Current Opinion in Immunology* 19 (2007): 301-308.

Prindull, G. "Apoptosis in the embryo and tumorigenesis." *European Journal of Cancer* , 1995: 116-123.

Reddy, A, E.V. Caler, and N.W. Andrews. "Plasma membrane repair is mediated by Ca2+-regulated exocytosis of lysosomes." *Cell* 106 (2001): 157-169.

Reed, JC. "Bcl-2 family proteins." *Oncogene* 17 (1998): 3225-3236.

Ricci, Jean, et al. "Disruption of Mitochondrial Function during Apoptosis Is Mediated by Caspase Cleavage of the p75 Subunit of Complex I of the Electron Transport Chain." *Cell* 117, no. 6 (June 2004): 773–786.

Ricci, Jean-Ehrland , et al. "Disruption of Mitochondrial Function during Apoptosis Is Mediated by Caspase Cleavage of the p75 Subunit of Complex I of the Electron Transport Chain." *Cell*, 2004: 773–786.

Richardson, H, and S Kumar. ""Death to flies: Drosophila as a model system to study programmed cell deat"." *J Immunol Methods* 265(1-2) (2002): 21-38.

Richter, C, JW Park, and BN Ames . "Normal oxidative damage to mitochondrial and nuclear DNA is extensive." *Proc Natl Acad Sci U S A*, 1998: 6465-7.

Rodriguez, J, and Y Lazebnik. "Capsase-9 and APAF-1 form an active holoenzyme." *Genes Dev* 13 (1999): 3179-3184.

Ross, T, et al. "Reverse electron flow-mediated ROS generation in ischemia-damaged 2 mitochondria: Role of complex I inhibition vs. depolarization of inner 3 mitochondrial membrane." *Biochimica et Biophysica Acta*, 2013: 4537–4542.

Rousalova, I, and E Krepela. "Granzyme B-induced apoptosis in cancer cells and its regulation (Review)." *International Journal of Oncology* 37 (2010): 1361-1378.

Roy, S, and DW Nicholson . "Cross-talk in cell death signaling." *J Exp Med* 192 (2000): 21-25.

Rubbo, H, et al. "Nitric oxide regulation of superoxide and peroxynitrite-dependent lipid peroxidation. Formation of novel nitrogen-containing oxidized lipid derivatives." *J.Biol.Chem.* 269 (1994): 26066-26075.

Russell, JH, and TJ Ley. "Lymphocyte-mediated cytotoxicity." *Annu Rev Immunol* 20 (2002): 323-370.

Saelens, X, N Festjens, LV Walle, M van Gurp, G van Loo, and P Vandenabeele. "Toxic proteins released from mitochondria in cell death." *Oncogene* 23 (2004): 2861-2874.

Saelens, X, N Festjens, LV Walle, M van Gurp, G van Loo, and P Vandenabeele. "Toxic proteins released from mitochondria in cell death." *Oncogene* 23 (2004): 2861-2874.

Saleh, A, M Srinivasa, Samir Acharya Srinivaula, Richard Fisheland, S Emad, and Alnemri. "Cytochrome c and dATP-mediated oligomerization of Apaf-1 is a prerequisite for procaspase-9 activation ." *J. Biol. Chem* 274 (1999): 17941-17945.

Salvesen, G, D Farley, J Shuman, A Przybyla, and J Travis. "Molecular cloning of human cathepsin G: structural similarity to mast cell and cytotoxic T lymphocyte proteinases." *Biochemistry*, 1987: 2289-2293.

Savill, J, and V Fadok. "Corpse clearance defines the meaning of cell death." *Nature* 407 (2000): 784-8.

Sazanov, LA, S.Y. Peak-Chew, I.M. Fearnley, and J.E. Walker. "Resolution of the membrane domain of bovine complex I into subcomplexes: implications for the structural organization of the enzyme." (Biochemistry) 39 (2000): 7229-7235.

Scaffaldi, C, I Schmitz, J Zha, S.J. Korsmeyer, P.H. Krammer, and M.E Peter. "Differential modulation of aoptosis sensitivity in CD95 type I and type II cells." *J. Biol. Chem* 274 (1999): 22532-22538.

Scaffidi, C, et al. "Two CD95 (APO-1/Fas) signaling pathways." *Embo J* 17(6) (1998): 1675-1687.

Schagger, H. "Native electrophoresis for isolation of mitochondrial oxidative phosphorylation protein complexes." *Methods Enzymol.* 260 (1995): 190-202.

Schagger, H, and K Pfeiffer. "Supercomplexes in the respiratory chains of yeast and mammalian mitochondria." *The EMBO journal* 19, no. 8 (2000): 1777-1783.

Schon, EA, and G Manfredi. "Neuronal degeneration and mitochondrial dysfunction." *J Clin Invest* 111 (2003): 303-312.

Schulte, U. "Biogenesis of Respiratory Complex I." *J. Bioenerg. Biomembr* 33 (2001): 205-212.

Scorrano, L, et al. "A Distinct Pathway Remodels Mitochondrial Cristae and Mobilizes Cytochrome c during Apoptosis." *Dev Cell* 2 (2002): 55-67.

Simon, H.U., A Haj-Yehia, and F Levi-Schaffer. "Role of reactive oxygen species (ROS) in apoptosis induction." *Apoptosis*, 2000: 415-418.

Smyth, Mark J, et al. "Unlocking the secrets of cytotoxic granule proteins." *Journal of Leukocyte Biology* 70 (2001).

Srinivasula, S.M., et al. "A conserved XIAP-interaction motif in caspase-9 and Smac/DIABLO regulates caspase activity and apoptosis." *Nature* 410 (2001): 112-116.

Stadtman, ER, and RL Levine. "Protein oxydation." *Ann N Y Acad Sci*, 2000: 191-208.

Stenger, S, DA Hanson, and R Teitelbaum. "An antimicrobial activity of cytolytic T cells mediated by granulysin." *science* 282 (1998): 121-125.

Stock, D, A.G. Leslie, and J.E. Walker. "Molecular architecture of the rotary motor in ATP synthase." *Science* 286 (1999): 1700-1705.

Sun, J, CH Bird, V Sutton, L McDonald, and PB Coughlin. "A cytosolic granzyme B inhibitor related to the viral apoptotic regulator cytokine response modifier A is present in cytotoxic lymphocytes." *J. Biol. Chem.* 271 (1996): 27802-9.

Sun, X, J Yin, MA Starovasnik, WJ Fairbrother, and VM Dixit. "Identification of a novel homotypic interaction motif required for the phosphorylation of receptor-interacting protein (RIP) by RIP3." *J. Biol. Chem* 277 (2002): 9505-9511.

Susin, SA, et al. "Molecular characterization of mitochondrial apoptosis-inducing factor." *Nature* 397 (1999b): 441-446.

Suzuki, Y, Y Imai, H Nakayama, K Takahashi, K Takio, and R Takahashi. "A serine protease, HtrA2, is released from the mitochondria and interacts with XIAP, inducing cell death." *Mol. Cell* 8 (2001): 613-621.

Taguchi, N, N Ishihara, A Jokufu, T Oka, and K Mihara. "Mitotic phosphorylation of dynamin-related GTPase participates in mitochondrial fission." *J Biol Chem* 282 (2007): 11521-11529.

Thiery, J, et al. "Perforin activates clathrin- and dynamin-dependent endocytosis, which is required for plasma membrane repair and delivery of granzyme Bfor granzyme-mediated apoptosis." *Blood* 115 (2010): 1582-1593.

Thiery, J, et al. "Perforin pores in the endosomal membrane trigger the release of endocytosed granzyme B into the cytosol of target cells." *Nat Immunol.* 12, no. 8 (2011): 770-7.

Thomas, D.A., L Scorrano, G.V. Putcha, S.J. Korsmeyer, and T.J. Ley. "Granzyme B can cause mitochondrial depolarization and cell death in the absence of BID, BAX and BAK." *Proc Natls Acad Sci*, 2001: 14985-14990.

Thomas, DA, C Du, M Xu, X Wang, and TJ Ley. "DFF45/ICAD can be directly processed by granzyme B during the induction of apoptosis." *Immunity*, 2000: 621-632.

Tompson, CB. "Apoptosis in the pathogenesis and tratment of disease." 267 (1995): 1456-62.

Trapani, JA, J Davis, VR Sutton, and MJ Smyth. "Proapoptotic functions of cytotoxic lymphocyte granule constituents in vitro and in vivo." *Curr Opin Immunol* 12 (2000): 323-329.

Turrens, J.F. "Mitochondrial formation of reactive oxygen species." *J. Physiol.* 552 (2003): 335-344.

Valko, M., D. Leibfritz , J. Moncol , MTD. Cronin , M Mazur, and J. Telser. "Free radicals and antioxidants in normal physiological functions and human disease. ." *Int J Biochem Cell Biol* 39 (2007): 44–84.

van Loo, G, et al. "The serine protease Omi/HtrA2 is released from mitochondria during apoptosis. Omi interacts with caspase-inhibitor XIAP and induces enhanced caspase activity." *Cell Death Differ* 9 (2002): 20-26.

Verhagen, A.M., et al. "Identification of DIABLO, a mammalian protein that promotes apoptosis by binding to and antagonizing IAP proteins." *Cell* 102 (2000): 43-53.

Vivier, Eric, et al. "Innate or Adaptive Immunity? The example of Natural Killer Cells." *Science* 331, no. 6013 (2011): 44-49 .

Voskoboinik, I, M Smyth, and J Trapani. "Perforin-mediated target-cell death and immune homeostasis." *Nature Rev. Immunol* 6 (2006): 940-952.

Walch, Michael et al. "Walch et al. 2014 Cell in press."

Wallace, DC. "A mitochondrial paradigm of metabolic and degenerative diseases, aging, and cancer: a dawn for evolutionary medicine." *Annu Rev Genet* 39 (2005): 359-407.

Wang, X. "The expanding role of mitochondria in apoptosis." *Genes Dev* 15, no. 22 (2001): 2922-33.

Wargnier, A, et al. "Identification of human granzyme B promoter regulatory elements interacting with activated T-cell-specific proteins: Implication of Ikaros and CBF binding sites in promoter activation." *Immunology*, 1995: 6930-6934.

Wiedemann, N, et al. "Machinery for protein sorting and assembly in the mitochondrial outer membrane. ." *Nature* 424 (2003): 565-571.

Wilson, N.S., V Dixit, and A Ashkenazi. "Death receptor signal transducers: nodes of coordination in immune signaling networks." *Nature Immunolo.* 10 (2009): 348-355.

Wu, G, et al. "Structural basis of IAP recognition by Smac/DIABLO." *Nature* 408 (2000): 1008-1012.

Yoon, Y, E.W. Krueger, B.J. Oswald, and M.A. McNiven. "The mitochondrial protein hFis1 regulates mitochondrial fission in mammalian cells through an interaction with the dynamin-like protein DLP1." *Mol.Cell.Biol.*, 2003: 5409-5420.

Zara, V, L Conte , and BL Trumpower. "Biogenesis of the yeast cytochrome bc(1) complex. ." *Biochim Biophys Acta* 1793, no. 1 (2009): 89-96.

Zhang, D, et al. "Mitochondrial DNA mutations activate the mitochondrial apoptotic pathway and cause dilated cardiomyopathy." *Cardiovasc Res* 57 (2003): 147-157.

Zhang, D, et al. "Mitochondrial DNA mutations activate the mitochondrial apoptotic pathway and cause dilated cardiomyopathy." *Cardiovasc Res* 57 (2003): 147-157.

Zhang, HG, X Su, and D Liu. "Induction of specific T cell tolerance by Fas ligand-expressing anti- gen-presenting cells." *J. Immunol.* 162 (1999): 1423-1430.

Zhao, T, et al. "Granzyme K cleaves the nucleosome assembly protein SET to induce single-stranded DNA nicks of target cells." *Cell Death and Differentiation* 14 (2007): 489-499.

Zou, H, Y Li, X Liu, and X Wang . "An APAF-1-cytochrome c multimeric complex is a functional apoptosome that activates procaspase-9." *J. Biol. Chem* 274 (1999): 11549-11556.

Granzyme B disrupts NADH:ubiquinone oxidoreductase electron transport complex I to induce ROS-dependent cell death

Guillaume Jacquemin[1#], Daniela Margiotta[1#], Atsuko Kasahara[1], Esen Yonca Bassoy[1], Michael Walch[2], Jerome Thiery[3], Judy Lieberman[4] and Denis Martinvalet*[1]

[1]CMU, Faculté de Médecine, Université de Genève, Genève Suisse
[2]Departement de Médecine, Unité d•Anatomie, Université de Fribourg, Fribourg, Suisse
[3]INSERM U753, Gustave Roussy Cancer Campus, Villejuif, France
[4]Program in Cellular and Molecular Medicine, Boston Children•s Hospital, Harvard Medical School, Boston MA USA

[#]Authors contributed equally to this work.

*Correspondence should be addressed to DM (Denis.Martinvalet@unige.ch)

SUMMARY

Caspases and the cytotoxic lymphocyte protease granzyme B (GB) induce ROS increase, loss of transmembrane potential, and mitochondrial outer membrane permeabilization (MOMP). How GB induces ROS and whether ROS is required for apoptosis is unclear. Here, we found that GB, independently of the caspases and MOMP, induces ROS-dependent death by cleaving NDUFV1, NDUFS2, and NDUFS1 subunits of the NADH:ubiquinone oxidoreductase complex I inside mitochondria. This leads to mitocentric ROS production, loss of complex I and III activity, disorganization of the respiratory chain, impaired mitochondrial respiration and loss of the mitochondrial cristae junctions. Furthermore, we have also found that GB-induced mitocentric ROS are necessary for optimal apoptogenic factor release, rapid DNA fragmentation and lysosomal rupture. Consequently GB-induced ROS significantly promote apoptosis.

INTRODUCTION

Cytotoxic lymphocytes kill infected or transformed cells by perforin (P)-mediated delivery of granzyme serine proteases[1-3]. There are five human and ten mouse granzymes, among which GB and Granzyme A (GA) are the most abundant and best characterized[4]. Like effector caspases, GB cleaves its substrates after aspartic acid residues to induce apoptotic cell death[4]. Human GB also directly cleaves caspase-3 and key caspase substrates, such as the proapoptotic Bcl-2 family member Bid, the inhibitor of the caspase-activated DNAses ICAD, PARP-1, lamin B, NuMa, DNA-PK_{cs} and tubulin[4-6]. Consequently, caspase inhibitors have little effect on human GB-mediated cell death and DNA fragmentation[5]. GB causes ROS production, dissipation of the mitochondrial transmembrane potential ($\Delta\Psi m$) and MOMP, which leads to the release of apoptogenic factors such as cytochrome c (Cyt c), HtrA2/Omi, endonuclease G (Endo G), Smac/Diablo and apoptosis-inducing factor (AIF), from the mitochondrial intermembrane space to the cytosol[7-14]. Human GB induces loss of $\Delta\Psi m$ and Cyt c release even in the presence of caspase inhibitors. Although much attention has focused on the importance of MOMP in the execution of GB-mediated cell death, mouse cells genetically deficient for Bid, Bax, and Bak, which are critical for MOMP, are still sensitive to GB-induced cell death[8,14-16]. This suggests that human GB targets the mitochondria in another way that needs to be characterized. Whether ROS production is a bystander effect or essential to the execution of GB-induced apoptosis is still an open question. GA induces Bcl2-insensitive caspase- and MOMP-independent programmed cell death in a ROS-dependent manner by cleaving complex I subunit NDUFS3[17-19]. Caspase 3 generates superoxide anion and other downstream ROS[20] by cleaving NDUFS1 subunit of the same complex I. The NADH-ubiquinone oxidoreductase complex I, the first enzyme complex of the mitochondrial ETC, which is ~1 MDa in size and composed of 45 subunits[21], catalyzes the transfer of 2 electrons from NADH to ubiquinone. This reaction is coupled with the translocation of 4 protons across the inner mitochondrial membrane to generate the proton gradient force ($\Delta\Psi m$). Here we show that GB also induces ROS-dependent cell death by directly attacking mitochondria in a caspase- and MOMP-independent manner to cleave NDUFS1, NDUFS2 and NDUFV1 in complex I. As a consequence, ETC complex I and III activities are reduced, mitochondrial ROS production is triggered and mitochondrial respiration is compromised. Moreover, GB disrupts the organization of the ETC and cristae junctions are lost. We also show that GB-mediated mitocentric ROS are necessary for proper apoptogenic factor

release from the mitochondrial intermembrane space to the cytosol and rapid DNA fragmentation. Moreover, GB-induced ROS are necessary for lysosomal membrane rupture. Thus ROS generation is not an adventitious side effect of cell death, but an essential mediator.

RESULTS

GB disrupts complex I by cleaving NDUFV1, NDUFS2 and NDUFS1

To test whether ROS are necessary for the rapid induction of cell death by GB, K562 cells were treated with a sublytic concentration of perforin (P) and GB in the presence or absence of the antioxidants Mn(III) tetrakis (4-benzoic acid) porphyrin Chloride (MnTBAP) or N-acetyl cysteine (NAC). Mitochondrial ROS were detected 15 minutes after treatment by staining with MitoSOX while cell death was assessed 45 min after treatment by annexin V/PI staining. MnTBAP and NAC reduced both GB-induced mitochondrial ROS production and cell death in a dose-dependent manner (Fig. 1a and supplementary Fig. 1a-b). MnTBAP also inhibits GB-induced ROS increase when detected with dihydroethidium that reacts with total cytosolic and mitochondrial ROS (supplementary Fig. 1c). Moreover, MnTBAP significantly protects the B cell line 721.221 from YT-Indy, a human NK cell line that doesn•t express GA or GK and only weakly expresses GM or GH but abundantly GB (Fig. 1b). These results strongly suggest that GB-mediated cell death depends on ROS generation. To define how GB induces ROS, we compared the proteome of mitochondria that were untreated or treated with GB or GA by 2D IEF-SDS PAGE gel electrophoresis. Spots that disappeared selectively from GB-treated mitochondria were analyzed by mass spectrometry as previously described[17]. NDUFV1 was identified as a putative GB target (Fig. 1c). NDUFV1 is a 51 kDa iron-sulfur (Fe-S) cluster-containing subunit that binds NADH and catalyzes the initial transfer of electrons from NADH across complex I to ubiquinone[22-25]. The critical role of NDUFV1 at the beginning of electron transport makes it a good candidate target for GB-induced ROS. To validate NDUFV1 as a physiological GB substrate, we examined its fate in K562 cells treated with GB and P (Fig. 1d). GB and P treatment induced dose- and time-dependent cleavage of NDUFV1 with similar kinetics as PARP-1 cleavage. The caspase inhibitors zVAD-fmk and DEVD-fmk have a marginal effect on NDUFV1 cleavage, while the GB inhibitor Ac-IETD-CHO prevented it. Thus NDUFV1 is a physiologically relevant, caspase-independent GB substrate.

The caspase 3 substrate NDUFS1 (Ricci et al., 2004) and other complex I subunits were not identified as putative GB substrates by our proteomics screen, possibly because we used a stringent criterion. Since GB and caspase 3 share many cellular substrates, we next looked at whether other mammalian complex I subunits are predicted GB substrates by the CutDB SitePrediction tool[26,27]. Of the 15 human core complex I subunits the most critical for its function, GB was predicted to have a high probability of cleaving NDUFV1 and 5 others (NDUFS2, NDUFS1, NDUFS3, NDUFS7 and NDUFA13). NDUFS1 was predicted to contain 11 possible cleavage sites. Like NDUFV1, both NDUFS1 and NDUFS2 were cleaved in K562 cells with similar kinetics as PARP-1 (Fig. 1e and data not shown). GB cleavage of NDUFS1 and NDUFS2 was slightly affected by zVAD-fmk (Supplementary Fig. 1d and data not shown). To evaluate further whether these complex I subunits are GB substrates, we expressed tagged versions of all 6 putative substrates in the B cell line 721.221 and used anti-tag antibodies to probe for their cleavage after cells were treated with GB and P. The overexpressed tagged subunits localized to mitochondria and integrated into complex I, based on their co-immunoprecipitation with other subunits, such as NDUFS3 (Supplemental Fig. 1e-g and data not shown). GB induced dose- and time-dependent cleavage of tagged NDUFV1, NDUFS2 and NDUFS1 that mimic the kinetics of cleavage of PARP-1 and the previously identified mitochondrial substrate HAX-1[14,15] (Supplementary Fig. 2a-c). GB did not cleave NDUFS3, NDUFS7 or NDUFA13 (data not shown). Tagged NDUFV1, NDUFS2 and NDUFS1 were also cleaved when transfected 721.221 cells were incubated with YT-Indy, (Fig. 1f-h). The caspase 3-uncleavable mutant of NDUFS1 (D255A-NDUFS1) was also cleaved when transfected target cells were incubated with YT-Indy, indicating that their cleavage was not secondary to caspase activation (Fig. 1g). Thus GB, independently of the caspases, cleaves NDUFV1, NDUFS2 and NDUFS1 in cells undergoing killer cell attack. Since NDUFV1, NDUFS2 and NDUFS1 are all Fe-S center-containing subunits involved in shuttling electrons across complex I, their cleavage could lead to mitochondrial ROS production[28].

GB cleaves recombinant NDUFV1, NDUFS1 and NDUFS2 and cleaves these proteins in intact mitochondria

CutDB predicts that GB will cleave NDUFV1 after D118 and D338/340 (Supplementary Fig. 3a), NDUFS1 after D364 (Supplementary Fig. 3b) and NDUFS2

after D317 (Supplementary Fig. 4). These cleavage site sequences are conserved between mice and humans. These proteins were *in vitro* labeled with ^{35}S-Methionine, and treated with GB. The cleavage fragment sizes corresponded roughly to predicted cleavage sites. To verify the cleavage sites, we expressed each protein with D-A mutations of the predicted cleavage sites. The mutant proteins were all resistant to GB, confirming that NDUFV1, NDUFS1 and NDUFS2 are direct GB substrates, cleaved at predicted aspartic acid residues. In isolated intact mitochondria, GB cleaved all 3 of these complex I subunits, but not NDUFS3 or NDUFA13, rapidly within one minute (Fig. 2a). Mitochondrial pretreatment with the protonophore valinomycin, which disrupts $\Delta\Psi$m, completely blocked this cleavage, suggesting that GB need an intact $\Delta\Psi$m to reach its substrates inside the mitochondrial matrix.

GB-induced ROS are mediated by complex I subunit cleavage, are independent of caspase activation and potentiate cell death

To investigate whether complex I inactivation by GB plays an important role in ROS generation and cell death we tested the effect of simultaneous overexpression of GB-uncleavable D118/338/340A-NDUFV1, D317A-NDUFS2 and D255/364A-NDUFS1 (Fig. 2b). Overexpression of GB-uncleavable forms of complex I subunits significantly reduced and slowed down GB-mediated ROS production, compared to cells overexpressing the WT substrates (Fig. 2c and d). Thus mitochondrial complex I proteolysis is a major contributor to ROS generation in this pathway. The presence of endogenous NDUFV1, NDUFS2 and NDUFS1 might account for some residual ROS production. Overexpression of these uncleavable mutant proteins also significantly inhibited and slowed down GB-mediated cell death (Fig. 2e and f). Pan-caspase inhibition had no significant effect on GB-mediated ROS production and cell death in cells expressing either WT or uncleavable complex I proteins (Fig. 2g and h). Thus GB induces mitocentric ROS by cleaving NDUFV1, NDUFS2 and NDUFS1, which occurs independently of the caspases and promotes cell death.

GB cleaves complex I subunits independently of MOMP

Mitochondrial outer membrane permeabilization (MOMP) is an important step in GB and caspase-induced apoptosis[7,9-13]. When GB cleaves cytosolic Bid, truncated Bid (t-Bid) interacts with Bak and Bax to disrupt the integrity of the mitochondrial outer membrane, causing the release of proapoptotic intermembrane space proteins. We therefore looked at whether GB-induced ROS generation and NDUFV1, NDUFS2

and NDUFS1 cleavage are linked to MOMP. Purified mitochondria were treated with GB in the presence or absence of S100 cytosolic fraction as a source of Bid, and the release of Cyt c and Endo G was followed to assess MOMP. As expected, GB induced Cyt c and Endo G release only in the presence of S100 (Fig. 3a). However cleavage of NDUFS1 occurred in the absence of S100, suggesting that MOMP is not required for GB cleavage of complex I proteins (Fig. 3a). Interestingly, NDUFS1 cleavage was increased in the presence of S100 most likely as the result of the combined action of GB and caspase 3. Moreover, in MEFs genetically deficient for both Bax and Bak, which do not undergo MOMP[29], GB still induced ROS and cell death although to a lower extent compared to the wild type counterpart (Fig. 3b-d). Note, the level of GB-induced ROS corresponds to the extent of cell death following GB treatment of $Bax^{-/-}$ and $Bak^{-/-}$. The high level of ROS observed in Wild type MEF could be due to the combined action of GB and caspase 3 actions on complex I subunits cleavage as observed in figure 3a. We also observed comparable cleavage of tagged NDUFV1, NDUFS2 and NDUFS1 in WT and $Bax^{-/-}$/$Bak^{-/-}$ MEFs (Figures 3f and g). Thus GB induces complex I subunits cleavage and ROS independently of MOMP.

GB-induced ROS are necessary for apoptogenic factor release and oligonucleosomal DNA fragmentation

Mitochondrial ROS may facilitate apoptogenic factor release from the mitochondrial intermembrane space into the cytosol. Cyt C, whose cytosolic release triggers apoptosome formation to activate caspase-9, is bound to cardiolipin in mitochondrial membranes by both electrostatic and hydrophobic interactions that are destabilized by ROS[30,31]. ROS also promotes release from mitochondria of Endo G, which may increase apoptotic DNA damage[32]. To test whether GB-mediated ROS enhances apoptogenic factor release, U937 cells were treated with P and GB in the presence or absence of the antioxidant NAC and the release of Cyt C, Endo G and Smac was assessed by immunoblot of cytosolic and mitochondrial fractions. Although NAC didn•t alter GB-induced Bid cleavage, NAC reduced and delayed the release of Cyt C, Endo G and Smac triggered by GB (Fig. 4a, b). Similarly overexpression of GB-uncleavable NDUFV1, NDUFS1 and NDUFS2 didn•t affect Bid cleavage while it inhibited GB-induced apoptogenic factor release (Fig. 4c, d). Thus GB-mediated mitochondrial ROS production promotes apoptogenic factor release. Factors release

requires at least two independent steps, MOMP, which is Bid/Bax/Bak-dependent, and ROS to untether factors in the intermembrane space to facilitate their release.

A hallmark of GB-mediated cell death is CAD activation of oligonucleosomal DNA fragmentation[33,34]. To investigate whether GB-induced ROS enhances apoptotic DNA damage, DNA from cells treated with P and GB in the presence or absence of NAC was analyzed by agarose gel electrophoresis (Fig. 4e, f). Oligonucleosomal DNA fragmentation was reduced and delayed by NAC treatment. Overexpression of GB-uncleavable NDUFV1, NDUFS1 and NDUFS2, which reduces ROS generation also largely abolished DNA fragmentation (Fig. 4g). Thus GB-induced ROS potentiates GB-mediated apoptotic DNA damage.

GB-induced ROS are necessary for lysosomal membrane rupture

A late event of apoptosis is caspase-9 and MOMP-dependent lysosomal membrane permeabilization, leading to the release of destructive lysosomal proteases into the cytosol. Mitochondrial ROS have been implicated in lysosomal disruption in TNF-mediated cell death[35]. Lysosomal membrane permeabilization can be assessed by staining with Lysosensor green, which fluoresces brightly in intact acidic lysosomes, but dims as the pH rises in compromised lysosomes. Lysosomal green staining began to decline in U937 cells within 30 min of GB + P treatment, suggesting that lysosomal permeabilization is a feature of GB-mediated death (Fig. 4h and supplementary fig. 5a). The loss of Lysosensor green staining was significantly inhibited by NAC. Moreover, overexpression of GB-uncleavable complex I subunits delayed lysosomal membrane permeabilization, suggesting that GB-induced mitochondrial ROS also potentiate this late event in apoptosis (Fig. 4i and supplementary fig. 5b).

GB-induced ROS requires a functional respiratory chain

Although our results strongly support a role for mitochondria in GB-induced ROS, it has been proposed that GB induces ROS, independently of mitochondria, *via* caspase-dependent activation of NADPH oxidase (NOX) enzymes[36]. However, pan-caspase inhibition with zVAD-fmk had no significant effect on GB-induced ROS production and cell death and overexpression of the uncleavable complex I subunits dramatically reduced ROS generation by GB (Fig. 2c-f). To evaluate further the role of mitochondrial respiration on GB induction of ROS, we compared ROS and cell

death of WT K562 and pseudo ρ^0 K562 cells, which have accumulated multiple mutations in mitochondrial DNA (mtDNA) after prolonged culture in ethidium bromide, leading to the lack of a functional respiratory chain and reliance on glycolysis for energy (Fig. 5a)[37]. GB-induced ROS and cell death were almost completely abrogated in K562 pseudo ρ^0 cells, indicating that GB requires a functional electron transport respiratory chain to trigger ROS-dependent cell death (Fig. 5b, c). We also investigated the role of the NADPH oxidases (NOX) in this pathway by comparing ROS generation and cell death in WT, *Nox1*$^{-/-}$ and *Nox4*$^{-/-}$ MEFs. GB still induced ROS and cell death in *NOX1*$^{-/-}$ or *NOX4*$^{-/-}$ MEFs, although less efficiently than in WT cells (Fig. 5d,e). Since MEF doesn•t express NOX1, this indicates that the NOX contribution in GB-induced ROS and cell death is marginal relative to the mitochondrial contribution.

The direct cleavage of complex I subunits suggests that GB enters mitochondria to reach its substrates. However, GB lacks a mitochondrial targeting sequence. Furthermore, cleavage of NDUFV1, NDUFS2 and NDUFS1 was MOMP-independent suggesting that permeabilization of the outer membrane is not needed. GA, which also does not have a mitochondrial targeting signal, enters the mitochondrial matrix in a $\Delta\Psi$m-dependent manner through an uncertain mechanism[17]. GB was previously shown to enter mitochondria to cleave HAX1[14]. We verified that GB enters mitochondria by flow cytometry and WB analysis of isolated mitochondria incubated with AlexaFluor647-labeled or unlabeled GB followed by gentle proteinase K (PK) treatment to remove externally bound proteins. GB mitochondrial import was inhibited by valinomycin, which disrupts the mitochondrial $\Delta\Psi$m (Fig. 5f, g). Valinomycin, which also disrupted the $\Delta\Psi$m of intact cells (Fig. 5h) without altering P-mediated GB uptake into cells (Fig. 5i), inhibited GB-induced ROS and cell death (Fig. 5j, k). Taken together, these results show that GB requires a functional respiratory chain and intact transmembrane potential to enter mitochondria and induce ROS and cell death.

GB disrupts complex I and III activities

We next wanted to understand how GB affects mitochondrial function. GB treatment rapidly reduced both the glutamate/malate- and succinate-dependent respiration of isolated mitochondria with kinetics that were similar to complex I cleavage (Fig. 6a. b). Thus GB decreases mitochondrial oxygen consumption. Glutamate/malate, which generate NADH, feed electrons into complex I, while succinate, which generates

$FADH_2$, feeds electrons directly to complex II; both complex I and II then transfer electrons to complex III. These results suggest that GB does more than disrupting complex I.

We next tested the effect of GB on ETC complex I activity. Purified intact mitochondria were treated or not with GB and respiratory complexes were analyzed by blue native gel electrophoresis (BNGE), which resolves ETC complexes in their native and active form to assess specific function by in-gel activity assays[38,39]. GB induced a dose-dependent inhibition of complex I activity that was significant within 1 min of GB treatment (Fig. 6c). Unexpectedly, GB also rapidly inhibited complex III activity, although less strongly than complex I. The activities of complexes IV and V were unaffected. Despite the change in complex III function, GB did not cleave the complex III subunits UGCRB, UQCRC1, UQCRC2 and UQCRFS1 (Fig. 6d). Because of the lack of good antibodies, we did not test whether GB cleaves the other complex III subunits MTCY, CYC1, CYCS, UQCRH, UQCR, UQCR10 or TTC19. Thus GB rapidly inhibits complex I and III activity and reduces mitochondrial respiration.

GB alters the organization of the mitochondrial respiratory chain

Mitochondrial ETC complexes organize into supercomplexes (SC) that channel electron in response to changes in substrate availability[40]. Complex I forms SCs with dimeric complex III (III_2, or with complexes III and IV) to facilitate transfer of electrons originating from NADH. The alteration in complex III activity we measured might be due to changes in SC formation caused by GB cleavage of complex I subunits. To determine whether GB treatment of isolated mitochondria causes changes in SC organization, purified mitochondria were treated or not with GB, and then solubilized with lauryl maltoside (LM) or digitonin (D) and analyzed by BNGE and immunoblot (Fig.6e-g). LM preserves ETC complexes but disrupts SCs, while D preserves both. In LM-solubilized mitochondria, GB reduced NDUFV1, NDUFS2 and NDUFS1, but had no effect on the complex III proteins UQCRC1, UQCR2 or UQCRS1 (Fig.6e). In D-solubilized mitochondria, however, $I+III_2$ SC formation was greatly enhanced by GB treatment, which was more evident when NDUFA13 and NDUFS3, complex I subunits not cleaved by GB, were probed (Fig.6g). We next looked at in gel complex I and III activity in monomeric complexes and SCs (Fig. 6f). GB induced a significant loss in monomeric complex I and III activities, as shown previously (Fig. 6c, f). In D-solubilized samples, complex I and III activities of supercomplex $I+III_2$ were not significantly changed by GB, even though much more SC was formed after GB

treatment, indicating that the specific activity of these complexes was reduced by GB treatment. Thus, GB alters mitochondrial respiratory chain organization by tilting the balance from monomeric complexes to an accumulation of SC I+III_2. This shift may enhance electron transport when complex I function is compromised. It may also help explain why GB compromises respiration of the complex II substrate succinate (Fig. 6b).

GB triggers loss of mitochondrial cristae junctions

The mitochondrial inner membrane is folded into large invaginations called cristae upon which respiratory chain complexes and SCs assemble. Cristae morphology is a critical determinant of ETC organization and respiratory efficiency[41]. Since GB affects the organization of respiratory complexes, we examined whether GB treatment might also affect the shape of cristae. The ultrastructure of intact mitochondria that were treated or not with GB was analyzed by electron microscopy. In GB-treated mitochondria many of the cristae appeared to have lost their junction (Fig. 6h). This was quantified by counting the number of mitochondria containing detached cristae, which was significantly increased in the GB treated samples. The functional significance of GB-induced cristae disorganization will require further study. Thus GB has a profound effect on mitochondrial respiration, electron transport activity and mitochondrial morphology.

DISCUSSION

Here we show that GB attacks mitochondria to cleave NDUFV1, NDUFS2 and NDUFS1 in ETC complex I, independently of the caspases, to trigger mitocentric ROS production and cell death. GB cleavage not only generates ROS, it also has a profound effect on mitochondrial function - it disrupts complex I and III function, and mitochondrial respiration of metabolites that feed into either complex I or complex II, modulates ETC supramolecular organization and causes cristae to detach. Generation of mitochondrial ROS in the form of superoxide, the species produced by complex I dysfunction[42], was previously shown to be necessary for killer lymphocyte-mediated death since superoxide scavengers virtually completely inhibit death[18,43]. GB can cause both caspase-dependent and caspase-independent cell death[16], which we have confirmed here. In fact, in our experiments pan-caspase inhibition had no significant effect on the extent of death (Fig. 2g and 2h). However, ROS generation is

key to caspase-independent programmed cell death and strongly promotes caspase-mediated death. Caspase-independent GB-mediated death occurs in *Bax*$^{-/-}$/*Bak*$^{-/-}$ cells, independently of MOMP. Here we show the importance of GB-induced ROS in both programmed cell death pathways by demonstrating that scavenging superoxide anion either with antioxidants or overexpressing GB-uncleavable mutants of GB complex I substrates strongly inhibits GB-mediated ROS and cell death. In particular, these maneuvers strongly inhibit both early events - apoptotic factor release from mitochondria (which amplifies caspase activation) - and more downstream DNA degradation and lysosomal disruption.

GA and caspase 3 also proteolyzed subunits of complex I to induced ROS-dependent apoptosis[17,20]. Mitochondria and mammalian complex I are evolutionarily derived from bacteria. We recently found that granzymes are delivered into bacteria by the killer cell antimicrobial peptide granulysin, where they also cleave multiple components of bacterial complex I to generate superoxide anion to rapidly kill bacteria (Walch *et al*., Cell in press). Thus, complex I disruption and ROS production are conserved biochemical mechanisms important for executing programmed cell death in widely diverse organisms in two evolutionary kingdoms. Given the essential role of complex I at the root of energy production, targeting complex I to induce death makes sense.

GB needs to enter the mitochondrial matrix to cleave its substrates in the matrix-protruding arm of complex I. How GB (or for that matter GA and caspase 3), which lack mitochondrial targeting sequences, get into the mitochondrial matrix is unknown. It will be important to figure this out, but that is beyond the scope of this study. Mitochondrial entry of GB does not require MOMP, which would only get the protease into the intermembrane space, but does require an intact $\Delta\Psi$m, since mitochondrial entry is blocked when it is dissipated by valinomycin. The same is true for caspase-3 and GA[17,20]. Although $\Delta\Psi$m is needed to initiate mitochondrial ROS and damage to mitochondrial function, it is soon disrupted when GB targets complex I and disrupts electron transport. Moreover, since MOMP dissipates the $\Delta\Psi$m, GB may only enter mitochondria that have not undergone MOMP or before MOMP dissipates the $\Delta\Psi$m. Studying in more detail the kinetics of GB mitochondrial entry, complex I subunit cleavage, MOMP and $\Delta\Psi$m dissipation in GB-treated isolated mitochondria and intact cells may help clarify how these two pathways interact. However, because of the

rapidity of these events, defining their sequencing may require high resolution, live cell imaging.

GB-induced ROS required mitochondrial electron transport since pseudo ρ^0 cells were resistant to both GB-induced ROS and cell death. This result and our finding that ROS generation is caspase-independent differ from[36], which implicated NOX oxidases in ROS generation by GB. However, we found that GB generation of ROS and cell death were not significantly reduced in *NOX1*$^{-/-}$ or *NOX4*$^{-/-}$ MEFs (MEFs express primarily *NOX4,* but not *NOX1*), suggesting that mitochondria rather than NOX proteins are the primary source of ROS in GB cell death pathway.

The crystal structure of *T*. *thermophilus* complex I shows that NDUFV1 (Nqo1/NuoF), NDUFV2 (Nqo2/NuoE) and NDUFS1 (Nqo2/NuoG) which form the N module of the electron entry site in complex I, are localized at the tip of the matrix protruding arm of complex I, exposed to solvent[21,44]. It is reasonable to conjecture that NDUFV1 and NDUFS1 occupy a similar position in mammalian complex I, and hence would be accessible to GB. Similar conclusions can be drawn for NDUFS2. We found that complex I within supercomplex I+III_2 is also altered by GB, suggesting that complex I subunits within SCs are accessible to GB. This is consistent not only with the function of those subunits in forming the electron entry site, but also with the topology of supercomplex I+III_2. Single-particle EM reconstructions show that dimeric complex III associates with the membrane segment of complex I, leaving the matrix-protruding arm free[45,46].

GB-mediated cleavage of NDUFV1, NDUFS2 and NDUFS1 inhibits complex I activity. NDUFV1 carries the NADH binding site and a Fe-S cluster while NDUFS2 and NDUFS1 only have Fe-S clusters. During electron flow down the ETC, electrons tunnel from Fe-S center to Fe-S center. Cleavage of these electron-transporting subunits would be expected to disrupt complex I function. Superoxide anion is produced by the one-electron reduction of O_2. In intact complex I, the Fe-S centers and their associated electrons are located within the heart of the complex, inaccessible to ambient oxygen dissolved in the matrix or the lipid bilayer of the inner mitochondrial membrane. However GB cleaves these subunits close to their Fe-S centers, possibly bringing electrons in proximity to dissolved oxygen to form superoxide. Reverse electron transport accounts for most $O_2^{\cdot -}$ production by complex

I under basal conditions in a process that involves reduced ubiquinone[47,48]. The GB substrate NDUFS2 establishes a groove with NDUFS7 to form the ubiquinone binding site[23-25]. GB cleavage of NDUFS2 may alter the ubiquinone binding site to favor ROS production in the reverse electron transfer mode. One possibility to explain ROS production in this pathway is by SC organization of the respiratory chain. GB treatment increases SC I+III_2 organization, which might be a compensatory mechanism to enhance electron transport when complex I function is compromised. Mitochondrial cristae morphology also influences respiratory chain organization[41,49]. GB reduces cristae junctions through an unknown mechanism, which likely contributes to mitochondrial dysfunction.

GB unexpectedly inhibited complex III activity and metabolism of a complex I-independent metabolic substrate. Although we did not observe cleavage of tested complex III subunits, other complex III subunits we did not evaluate might be proteolyzed by GB. Increased SC I+III_2 formation may help explain why GB compromises respiration of the complex II substrate succinate. Complex I outcompetes complex II for binding to complex III; more I+III_2 formation may lead to decreased SC II + III, but this requires further study.
Taken together our results demonstrate that GB-induced complex I disruption triggers ROS production that potentiate cell death.

Acknowledgments

This work was supported by Ambizione SNSF PZ00P3_126710 / 1, ERC starting grant ERC-2010-StG_20091118, and subsides from the Carlos and Elsie de Reuter Foundation and Schmidheiny Foundation. We thank Prof. Krause for $NOX1^{-/-}$ and $NOX4^{-/-}$ embryos (University of Geneva) and Olivier Dupont for technical assistance.

METHODS

Antibodies

Anti-V5 (V5-10) and anti-FLAG (M2) (Sigma Aldrich); anti-PARP (H-250), anti-HSP60 (H-300), anti-tubulin (B-7), anti-Tom40 and anti-HAX-1 (FL-279) (Santa Cruz Biotechnology); anti-HA (3F10) (Roche); anti- -light chain-HRP (Bethyl Laboratories); anti-NDUFS1 and anti-NDUFS2 (Epitomics); anti-Tom20 and anti-cytochrome c (BD Biosciences); anti-NDUFV1 (Aviva Systems Biology); anti-NDUFS3 (3F9DD2)

(Invitrogen); anti-NDUFS7 (Acris, AP21286PU-N); NDUFS13 (Mitosciences, MS103); anti-CORE1/UQCRC1 (MS303), anti-CORE2/UQCRC2 (MS304) and anti-UQCRFS1 (MS305) (Abcam); anti-Endo G (Novus Biological); anti-Caspase 3 (3G2) and anti-Histone H3 (Cell Signaling).

P and GB treatment

Perforin (P) was purified from the rat RNK-16 cells and GB from the human YT-Indy NK cells[50]. GB was first added to cells ($5x10^4$) suspended in 30 µl cell buffer (HBSS with 10 mM HEPES, pH 7.4, 0.4% BSA, 4 mM $CaCl_2$) and immediately thereafter an equal volume of P in HBSS with 10 mM HEPES, pH 7.4, was added. The P concentration was chosen as the sublytic concentration that lyses 5%..15% of cells. Cells were incubated at 37°C for the indicated time. In some cases cells were preincubated with 100 µM of the caspase inhibitors zVAD-fmk + DEVD-fmk or 100 µM of the GB inhibitor Ac-IETD-CHO for 30 min at 37°C before P and GB treatment. When antioxidants were used, cells were pretreated with N-Acetyl-L-cysteine (Sigma-Aldrich) for 1 hour, or with Mn(III)tetrakis(4-benzoic acid)porphyrin Chloride (MnTBAP) (Calbiochem) for 30 min before addition of P and GB.

Measurement of apoptosis, ROS production and $\Delta\Psi m$

Treated cells were washed in PBS and stained with Annexin V Alexa Fluor 647 and propidium iodide (Life Technologies) to detect apoptotic cells. Alternatively, cells were fixed with 0.5% paraformaldehyde in PBS and nuclei were stained with 5 ug/ml Hoechst 33342 (Molecular Probes) and analyzed by microscopy. Condensed or fragmented nuclei were considered as apoptotic. For each individual experiment, at least 300 nuclei were counted per condition. For detection of ROS, cells were stained with 5 µM MitoSOX or 2 µM dihydroethidium (HE) (Life Technologies) for 5 min at room temperature and analyzed by flow cytometry. To assess m, cells were labeled with 500 nM Tetramethylrhodamine, Methyl Ester (TMRM) for 15 min at room temperature and washed 3 times in PBS before flow cytometry analysis with an Accuri C6 flow cytometer (BD Biosciences).

Site-directed mutagenesis

pCMV6 vectors containing NDUFS1, NDUFS2 and NDUFV1 cDNA sequences were purchased from OriGene Technologies. Site-directed mutagenesis was performed by polymerase chain reaction with Herculase II Fusion DNA Polymerase (Agilent

Technologies) using overlapping primers, followed by restriction digest with DpnI. PCR products were transformed into One Shot TOP10 Competent E. coli (Life Technologies).

The following primers were used (5•-3•):

S1D255A forward, GACAGAATCCATTGATGTAATGGCTGCGGTTGGAAG

S1D255A reverse, CTTCCAACCGCAGCCATTACATCAATGGATTCTGTC

S1D364A forward, GAGTGGACTCTGCCACCTTATGCACTGAAG

S1D364A reverse, CTTCAGTGCATAAGGTGGCAGAGTCCACTC

S2D317A forward, CGACCAGGTTGAGTTTGCTGTTCCTGTTGGTTCTC

S2D317A reverse, GAGAACCAACAGGAACAGCAAACTCAACCTGGTCG

V1D118A forward, TGGTGAACGCAGCCGAGGGGGAGCC

V1D118A reverse, GGCTCCCCCTCGGCTGCGTTCACCA

V1D338/340A forward, CGGTGCTGATGGCCTTCGCTGCGCTGGTGCA

V1D338/340A reverse, TGCACCAGCGCAGCGAAGGCCATCAGCACCG

Generation of stable cell lines

Retroviral vectors were obtained by subcloning the cDNA sequence of human NDUFS1, NDUFS2 or NDUFV1 into pQCXIH, pQCXIP or pQCXIN (Clontech), respectively. The following primers were used (5•-3•):

V1 forward, AAAAAATTAATTAAGCCACCATGCTGGCAACACGGCGGC

V1 reverse (3xFLAG tag),

AAAAATTAATTAACTACTTGTCATCGTCATCCTTGTAGTCGATGTCAT

GATCTTTATAATCACCGTCATGGTCTTTGTAGTCAGAGGCAGCCTGCCGGGC

S1 forward, AAAAAAGCGGCCGCGCCACCATGTTAAGGATACCTGTAAGAAAG

S1 reverse (V5 tag),

AAAAAAGGATCCTCACGTAGAATCGAGACCGAGGAGAGGGTTAGGGATA

GGCTTACCGCATATGGATGGTTCCTCTAC

S2 forward, AAAAAAGCGGCCGCGCCACCATGGCGGCGCTGAGGGCTTTG

S2 reverse (HA tag),

TGCTTCTGAATTCTCAAGCGTAGTCTGGGACGTCGTATGGGTACCGATCT

ACTTCTCCAAATACAATATCTTGG

Retroviruses were produced by $CaCl_2$ transfection of the GP2-293 packaging cell line with the retroviral vectors encoding complex I genes and pVSV-G. Twelve hours after transfection, cells were washed and stimulated with 10 mM sodium butyrate for 12 h before changing the medium. Retroviral supernatants were collected after 48 hr.

Cells were transduced by 12 h incubation with the retroviral supernatant in the presence of 8 µg/mL polybrene. Puromycin, G-418 and hygromycin selection was begun 48 hr after infection.

Effector-target killing assay

Target cells (721.221, $0.05x10^6$) in 100 µl of medium (HBSS containing 1.55 mM $CaCl_2$, 17.5 mM glucose, 10 mM Hepes, pH 7.4) were mixed with an equal volume of effector cells (YT-indy) at the indicated effector-to-target (E:T) ratios and incubated at 37°C for the indicated times. 5X loading buffer with β-mercaptoethanol was directly added to the mixture prior to SDS-PAGE and immunoblot. For caspase inhibition, target cells were pretreated for 15 min with 10 µM zVAD-fmk before incubation with effector cells. For calcein release assay, target cells were preloaded with 10 µM Calcein AM (Life Technologies) for 30 min, then washed three times and incubated with effector cells as previously for the indicated time. Specific killing were determine by monitoring the calcein released in the supernatant.

$$\%\text{Specific release} = 100\,\frac{release - spontaneous\ release}{\max release - spontaneous\ release}$$

Generation of pseudo ^{0} cells

K562 cells were cultured in DMEM supplemented with ethidium bromide (250 ng/ml), sodium pyruvate (110 µg/ml) and uridine (50 µg/ml) for at least 2 weeks. Mitochondrial DNA was quantified by qPCR using primers specific for *COX1* and normalized to nuclear DNA using primers for *RNaseP*.

Cell fractionation

Treated cells ($1x10^6$) were washed with PBS and resuspended in 100 µl of cytosolic extraction buffer (70 mM KCl, 137 mM NaCl, 1.4 mM KH_2PO_4 pH 7.2, 4.3 mM Na_2HPO_4, 250 mM Sucrose, 50 µg/ml digitonin, protease inhibitors) and placed on ice for 5 min. Cells were centrifuged at 1000xg for 5 min and the supernatant was stored as the cytosolic fraction. The pellet was resuspended in 100 µl of mitochondrial lysis buffer (50 mM Tris pH7.4, 150 mM NaCl, 2 mM EDTA, 2 mM EGTA, 2% Triton X-100, 0.3% NP-40, protease inhibitors). After 10 min centrifugation at 10,000xg, the supernatant was kept as the mitochondrial-enriched fraction.

Quantification of GB uptake

Cells were washed in HBSS and resuspended in cell buffer (HBSS with 10 mM HEPES, pH 7.4, 0.4% BSA, 4 mM $CaCl_2$). GB, labeled with AlexaFluor-647 using the Alexa Fluor® 647 labeling kit from Life Technologies according to the manufacturer•s protocol, was added to cells just before adding a sublytic dose of P. After 10 min at 37°C, cells were extensively washed with HBSS at 4°C before flow cytometry analysis.

DNA laddering assay

Treated cells ($1.5x10^6$) were washed with cold PBS, resuspended in lysis buffer (10 mM Tris-HCL, pH 7.4, 10 mM EDTA, 0.5% SDS) and incubated for 10 min on ice. RNAse A (100 μg/mL) was added for 1 hr at 37°C, followed by addition of 100 μg/mL proteinase K for 4 hr at 50°C. After adding 300 mM sodium acetate pH 5.2, DNA was precipitated with ethanol overnight at -20°C. The pellet obtained after centrifugation at 14,000xg for 30 min was dissolved in TE buffer (10 mM Tris pH 8.0, 1 mM EDTA). DNA (6 μg) was electrophoresed through 1.2% agarose gels containing 0.5 μg/mL ethidium bromide.

Isolated mitochondria assays

Mitochondria isolated from mouse liver as described[51] were freshly prepared for all assays. Mitochondria (2.5 mg/ml protein) in 40 μl import buffer (600 mM Sorbitol, 160 mM KCl, 20 mM Magnesium Acetate, 4 mM KH_2PO_4, 5 mM EDTA, 5 mM $MnCl_2$, 200 mM Hepes pH 7.2) were incubated with GB (450 nM) for 5 min at 37°C and 10 μl of reactions were analyzed by immunoblot. For apoptogenic factor release experiments, mitochondria were incubated with GB (450 nM) alone or with 25 μg of S100 for 1 hr at 37°C. After centrifugation at 8000xg, supernatant and pellet were analyzed by immunoblot. For O_2 consumption and electron microscopy experiments, mitochondria were purified as described[52]. Mitochondrial pellet was resuspended in respiration buffer (150 mM KCl, 10 mM Tris/MOPS and 10 μM ATP). Mitochondria (400 μg) were transferred to a Clark electrode chamber to measure oxygen consumption. Succinate (5 mM) or glutamate and malate (5 and 2.5 mM, respectively) were added and 5 min later GB (450 nM) was added. Oxygen consumption was recorded over 20 min. Mitochondrial import assays were performed accordingly to[53]. 50 μg of mitochondrial in import buffer were incubated with 200 ng of unlabeled or Alexa-647 GB for 15 min at 37°C. Half of the reactions were treated with 50 μg/ml of proteinase K (PK) for 15 min on ice to give the imported fraction. PK was inactivated with 5 μl of 0.2 M PMSF

and sample spun at 12000 g for 15 min. Pellets were resuspended in either PBS or 1x SDS sample buffer for FACS and WB analysis respectively. The second halves ware use as input. In some case mitochondria in SH buffer were preincubated with 0.4 µM of valinomycin for 15 min to disrupt the $\Delta\Psi$ before carrying the import assay.

Respiratory complex in-gel activity

Mitochondria (400 µg in 40 µl of import buffer) were treated with 450 nM of GB for 5 min at 37°C. The reaction was stopped by adding 3 µl of 0.2 M PMSF. After 5 min on ice, samples were spun for 30 min at 12000xg. Pellets were solubilized on ice for 15 min with 40 µl of lysis buffer. For monomeric complex resolution, pellets were resuspended in lauryl maltoside buffer (50 mM NaCl, 1 mM EDTA, 50 mM Imidazole/HCl, 2 mM 6-Aminohexanoic acid, pH 7.0, 2% freshly prepared lauryl maltoside). To resolve SCs, pellets were solubilized in digitonin buffer (30 mM Hepes pH 7.4, 150 mM potassium acetate, 10% glycerol and 5% freshly prepared digitonin). Samples were spun for 20 min at 20,000xg at 4°C. 6 µl of 50% glycerol and 5 µl of 5% Coomassie blue G-250 were added to the supernatant to give a detergent/dye mass ratio of 8. Mitochondria (100 µg) were electrophoresed at 30 V for 30 min through native 3-13% gradient acrylamide gels using anode buffer (imidazole 25 mM, pH 7) and cathode buffer B (50 mM Tricine pH 7, 7.5 mM imidazole, 0.02% Coomassie blue G-250). Then the cathode buffer B was replaced by cathode buffer A (50 mM Tricine pH 7.0, 7.5 mM imidazole, 0.002% Coomassie blue G-250) and electrophoresis was continued at 80 V until the dye front reached the gel bottom. Complex I, IV and V were assayed as described[38]. Briefly, gels were washed in distilled water before incubation at room temperature (RT) with the following solutions: Complex I solution: 2 mM Tris–HCl pH 7.4, 0.1 mg/ml NADH, 2.5 mg/ml nitrotetrazolium blue for 15 min at RT. Complex IV solution: 5 mg 3:3'-Diamidobenzidine tetrahydrochloride dissolved in 9 ml of 5 mM phosphate buffer (0.05 M, pH 7.4), 1 nM catalase (20 U/ml), 10 mg Cyt c, and 750 mg sucrose overnight at RT. Complex V solution: 35 mM Tris pH 7.8, 270 mM glycine, 14 mM $MgSO_4$, 0.2% $Pb(NO_3)_2$, 8 mM ATP, overnight at RT. Gels were washed in distilled water and scanned immediately. Complex III activity was assayed as described in[39]. Briefly, gels were incubated in Complex III solution: 1-STEP TMB-BLOT (Pierce) overnight at RT.

Blue Native-PAGE immunoblot

Mitochondria (10 μg), resolved by BNGE as above, were transferred onto PVDF membranes using a semi-dry Hoefer transfer apparatus. Membranes were fixed in 100% methanol before blocking and incubation at 4^0C overnight with primary antibodies.

Electron microscopy

Mouse liver mitochondria (400 μg) in 40 μl import buffer were treated with 450 nM GB with or without 25 μg S100 for 1 h at 37°C. Samples were washed twice in 1X PBS then fixed for 30 min at RT with 1.25% glutaraldehyde, 100 mM sodium cacodylate. Embedding and staining were performed as in[54]. Thin sections were imaged on a Tecnai-20 electron microscope (Philips-FEI). The number of mitochondria with disrupted cristae junctions was counted in 1200 mitochondria for each condition.

Electron microscopy

Mouse liver mitochondria (400 μg) in 40 μl import buffer were treated with 450 nM GB with or without 25 μg S100 for 1 h at 37°C. Samples were washed twice in 1X PBS then fixed for 30 min at RT with 1.25% glutaraldehyde, 100 mM sodium cacodylate. Embedding and staining were performed as in[54]. Thin sections were imaged on a Tecnai-20 electron microscope (Philips-FEI). The number of mitochondria with disrupted cristae junctions was counted in 1200 mitochondria for each condition.

References

1 Law, R. H. *et al.* The structural basis for membrane binding and pore formation by lymphocyte perforin. *Nature* **468**, 447-451, doi:10.1038/nature09518 (2010).

2 Thiery, J. *et al.* Perforin pores in the endosomal membrane trigger the release of endocytosed granzyme B into the cytosol of target cells. *Nat Immunol* **12**, 770-777, doi:10.1038/ni.2050 (2011).

3 Thiery, J. *et al.* Perforin activates clathrin- and dynamin-dependent endocytosis, which is required for plasma membrane repair and delivery of granzyme B for granzyme-mediated apoptosis. *Blood* **115**, 1582-1593, doi:10.1182/blood-2009-10-246116 (2010).

4 Chowdhury, D. & Lieberman, J. Death by a thousand cuts: granzyme pathways of programmed cell death. *Annu Rev Immunol* **26**, 389-420 (2008).

5 Cullen, S. P., Adrain, C., Luthi, A. U., Duriez, P. J. & Martin, S. J. Human and murine granzyme B exhibit divergent substrate preferences. *J Cell Biol* **176**, 435-444, doi:10.1083/jcb.200612025 (2007).

6 Andrade, F. *et al.* Granzyme B directly and efficiently cleaves several downstream caspase substrates: implications for CTL-induced apoptosis. *Immunity* **8**, 451-460 (1998).

7 Kroemer, G., Galluzzi, L. & Brenner, C. Mitochondrial membrane permeabilization in cell death. *Physiol Rev* **87**, 99-163 (2007).

8 MacDonald, G., Shi, L., Vande Velde, C., Lieberman, J. & Greenberg, A. H. Mitochondria-dependent and -independent regulation of Granzyme B-induced apoptosis. *J Exp Med* **189**, 131-144 (1999).

9 Sutton, V. R., Wowk, M. E., Cancilla, M. & Trapani, J. A. Caspase activation by granzyme B is indirect, and caspase autoprocessing requires the release of proapoptotic mitochondrial factors. *Immunity* **18**, 319-329 (2003).

10 Waterhouse, N. J. *et al.* A central role for Bid in granzyme B-induced apoptosis. *J Biol Chem* **280**, 4476-4482, doi:10.1074/jbc.M410985200 (2005).

11 Goping, I. S. *et al.* Granzyme B-induced apoptosis requires both direct caspase activation and relief of caspase inhibition. *Immunity* **18**, 355-365 (2003).

12 Alimonti, J. B., Shi, L., Baijal, P. K. & Greenberg, A. H. Granzyme B induces BID-mediated cytochrome c release and mitochondrial permeability transition. *J Biol Chem* **276**, 6974-6982, doi:10.1074/jbc.M008444200 (2001).

13 Kaiserman, D. *et al.* The major human and mouse granzymes are structurally and functionally divergent. *J Cell Biol* **175**, 619-630, doi:10.1083/jcb.200606073 (2006).

14 Han, J. *et al.* Deregulation of mitochondrial membrane potential by mitochondrial insertion of granzyme B and direct Hax-1 cleavage. *J Biol Chem* **285**, 22461-22472, doi:10.1074/jbc.M109.086587 (2010).

15 Heibein, J. A., Barry, M., Motyka, B. & Bleackley, R. C. Granzyme B-induced loss of mitochondrial inner membrane potential (Delta Psi m) and cytochrome c release are caspase independent. *J Immunol* **163**, 4683-4693 (1999).

16 Thomas, D. A., Scorrano, L., Putcha, G. V., Korsmeyer, S. J. & Ley, T. J. Granzyme B can cause mitochondrial depolarization and cell death in the absence of BID, BAX, and BAK. *Proc Natl Acad Sci U S A* **98**, 14985-14990, doi:10.1073/pnas.261581498 (2001).

17 Martinvalet, D., Dykxhoorn, D. M., Ferrini, R. & Lieberman, J. Granzyme A cleaves a mitochondrial complex I protein to initiate caspase-independent cell death. *Cell* **133**, 681-692, doi:S0092-8674(08)00461-3 [pii]
10.1016/j.cell.2008.03.032 (2008).

18 Martinvalet, D., Zhu, P. & Lieberman, J. Granzyme A induces caspase-independent mitochondrial damage, a required first step for apoptosis. *Immunity* **22**, 355-370, doi:S1074-7613(05)00068-3 [pii]
10.1016/j.immuni.2005.02.004 (2005).

19 Beresford, P. J., Xia, Z., Greenberg, A. H. & Lieberman, J. Granzyme A loading induces rapid cytolysis and a novel form of DNA damage independently of caspase activation. *Immunity* **10**, 585-594, doi:S1074-7613(00)80058-8 [pii] (1999).

20 Ricci, J. E. *et al.* Disruption of mitochondrial function during apoptosis is mediated by caspase cleavage of the p75 subunit of complex I of the electron transport chain. *Cell* **117**, 773-786 (2004).

21 McKenzie, M. & Ryan, M. T. Assembly factors of human mitochondrial complex I and their defects in disease. *IUBMB Life* **62**, 497-502, doi:10.1002/iub.335 (2010).

22 Sherwood, S. & Hirst, J. Investigation of the mechanism of proton translocation by NADH:ubiquinone oxidoreductase (complex I) from bovine heart mitochondria: does the enzyme operate by a Q-cycle mechanism? *Biochem J* **400**, 541-550, doi:10.1042/BJ20060766 (2006).

23 Ngu, L. H. *et al.* A catalytic defect in mitochondrial respiratory chain complex I due to a mutation in NDUFS2 in a patient with Leigh syndrome. *Biochim Biophys Acta* **1822**, 168-175, doi:10.1016/j.bbadis.2011.10.012 (2012).

24 Pagniez-Mammeri, H. *et al.* Mitochondrial complex I deficiency of nuclear origin I. Structural genes. *Mol Genet Metab* **105**, 163-172, doi:10.1016/j.ymgme.2011.11.188 (2012).

25 Pagniez-Mammeri, H. *et al.* Mitochondrial complex I deficiency of nuclear origin II. Non-structural genes. *Mol Genet Metab* **105**, 173-179, doi:10.1016/j.ymgme.2011.10.001 (2012).

26 Hirst, J., Carroll, J., Fearnley, I. M., Shannon, R. J. & Walker, J. E. The nuclear encoded subunits of complex I from bovine heart mitochondria. *Biochim Biophys Acta* **1604**, 135-150 (2003).

27 Igarashi, Y. *et al.* CutDB: a proteolytic event database. *Nucleic Acids Res* **35**, D546-549, doi:10.1093/nar/gkl813 (2007).

28 Carroll, J., Fearnley, I. M., Shannon, R. J., Hirst, J. & Walker, J. E. Analysis of the subunit composition of complex I from bovine heart mitochondria. *Mol Cell Proteomics* **2**, 117-126, doi:10.1074/mcp.M300014-MCP200 (2003).

29 Wei, M. C. *et al.* Proapoptotic BAX and BAK: a requisite gateway to mitochondrial dysfunction and death. *Science* **292**, 727-730, doi:10.1126/science.1059108 (2001).

30 Petrosillo, G., Ruggiero, F. M. & Paradies, G. Role of reactive oxygen species and cardiolipin in the release of cytochrome c from mitochondria. *FASEB J* **17**, 2202-2208, doi:10.1096/fj.03-0012com (2003).

31 Petrosillo, G., Ruggiero, F. M., Pistolese, M. & Paradies, G. Ca2+-induced reactive oxygen species production promotes cytochrome c release from rat liver mitochondria via mitochondrial permeability transition (MPT)-dependent and MPT-independent mechanisms: role of cardiolipin. *J Biol Chem* **279**, 53103-53108, doi:10.1074/jbc.M407500200 (2004).

32 Kim, J. S. *et al.* Reactive oxygen species-dependent EndoG release mediates cisplatin-induced caspase-independent apoptosis in human head and neck squamous carcinoma cells. *Int J Cancer* **122**, 672-680, doi:10.1002/ijc.23158 (2008).

33 Shresta, S., MacIvor, D. M., Heusel, J. W., Russell, J. H. & Ley, T. J. Natural killer and lymphokine-activated killer cells require granzyme B for the rapid induction of apoptosis in susceptible target cells. *Proc Natl Acad Sci U S A* **92**, 5679-5683 (1995).

34 Parrish, J. *et al.* Mitochondrial endonuclease G is important for apoptosis in C. elegans. *Nature* **412**, 90-94, doi:10.1038/35083608 (2001).

35 Huai, J. *et al.* TNFalpha-induced lysosomal membrane permeability is downstream of MOMP and triggered by caspase-mediated NDUFS1 cleavage and ROS formation. *J Cell Sci* **126**, 4015-4025, doi:10.1242/jcs.129999 (2013).

36 Aguilo, J. I. *et al.* Granzyme B of cytotoxic T cells induces extramitochondrial reactive oxygen species production via caspase-dependent NADPH oxidase activation. *Immunol Cell Biol* **88**, 545-554, doi:10.1038/icb.2010.5 (2010).

37 Kaminski, M., Kiessling, M., Suss, D., Krammer, P. H. & Gulow, K. Novel role for mitochondria: protein kinase Ctheta-dependent oxidative signaling organelles in activation-induced T-cell death. *Mol Cell Biol* **27**, 3625-3639, doi:10.1128/MCB.02295-06 (2007).

38 Nijtmans, L. G., Henderson, N. S. & Holt, I. J. Blue Native electrophoresis to study mitochondrial and other protein complexes. *Methods* **26**, 327-334, doi:10.1016/S1046-2023(02)00038-5 (2002).

39 Smet, J. *et al.* Complex III staining in blue native polyacrylamide gels. *J Inherit Metab Dis* **34**, 741-747, doi:10.1007/s10545-011-9315-7 (2011).

40 Lapuente-Brun, E. *et al.* Supercomplex assembly determines electron flux in the mitochondrial electron transport chain. *Science* **340**, 1567-1570, doi:10.1126/science.1230381 (2013).

41 Cogliati, S. *et al.* Mitochondrial cristae shape determines respiratory chain supercomplexes assembly and respiratory efficiency. *Cell* **155**, 160-171, doi:10.1016/j.cell.2013.08.032 (2013).

42 Murphy, M. P. How mitochondria produce reactive oxygen species. *Biochem J* **417**, 1-13, doi:10.1042/BJ20081386 (2009).

43 Malassagne, B. *et al.* The superoxide dismutase mimetic MnTBAP prevents Fas-induced acute liver failure in the mouse. *Gastroenterology* **121**, 1451-1459 (2001).

44 Sazanov, L. A. & Hinchliffe, P. Structure of the hydrophilic domain of respiratory complex I from Thermus thermophilus. *Science* **311**, 1430-1436, doi:10.1126/science.1123809 (2006).

45 Dudkina, N. V., Eubel, H., Keegstra, W., Boekema, E. J. & Braun, H. P. Structure of a mitochondrial supercomplex formed by respiratory-chain complexes I and III. *Proc Natl Acad Sci U S A* **102**, 3225-3229, doi:10.1073/pnas.0408870102 (2005).

46 Dudkina, N. V., Kouril, R., Peters, K., Braun, H. P. & Boekema, E. J. Structure and function of mitochondrial supercomplexes. *Biochim Biophys Acta* **1797**, 664-670, doi:10.1016/j.bbabio.2009.12.013 (2010).

47 Lambert, A. J. & Brand, M. D. Inhibitors of the quinone-binding site allow rapid superoxide production from mitochondrial NADH:ubiquinone oxidoreductase (complex I). *J Biol Chem* **279**, 39414-39420, doi:10.1074/jbc.M406576200 (2004).

48 Lambert, A. J. & Brand, M. D. Superoxide production by NADH:ubiquinone oxidoreductase (complex I) depends on the pH gradient across the mitochondrial inner membrane. *Biochem J* **382**, 511-517, doi:10.1042/BJ20040485 (2004).

49 Frezza, C. *et al.* OPA1 controls apoptotic cristae remodeling independently from mitochondrial fusion. *Cell* **126**, 177-189, doi:10.1016/j.cell.2006.06.025 (2006).

50 Thiery, J., Walch, M., Jensen, D. K., Martinvalet, D. & Lieberman, J. Isolation of cytotoxic T cell and NK granules and purification of their effector proteins. *Curr Protoc Cell Biol* **Chapter 3**, Unit3 37, doi:10.1002/0471143030.cb0337s47 (2010).

51 Susin, S. A., Larochette, N., Geuskens, M. & Kroemer, G. Purification of mitochondria for apoptosis assays. *Methods Enzymol* **322**, 205-208 (2000).

52 Frezza, C., Cipolat, S. & Scorrano, L. Organelle isolation: functional mitochondria from mouse liver, muscle and cultured fibroblasts. *Nat Protoc* **2**, 287-295, doi:10.1038/nprot.2006.478 (2007).

53 Mokranjac, D. & Neupert, W. Protein import into isolated mitochondria. *Methods Mol Biol* **372**, 277-286, doi:10.1007/978-1-59745-365-3_20 (2007).

54 Scorrano, L. *et al.* A distinct pathway remodels mitochondrial cristae and mobilizes cytochrome c during apoptosis. *Dev Cell* **2**, 55-67, doi:S1534580701001162 [pii] (2002).

FIGURE LEGENDS

Figure 1. GB cleaves complex I subunits NDUFS1, NDUFV1 and NDUFS2

(a) K562 cells were treated with P +/- GB as indicated in the presence of MnTBAP. ROS (MitoSox+ left panel) and cell death (Annexin V/PI, right panel) were monitored at 15 and 45 min, respectively. (b) 721.221 target cells preincubated or not with MnTBAP were mixed with YT-Indy effector cells expressing only GB at an E:T ratio of 6:1. Target cell killing was monitored by calcein release assay. Panels (a-b) show mean +/- SEM of at least 3 independent experiments, **p<0.01, ***p<0.001. (c) Close up of 2D IEF-SDS-PAGE gels of purified intact mouse liver mitochondria treated or not with GB or GA. The spot indicated by the arrow was identified by mass spectrometry as NDUFV1. (d-e) K562 cells, treated with P +/- GB as indicated, were analyzed by immunoblot probed for NDUFV1 (d) and NDUFS1 (e), PARP-1 and Hsp60. Some cells were treated with the caspase inhibitors zVAD-fmk and DEVD-fmk or with the GB-specific inhibitor Ac-IETD-CHO. (f-h) 721.221 target cells, transfected with tagged NDUFV1 (f), caspase 3-uncleavable (D255A) NDUFS1 (g) or NDUFS2 (h) were treated with YT-Indy NK cells at indicated effector: target (E:T) ratios and probed for the ectopically expressed complex I proteins using anti-tag antibodies. Experiments in (B-E) were repeated at least 3 times with similar results.

Figure 2. Overexpression of GB-uncleavable NDUFS1, NDUFS2 and NDUFV1 protects against GB-induced ROS production and cell death

(a) Purified intact mouse liver mitochondria pretreated or not with valinomycin, were incubated with GB and probed for complex I subunits. (b) Expression of wild type (Triple WT) and GB-uncleavable NDUFV1-3xFLAG, NDUFS2-HA, and NDUFS1-V5 (Triple mutant) proteins in untransfected or transfected K562 cells. (c-h) Transfected K562 cells were treated with P +/- GB as indicated and assessed for mitochondrial ROS by MitoSOX staining and flow cytometry (c, d and g) and for cell death by annexin V/PI staining and flow cytometry (e, h) or counting of apoptotic nuclei stained by Hoechst 33342 (f, mean of at least 300 nuclei per conditions, from 3 independent experiments). P+GB (red lines), P alone (blue lines), GB alone (black lines), triple WT (circles) and triple mutant (triangles). In (g, h) cells were pretreated or not with zVAD-fmk to inhibit caspases. Mean +/- SEM of at least 3 independent experiments is shown, *p<0.05, **p<0.01.

Figure 3. GB cleaves NDUFS1, NDUFV1 and NDUFS2 independently of MOMP

(a) Cyt c and Endo G release and NDUFS1 cleavage were assessed by immunoblot of supernatants and mitochondrial pellets from purified intact mouse liver mitochondria treated with 50 and 450 nM of GB in the presence or absence of S100 cytosolic fraction. Hsp60 was probed as a loading control protein that is not released.
(b) *Bax*$^{-/-}$*Bak*$^{-/-}$ cells do not express Bax or Bak as assessed by immunoblot.
(c, d) ROS production (c) and cell death (d) assessed by mitoSOX and annexin V-PI staining, respectively, in wild type (WT) and *Bax*$^{-/-}$*Bak*$^{-/-}$ MEFs treated with GB and P for 1 hr. Mean +/- SEM of 3 independent experiments is shown, *p<0.05, **p<0.01.
(e, f) Wild type (e) and *Bax*$^{-/-}$*Bak*$^{-/}$ (f) MEFs overexpressing NDUFS1-V5, NDUFV1-3xFLAG and NDUFS2-HA were treated with GB and P as indicated and probed for NDUFS1, NDUFV1 and NDUFS2 using anti-tag antibodies. PARP-1 was probed as a control for GB activity and Hsp60 is a loading control. Blots are representative of at least 3 independent experiments.

Figure 4. GB-induced ROS are required for proper apoptogenic factor release, DNA laddering and lysosomal membrane permeabilization

(a) Total cell lysate, (b) cytosolic (cyto) and mitochondrial (mito) fractions of U937 cells treated or not with P and GB, with or without NAC pretreatment were analyzed by WB for Bid cleavage and the release of Cyt c, Smac and EndoG from the mitochondria. Tom40 and GAPDH were probed as loading controls and to verify proper fractionation. (c, d) K562 stably expressing wild type (Triple WT) or GB-uncleavable (Triple mutant) NDUFV1, NDUFS1 and NDUFS2 were treated as in (a) to assess Bid cleavage or as in (b) for the release of the apoptogenic factors. (e-f) DNA from U937 cells, treated as in (a), was analyzed by agarose gel electrophoresis (e) and the % of DNA that migrated below 3 Kb was quantified. (e) shows a representative gel and (f), the mean +/- SEM of 3 independent experiments. **p<0.01
(g) K562 triple WT or triple mutant cells were treated and analyzed as in (e). A representative gel of 3 independent experiments is shown. (h) U937 cells treated as indicated with or without 5 mM NAC, were stained with Lysosensor, which only fluoresces in lysosomes that maintain acidic pH. Mean +/- SEM of 3 independent experiments. *p<0.05, **p<0.01. (i) K562 cells overexpressing triple WT or triple mutant complex I subunits were treated and analyzed as in (h).

Figure 5. GB-induced ROS generation and cell death require mitochondrial respiration

(a) Quantification of mitochondrial and genomic DNA in wild type and pseudo ρ^0 K562 cells as measured by qPCR amplification of representative genes.

(b, c) Pseudo ρ^0 K562 cells are highly resistant to GB-induced ROS production (b), assessed by MitoSOX staining, and cell death (c), assessed by annexin V/PI staining. (d, e) WT, *NOX1*$^{-/-}$ and *NOX4*$^{-/-}$ MEFs were treated with P + GB and analyzed as above for ROS production (d) and cell death (e).

(f) Purified intact mouse liver mitochondria treated or not with valinomycin were incubated with Alexa 647-GB before partial treatment with proteinase K (PK) to remove externally bound proteins and analyzed by FACS. (g) Same as in (f) using unlabeled GB and analyzed by immunoblot.

(h-k) Although valinomycin treatment of K562 cells depolarizes mitochondria (h), it has no effect on GB uptake into cells assessed by flow cytometry (i). Valinomycin inhibits GB-induced ROS (j) and cell death (k) in a dose-dependent manner, even in the presence of the pan-caspase inhibitor zVAD. The color code for valinomycin concentrations is as in (h). All graphs show mean +/- SEM of at least 4 independent experiments. *p<0.05, **p<0.01, ***p<0.001

Figure 6. GB disrupts complex I and III activity

(a, b) Purified mouse liver mitochondria in respiration buffer were stimulated with glutamate/malate (a) or succinate (b) and O_2 consumption was measured using a Clark electrode. Within 1 min of adding GB, respiration of GB-treated mitochondria (purple and orange lines) was reduced compared to untreated mitochondria (black lines). Data are representative of at least 3 independent experiments.

(c) Purified mitochondria were treated with GB as indicated. Monomeric mitochondrial respiratory complexes were solubilized using LM and resolved by BNGE before measuring in-gel ETC complex activities. Mean +/- SEM of 3 independent experiments is shown. *p<0.05, **p<0.01.

(d) 721.221 cells, treated with GB and P, were probed for complex III proteins. GB substrates, NDUFS1 and PARP-1, were probed as positive controls and HSP60 as loading control. Blots are representative of at least 3 independent experiments.

(e-g) Isolated liver mitochondria treated with 450 nM GB for 5 min were solubilized with LM to resolve monomeric complexes (e) or D to preserve SCs (g) and analyzed by BNGE and immunoblot. Blots are representative of at least 4 independent experiments. (f) Complex I and III in-gel activity was monitored in monomeric

complexes after LM solubilization and I + III_2 SC after D solubilization. Shown are mean +/- SEM of 4 independent experiments. **p<0.01.

(h) Representative electron micrographs after mouse liver mitochondria were treated with buffer or GB. GB treatment triggers loss of mitochondrial cristae junctions. White arrows indicate detached cristae, while black arrows show attached cristae. (i) The proportion of mitochondria with detached cristae was quantified and represented as the mean +/- SEM of 3 independent experiments is shown. *p<0.05, **p<0.01.

Jacquemin et al Fig 1

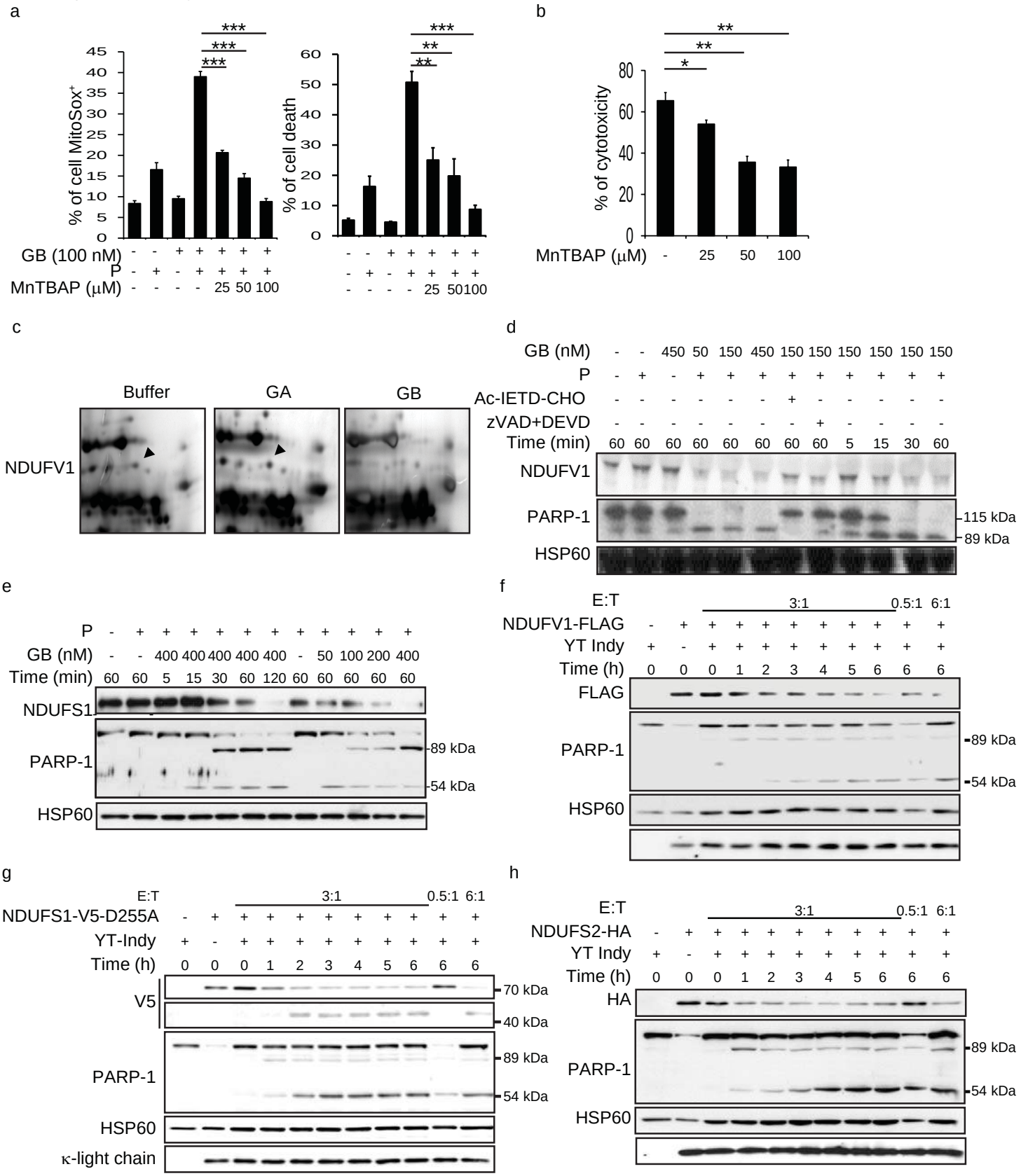

Jacquemin et al Fig 2

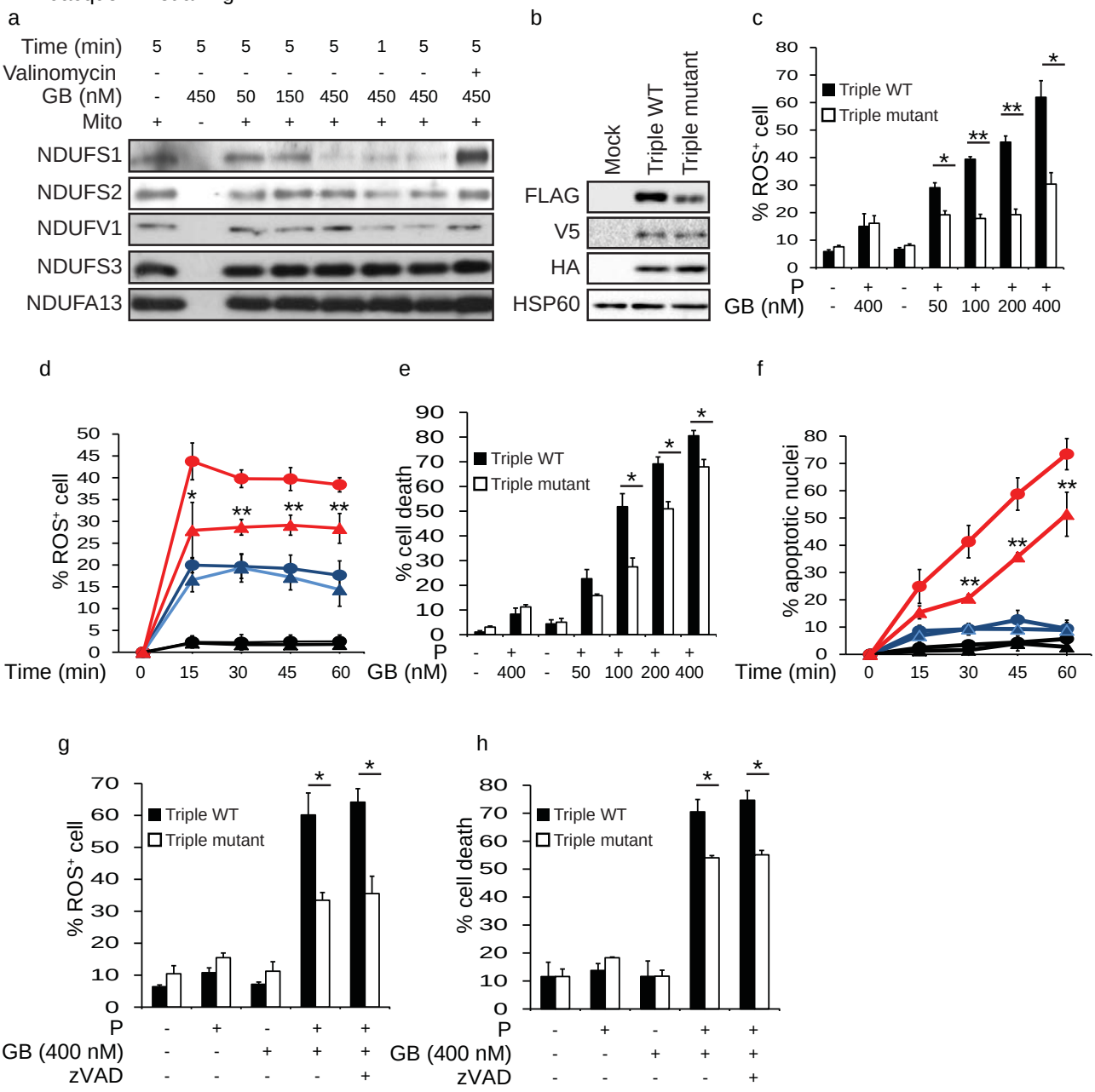

Jacquemin et al Fig 3

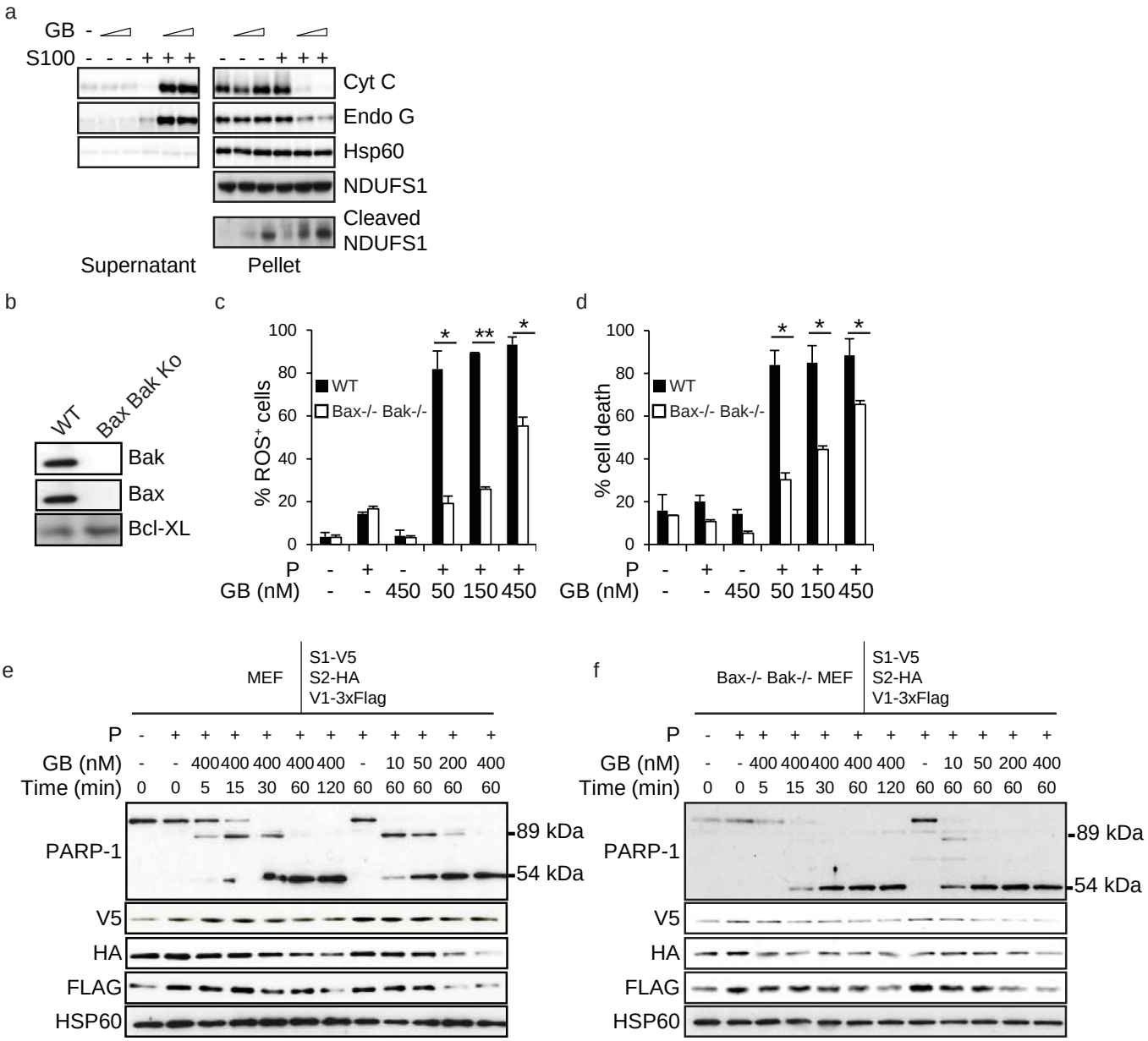

Jacquemin et al Fig 4

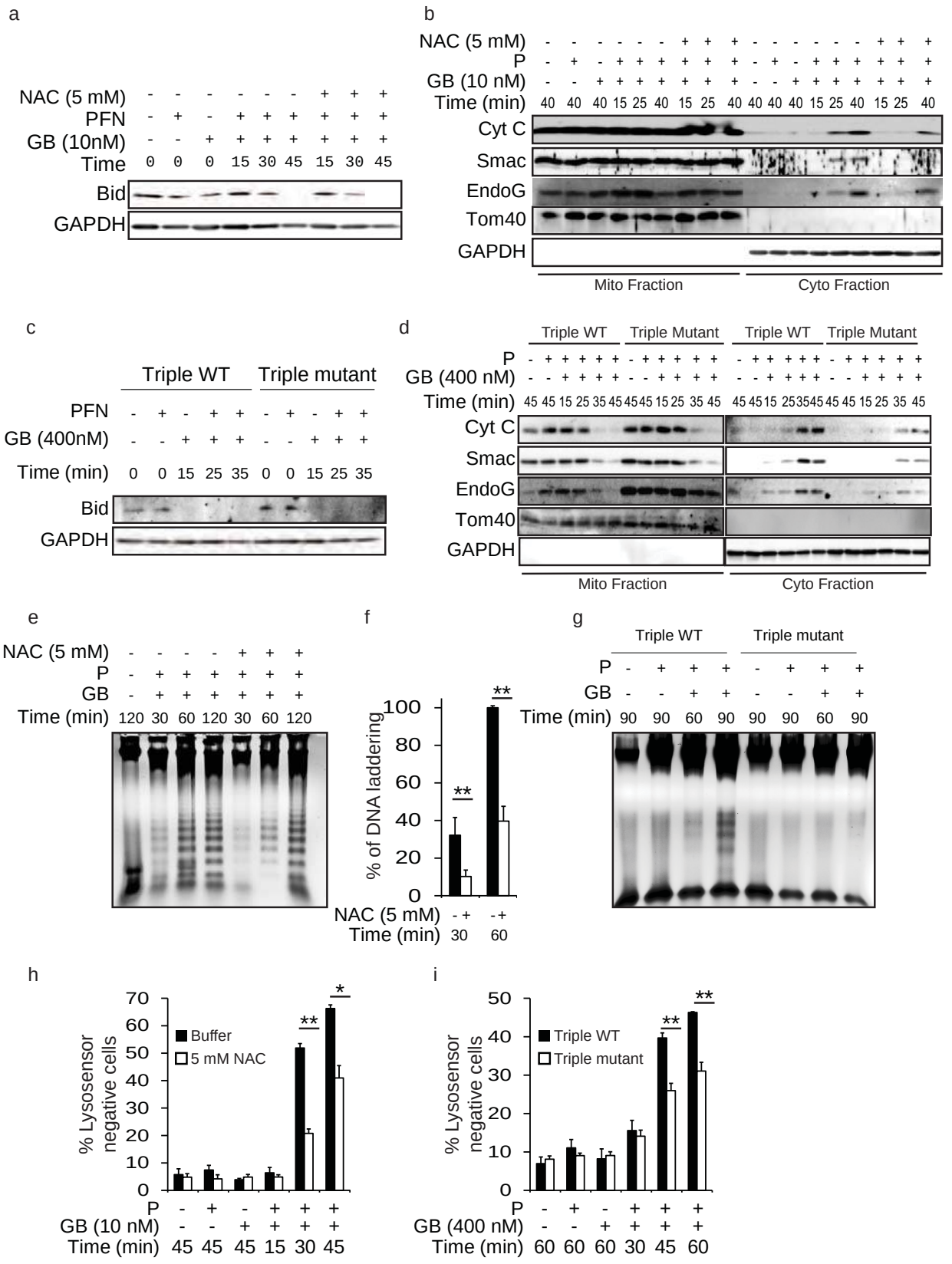

Jacquemin et al Fig 5

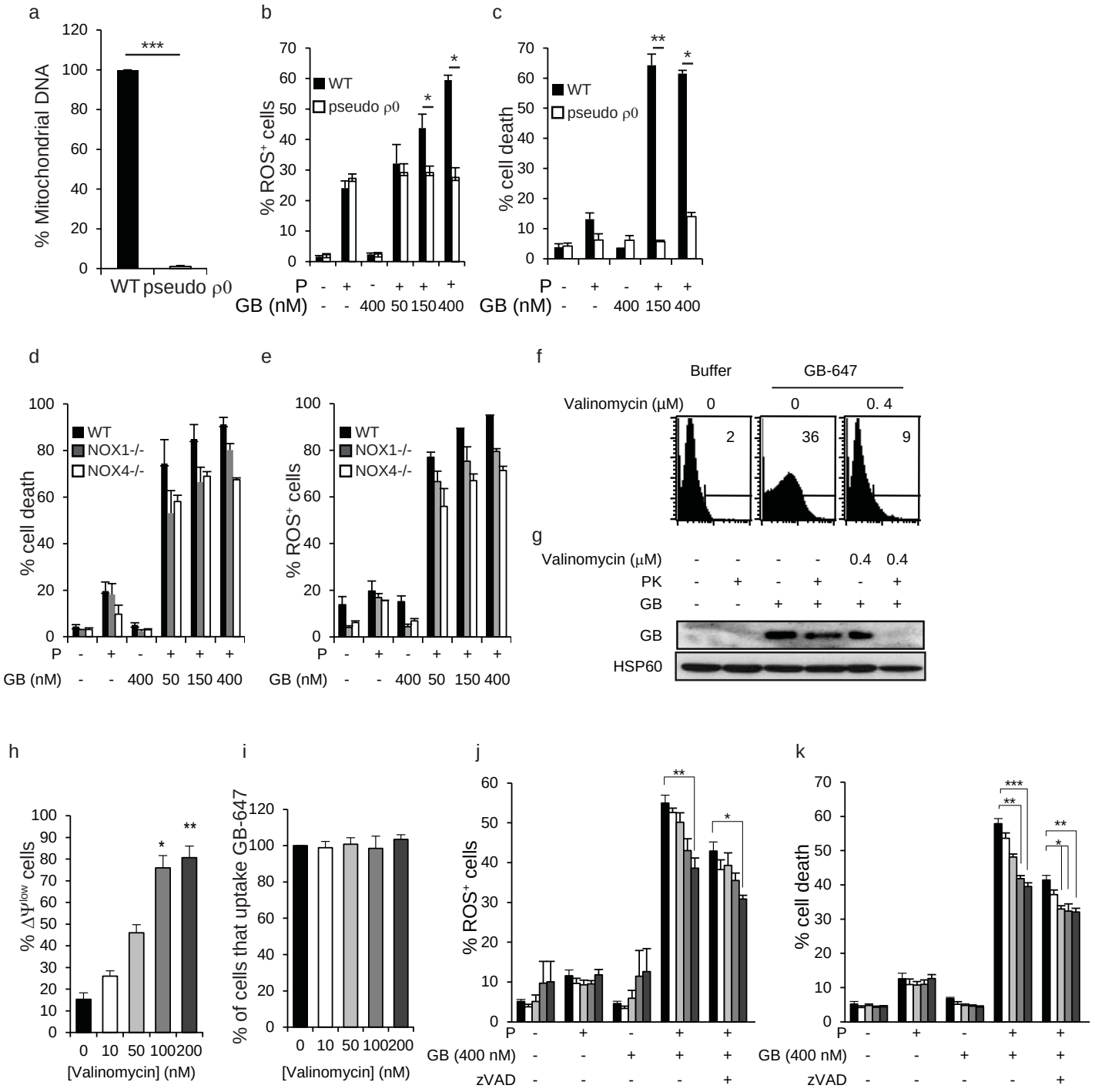

Jacquemin et al Fig 6

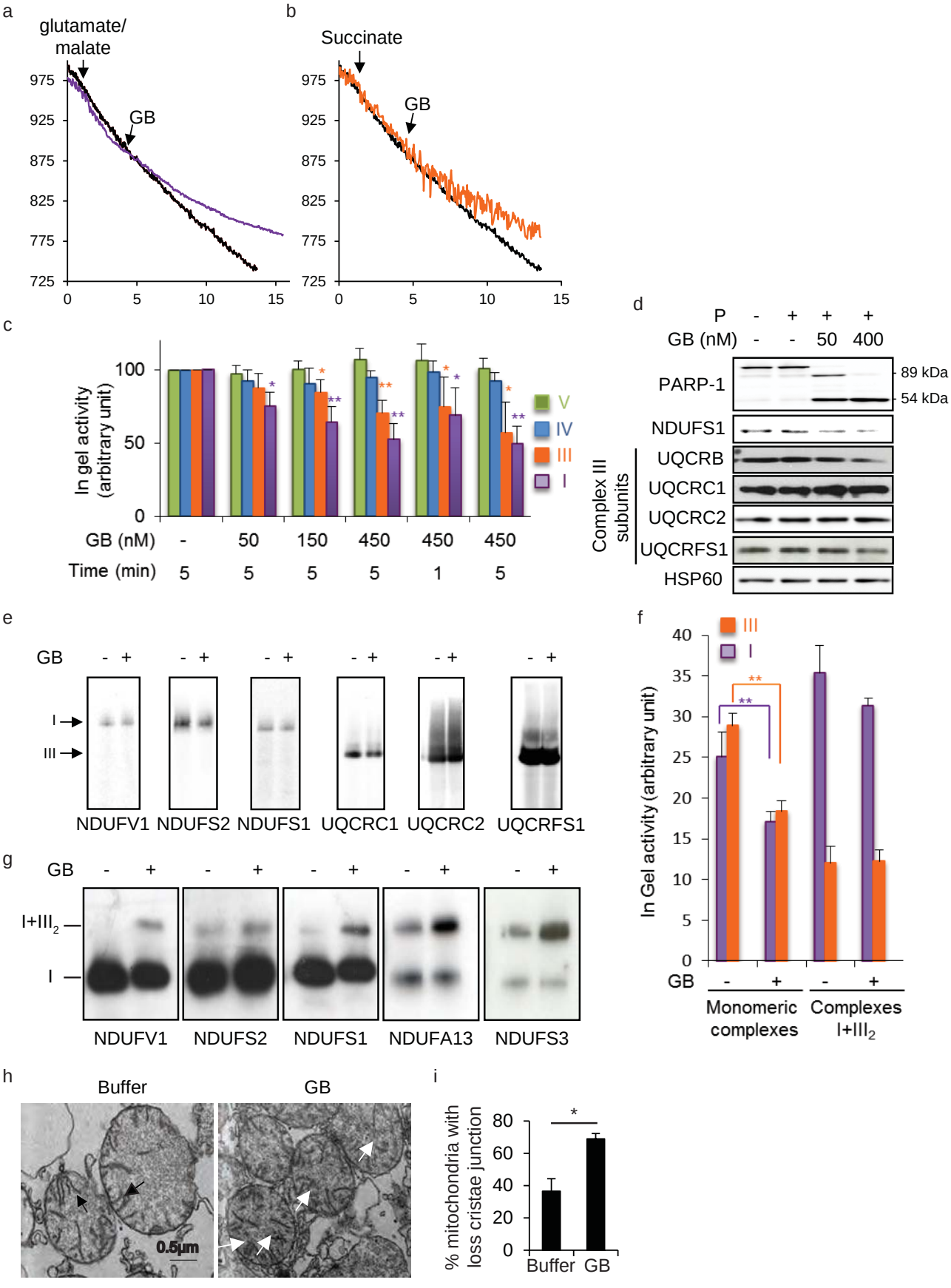

AKNOWLEDGMENT

I would like to express the deepest appreciation to my thesis director Professor Denis Martinvalet, who has supervised my thesis and the last four years of my life. He continually and convincingly conveyed a spirit of profound and total dedication in regard to research and an excitement in regard to teaching everything he knows.

I would like to thank my co-director Professor Jean-Claude Martinou and my committee members Professor Michael Walch and Professor Jerome Thiery who have carefully reviewed my PhD thesis.

A special thanks goes to all Martnvalet lab members, Olivier, Guillaume, Yonca, Valentina, Seba and Atzuko, who gave me more than I was expecting: suggestions, scientific advice, supports and beautiful memories.

I would like to thank all the members of the PHYM Department, Professors, PhD students, Post Docs, technicians, staff members, for their scientific advice, knowledge and willingness.

I would also like to extend huge, warm thanks to my family who provided unconditional love and care, to my friends (too many to list here but you know who you are!) for providing support and friendship here in Geneva and even from 1300 Km.

I take this opportunity to sincerely thank the person who came along with me to Geneva and supported me over the first year of this travel.

Last but not least, many thanks go to the one who is here beside me. I'm here with you beside me.